SEMICONDUCTING TIN OXIDE AND COBALT OXIDE FILMS FOR FUTURE SOLAR ENERGY APPLICATIONS

by

Alan F. Carroll

Thesis submitted to the Graduate Faculty of the

Virginia Polytechnic Institute and State University

in partial fulfillment of the requirements for the degree of

MASTER OF SCIENCE

in

Ceramic Engineering

APPROVED:

L. H. Slack, Chairman

W. R. Hibbard, Jr.

J. J. Brown, Jr.

January, 1976

Blacksburg, Virginia

ACKNOWLEDGMENTS

The author would like to thank the many people who contributed some of their time and effort in the work of preparing this thesis.

Special thanks go to Dr. Lyle H. Slack, Associate Professor of Ceramic Engineering, for his advice and encouragement given throughout the past year and three months and for his review of the manuscript.

The author is also grateful to Dr. Walter R. Hibbard, Jr., Chairman of the Materials Engineering Department at V.P.I.& S.U., and Dr. Jesse J. Brown, Jr., Associate Professor of Ceramic Engineering for their willingness to serve on the graduate committee.

He would also acknowledge the financial assistance given him by the National Science Foundation in the form of a solar energy related graduate traineeship.

Thanks are due to others who assisted. Mr. Fred Battrell assisted in gathering of ESCA data, Mr. Andrew Wnuk assisted in sputtering procedures, and Mrs. Teresa Belcher assisted in typing.

The author is also thankful for his parents, Mr. and Mrs. Laurence Carroll, and the love and encouragement they continue to give to him.

TABLE OF CONTENTS

LIST OF TABLES

LIST OF FIGURES

Figure | Page

Figure | Page

I. INTRODUCTION

A common feature of oxide materials is their high electrical resistivity. If these materials are formed into thin films, (two microns or less in thickness) their electrical resistivity generally is much less due to semiconduction. This semiconduction is caused by the many defects in the crystal structure of a film with its high surface to volume ratio.

In order to make use of semiconducting oxide thin films, an understanding of their electrical behavior and its causes must be obtained. This understanding can be reached by carrying out a thorough characterization of the films.

Recent events have shown our nation's supply of petroleum-based energy to be inadequate for the demands of its industry. This awareness has stimulated a search for alternative forms of energy that will supplement and/or eventually replace petroleum fuels.

One of these alternative energy sources under consideration by many is direct conversion of solar energy into electrical energy (photovoltaic effect). It is being considered as an energy supplement for remote locations such as military warning stations. Large scale applications are not presently in operation. The reason for this is that photovoltaic conversion with current technology of single crystal silicon is inefficient and capital intensive. Large quantities of expensive solar cells costing approximately $1,000 per square foot are required to produce sufficient electrical energy for industrial use. For example the cost of producing 1 KW of energy with solar cells is

approximately $20,000. Reduction of solar cell unit costs by mass production would still leave energy costs at levels much higher than those of other sources.

Previous work done at VPI&SU on semiconducting thin films engendered interest in investigating the feasibility of using these in solar cells. A cost estimation of preparing these by performing both pyrolytic and vacuum deposition of oxides and metals on window glass in mass production is $.30 per square foot. The fact that these films could be readily deposited on glass pointed to their potential use on large glass covered buildings. They would be able to serve the dual purpose of reflecting sunlight and producing electricity. This function would be most helpful during the hottest period of a typical summer day when air conditioning demand for electric power would be greatest.

To form these solar cells a p-type and n-type film are brought together. Electronic equilibrium is lost and instantly regained as free charge carriers near the junction of the films cross the junction into the neighboring film. In the resulting equilibrium the electronic energy bands of the p-type film exist at a higher energy than those of the n-type film while their Fermi levels are at equal energy. The transition region near to the junction is depleted of charge carriers and undergoes a gradual decrease in energy on going from p-type to n-type regions. Due to this difference in electrical energy there exists a voltage drop on moving from the p-type to n-type region.

Photo-energy is capable of exciting electrons from the valence band to the conduction band of semiconducting materials. This leaves a corresponding positive hole in the valence band. If an electron-hole pair is excited in the p-type film, the electron (minority carrier) can flow across the junction into the n-type film and on into an external circuit. The same process can occur in reverse for photo-excited holes in the n-type film.

These minority carriers are in constant danger of annihalation by recombination with the predominant type of charge carrier (majority carrier) in the film. Only those minority carriers generated near to the junction can exist for periods long enough to assure their successful transfer into the neighboring material where they become majority carriers.

The efficiency of the above mentioned process (photovoltaic effect) hinges upon the structural and electrical nature of each film. Optimum films would have an energy gap between valence and conduction bands of energy equal to the energy most available from the solar spectrum. This would allow the excitation of a large amount of electron-hole pairs. The films would need to be relatively free of impurities and other obstructions such as grain boundaries at which recombination could occur. An abrupt junction between these films would enable more minority carriers having a given life time to successfully cross it since they would have less distance to travel. However, too sharp a junction would not be desired for it would then be possible for a tunneling transition of electrons in the conduction

band of the n-type film to the valence band of the p-type film to effectively short circuit the process.

The basic properties needing study prior to forming this junction are

(1) compatibility of crystal structures of the n- and p-type films,

(2) the conductivity mechanism of these films with information concerning mobility of charge carriers,

(3) the optical properties of the films giving information about the films' ability to absorb photo-energy in the vicinity of the junction, and

(4) methods of fabrication and their effect on the above properties.

The main objective of this work was to reproducibly deposit n-type and p-type semiconducting films of tin oxide and cobalt oxide for possible application in the conversion of solar energy into electrical or thermal energy. This study entailed a thorough characterization of the films that were deposited. This characterization included their crystal structures as revealed by X-ray diffraction, their electronic structures as revealed by electron spectroscopy, scanning electron microscopy study of the films' morphology, and studies of the electrical conductivity mechanisms in these films. Because solar energy must be absorbed by these films in order to be converted to electrical energy, it was also necessary to study the films' optical characteristics. Although it was not a specific objective of this work to develop a working solar cell, prototype

solar cells of n-type tin oxide and p-type cobalt oxide films were prepared in a brief effort to test the applicability of these films.

II. LITERATURE REVIEW

A. Tin Oxide

1. Preparation Methods. Thin films of tin dioxide have been prepared by pyrolytic deposition, d.c. sputtering, and oxidation of tin monoxide films. Bulk samples have been prepared by chemical precipitation methods.

Pyrolytic deposition has been accomplished by spraying $SnCl_2$ vapor onto substrates heated to 400-500°C.[1-5] Other investigators have sprayed solutions of $SnCl_4$ in ethanol onto substrates having temperatures from 500-600°C.[6-11] Incorporation of dopants was readily accomplished along with the dissolution of $SnCl_4$ prior to spraying.[9,11]

Optimum pyrolytic films were described as those having uniform thickness.[12] Films formed on an industrial scale have been found to have variable thickness. This variability was either a tapering effect or a localized change of thickness. The former was evidenced by interference fringes and the latter by abrupt changes in absorption. Non-uniform atomization and contamination were responsible for the localized variations.

Another method used to form insulating thin films of tin dioxide took pyrolytic films of tin dioxide or evaporated films of tin monoxide and heated them in air at a temperature greater than 250°C.[7] The resulting film had an activation energy of 3.4 eV that indicated attainment of stoichiometry.

D.C. sputtering of tin dioxide (hereafter called tin oxide) and tin oxide doped with antimony was accomplished by using hot pressed or sintered ceramic targets of tin oxide.[13,14] Glass substrates were placed on a water cooled holder which was from 5.0 to 7.5 cm below the targets within a chamber evacuated to 10^{-6} torr. Argon gas was let into the chamber at a pressure of 2×10^{-3} torr. It was accelerated toward the tin oxide targets by voltages of 4-5 KV. Tin oxide ejected from the targets by the argon deposited at an approximate rate of 1 micron per hour.

To form bulk specimens of tin oxide or tin oxide doped with antimony a chemical precipitation method was used. In this method a gel of tin hydroxide precipitated from tin chloride dissolved in hydrochloric acid as ammonium hydroxide was added. Decanting of the solution was carried out to remove chlorine. The residual gel was dried at $45^{o}C$[15] or $110^{o}C$.[16,17]

2. Structure. X-ray diffraction studies of bulk specimens of tin oxide have indicated small crystals of the rutile structure which is the form of naturally occurring tin oxide, cassiterite.[15,16] In this structure the Sn^{4+} has a coordination number of 6 while the O^{-2} has a coordination number of 3. Electron diffraction patterns have also shown crystallinity but of a different nature. This difference would be due to the presence of tin oxyhydroxide compounds that form prior to complete oxidation.[17] X-ray diffraction studies of pyrolytic and sputtered thin films of tin oxide have also yielded cassiterite patterns.[11,14]

The structure of pyrolytic films has been described as defective on both cation and anion lattices. In the latter case residual Cl^- from the tin chloride spray solution has been noted as the most likely cause for high conductivities measured.[6,8,15,18] The cation lattice was able to accommodate substitutionary cations such as antimony, phosphorous, indium, and thallium.[11] Doping with antimony has received the most attention, as it has caused the greatest increase in conductivity.[4,7-11,15,18]

3. Electrical Properties. Pyrolytic films of tin oxide have exhibited high conductivities on the order of $10^2(\text{ohm-cm})^{-1}$.[4,6,7,9,11] Additions of pentavalent antimony has enhanced conductivity to approximately $10^3(\text{ohm-cm})^{-1}$.[4,7,9,11,15] This high conductivity would not be found if the reaction

$$SnCl_4 + 2H_2O \rightarrow SnO_2 + 4HCl \qquad (1)$$

went to completion. Two possible alternative reactions have been proposed.[7]

$$2SnCl_4 + 4H_2O \rightarrow SnO_2 + SnO + 8HCl + \tfrac{1}{2}O_2 + 2e \qquad (2)$$

$$2SnCl_4 + 4H_2O \rightarrow SnO_2 + SnO + 7HCl + \tfrac{1}{2}H_2 + \tfrac{1}{2}O_2 + \tfrac{1}{2}Cl_2 + e \qquad (3)$$

The first of these shows the effect of oxygen vacancies while the second reaction accounts for residual Cl.

The free charge carriers responsible for high conductivity have been identified as negatively charged and quantified by use of the Hall technique.[4,7,9,11] Typical concentrations range from $10^{19}cm^{-3}$ to $10^{21}cm^{-3}$. On adding antimony these concentrations increased.

Films with little or no antimony showed higher concentrations than would normally be expected. For example, the carrier concentration of films containing 0.2 m/o antimony was found to be equivalent to the concentration expected for films containing 0.95 m/o antimony.[4] This phenomenon was attributed to residual chlorine.[15,19]

Methods of controlling the carrier concentration and thereby the conductivity have been investigated. These have taken the form of systematic doping with materials having pentavalent or trivalent ions with radii suitably close to that of tetravalent tin.[9,11] In one study the relative effects of antimony and indium were seen to be the most marked.[11] Pentavalent antimony increased conductivity while trivalent indium decreased it.

The temperature dependence of conductivity was studied in order to give some insight into the causes for conductivity behavior.[7,9,11] Highly conductive films doped with antimony showed little or no temperature dependence. This zero activation energy effect was ascribed to overlapping of the antimony donor band with the tin conduction band.[9] Other less conductive films had conductivities that increased with temperature while carrier concentration remained constant. This increase was attributed to an increased carrier mobility resulting from the transition of electrons from an impurity band where mobility was low to the conduction band where it was higher.[9] As temperature exceeded 250^{o}C conductivity was permanently decreased due to some structural changes (Figure 1). This effect was thought to be possibly brought about by both removal of the residual chlorine and oxidation of the film.[7,9,15]

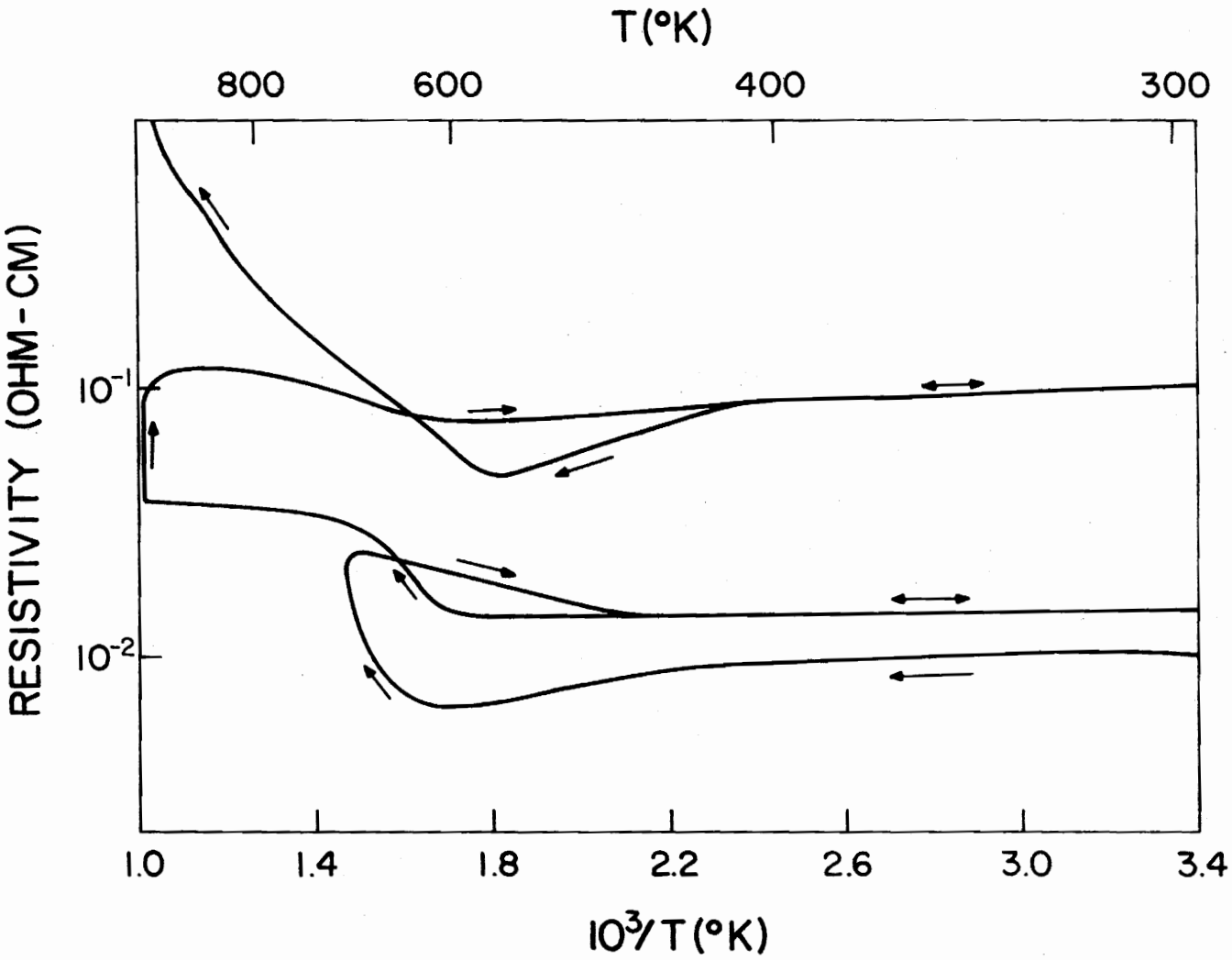

Figure 1. Resistivity of Thin Film Tin Oxide as a Function of 1/T (after Arai).

Some have plotted log conductivity vs. reciprocal temperature to obtain activation energies ranging from 10^{-2} to 4×10^{-2} eV for pure tin oxide.[7,11] Others have thought the temperature dependence to be better described by a plot of $\ln \sigma T^{-3/4}$ vs. T^{-1}.[8] Highly resistive tin oxide prepared by the oxidation method had an activation energy of 3.4 eV which as stated previously indicated negligable extrinsic contributions to conductivity.[7]

4. Optical Properties. Thin films of tin oxide have been found to be nearly transparent to visible light. Percent transmission was measured to be 90%.[6] Additions of antimony have brought about either black or blue coloration.[8,9,15] A possible cause given for this coloration was the formation of a dimeric complex of trivalent antimony and tetravalent tin whose parts interacted with each other in the process of absorbing light.[15,22]

Infrared transmission was found to decrease gradually from 85% to 50% as wavelength increased from 0.7 to 2.5 microns.[6] In the far infrared region two absorption bands were observed at wavelengths of 9 microns and 16.4 microns.[8]

The absorption bands in the far infrared were attributed to chlorine content in that films free of chlorine lacked these.[8] The increased availability of excitable electrons was given as the explanation of absorption by films containing chlorine.

Infrared reflectivity increased with wavelength from wavelengths of 1.5 microns to 3.0 microns. Beyond 3.0 microns it remained at a constant high value.[9] Another study showed a more gradual increase

of reflectivity with wavelength to a maximum value of 30% at a wavelength of 9.0 microns.[6]

To perform these measurements the investigators used thin film samples on substrates of fused silica or rock salt[6] or rock salt only.[8] Bulk samples for reflectivity measurement were prepared as 1% KBr disks in another study.[15]

5. Use in Electronic Devices. Pyrolytic tin oxide has been used in semiconductor junction devices. It has served as an active component of the device[5,22] or as a transparent electrode for junctions composed of cadium sulfide with cadium telluride or copper sulfide.[20,21]

Photovoltaic devices with tin oxide deposited onto single crystals of either silicon, germanium, or gallium arsenide have been fabricated.[5] These photocells gave best electrical output for incident light of high energy. The best cell made had an efficiency of approximately 0.16 that of a typical silicon solar cell. The rectifying properties of these n-n cells were explained as being caused by an upward bending of silicon energy bands at the junction.[5,23] This bending provided a sharp potential hill of approximately 0.5 eV. Electrons excited by incident light (photo-electrons) could leap over this barrier and consequently move through the tin oxide.

B. Cobalt Oxide

1. Preparation Methods. Cobalt oxide can exist in several forms: CoO, Co_3O_4, and Co_2O_3. The most influential conditions involved in preparing these are atmosphere and temperature.[26,29,30]

Pyrolytic thin films formed by spraying a solution of cobalt acetate in ethanol have crystallized in the spinel structure of Co_3O_4.[24,25]

Other films formed by triode sputtering were CoO, Co_3O_4, or Co_2O_3. Increasing the partial pressure of oxygen in the sputtering device increased the oxygen in the film.[26]

Bulk specimens of CoO have been prepared by several sintering methods.[27-31] Vacuum pressure sintering of preheated Co_3O_4 to a temperature of 950°C and a pressure of 11,750 psi with a vacuum of 50 microns is a recently developed method.[27]

2. Structure. CoO has the NaCl type crystal structure with a coordination number of 6 for both cobalt and oxygen. Co_3O_4 is of the spinel structure.[32]

Studies of the diffusion and electrical conduction of CoO have shown it to be non-stoichiometric with an excess of oxygen arising from cobalt vacancies.[28-31] At temperatures above 70°K the vacancies contribute either one or two positive holes to the valence band of CoO by accepting electrons. At lower temperatures they are un-ionized.[30]

The effect of doping CoO with monovalent lithium has also been studied.[28,31,33] Addition of 0.15 m/o lithium decreased cobalt vacancy concentration but nevertheless increased concentration of holes. At low partial pressures of oxygen ($10^{-.025}$ atmos.) gravimetric measurements showed the material to have a slight oxygen deficiency. Thermoelectric tests indicated the presence of negative charge carriers

that were noted as being supplied by interstitial cobalt atoms.[31] Diffusion of oxygen in CoO was aided by adding lithium. This was due to the rise in oxygen vacancy concentration with cobalt vacancy decrease. Doping with trivalent aluminum was found to produce opposite effects.[28]

3. Electrical Properties. CoO has been shown to be a p-type semiconductor.[30] Its conductivity is dependent on concentration of cobalt vacancies or lithium dopant. Therefore, the conductivity increased with increasing partial pressure of oxygen (increasing cobalt vacancies) up to a point where CoO was transformed to Co_3O_4. Beyond this point, conductivity was constant.[29]

Conductivity was also increased by increases in temperature. The cause given for this behavior was an exponential increase in hole mobility with temperature.[30,33] This increase in conductivity showed a two slope behavior on plots of logarithm of conductivity versus reciprocal absolute temperature. There was an abrupt change in slope at temperatures near the Neél temperature. This phenomenon was attributed to the anti-ferromagnetic nature of CoO. Activation energies (E_a) calculated from these plots were smallest for samples having the greatest departure from stoichiometry and for temperatures below the Neél temperature (19°C). The room temperature E_a values ranged from 0.44 eV for $CoO_{1.988}$ to 0.70 eV for $CoO_{1.999}$.

In Co_3O_4 addition of monovalent lithium increased the conductivity.[34] The mechanism for conduction was claimed to be that of the Wagner model for conduction in crystals having the spinel structure.

4. Optical Properties. A bulk sample of CoO was prepared by sectioning to a thickness of 30 microns that allowed light to penetrate. Transmission steadily increased from 0% at wavelength of 0.5 micron to 89% at 1.7 microns with a dip to 10% at 1.3 microns.[35]

These data were correlated to a theoretical model based on the principle of energy level transition of the paramagnetic Co^{++} ion in the cubic NaCl crystal structure. The energy levels available for these transitions were formed as normal Co^{++} energy levels were perturbed (split) under the influence of the surrounding crystal environment. Photon energy would be absorbed as part of a complex process of interaction with these ions and other waves (phonon, excitation, spin).

Thin films of Co_3O_4 were more transparent in the visible region than CoO due to thinness. Transmission was found to have a maximum value of 30% at 0.6 microns in the visible region. In the near infrared region, transmission rapidly reached a constant value of 30%. No theoretical reasons were given for this behavior. The characteristic of selective transmission in the visible region was noted as aesthetically advantageous in that a greenish color effect was produced.[25]

III. EXPERIMENTAL PROCEDURE

A. Sample Preparation

1. Types of Samples. Several experiments were performed in this study in order to characterize thin film thickness, structure, morphology, composition, electrical resistivity and rectification, solar response, and optical properties. In order to perform these tests four different types of samples were prepared.

For investigation of thickness, structure, morphology, and optical properties a glass slide* was used as a substrate for the films.

A second type of sample was designed with four terminal resistivity measurements in mind (Fig. 2). It was prepared in two sizes: a full sized glass slide of 1-3/4 inch length and 1 inch width and a smaller size capable of being mounted onto the sample holder of the ESCA apparatus. To accomodate four contacts leading to both an electric power supply and voltmeter, four thin film strips of gold on nichrome were evaporated onto the slide across its width. These strips were separated by three gaps of approximately .06 inch (full size) or .02 inch (ESCA) that were formed by masking the glass during the evaporation process.

To test for rectification of current passing through the junction of combined tin oxide and cobalt oxide films a configuration with gold leads above and below the films was used (Fig. 3). Depositing the

---

*Arthur H. Thomas Co., Philadelphia, Pennsylvania.

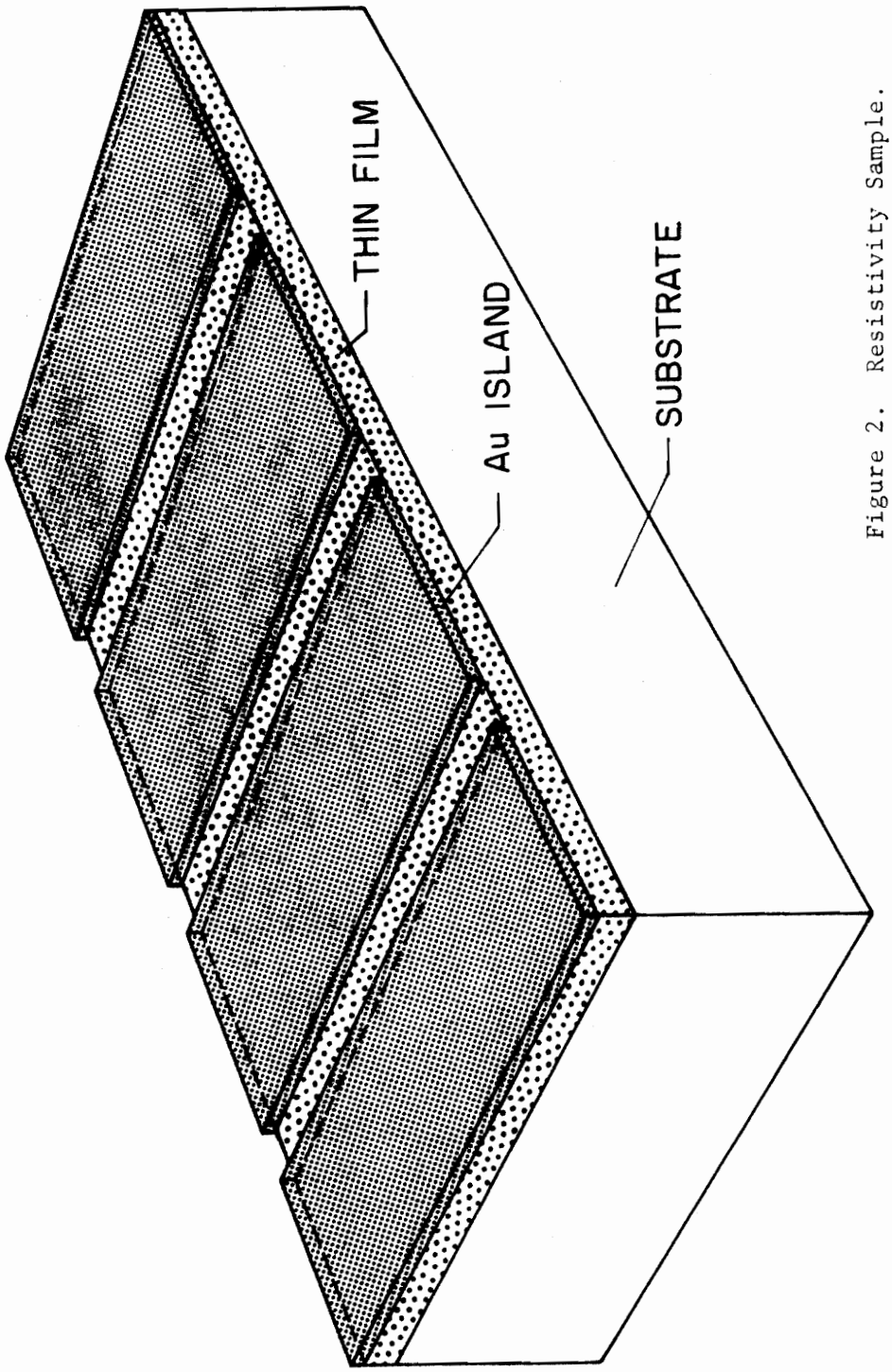

Figure 2. Resistivity Sample.

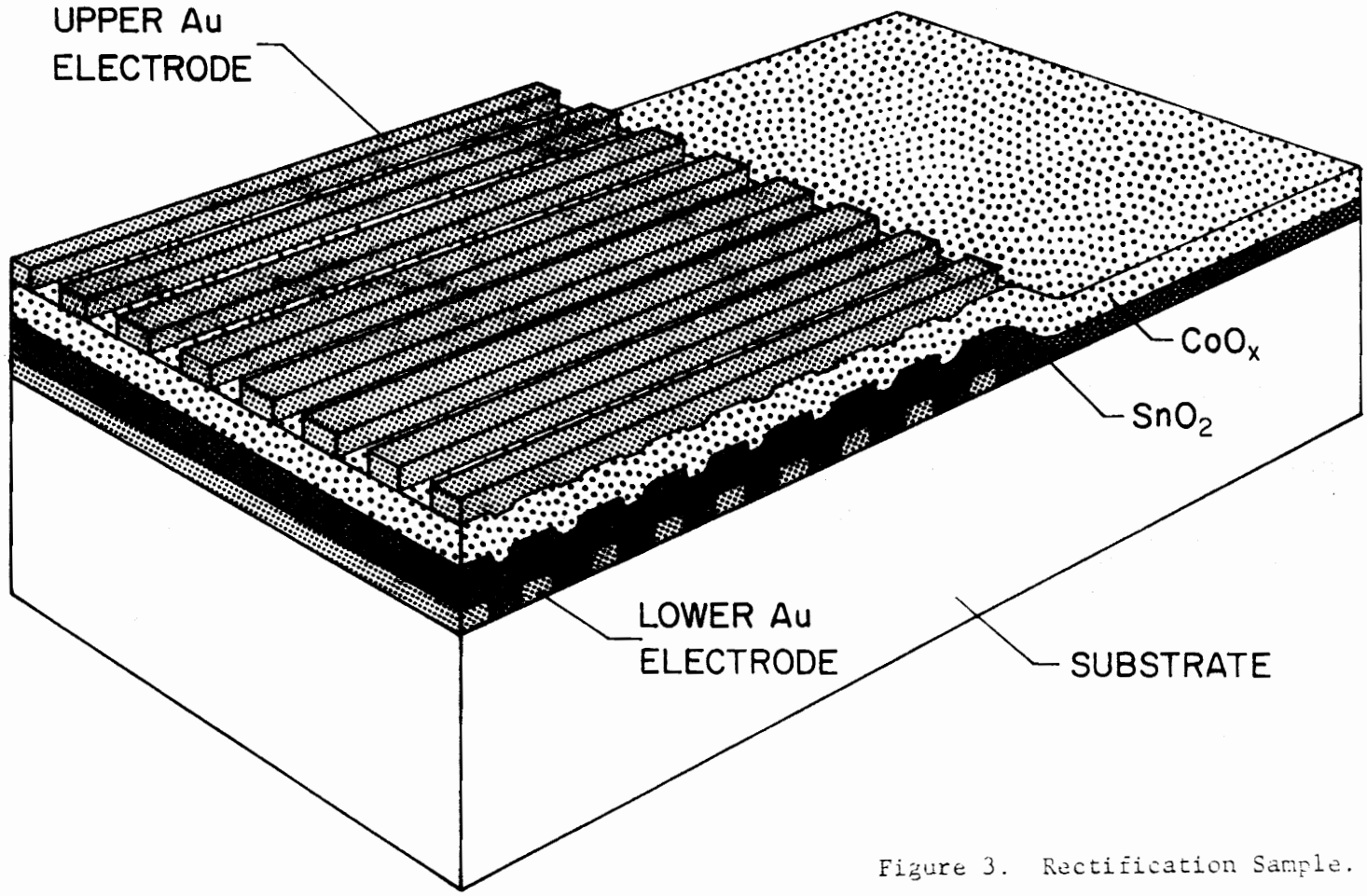

Figure 3. Rectification Sample.

upper electrodes normal to the lower ones enabled testing of different small areas of the combined films.

Detection of the photovoltaic effect was attempted with the sample shown in Figure 4. In this sample the lower electrode nearly covered the entire slide.

2. Pyrolytic Deposition. Tin oxide thin films were prepared by pyrolytic deposition. This technique involved the spraying of a 2.85 M solution of $SnCl_4 \cdot 5H_2O$* in ethanol onto a glass substrate heated to a temperature of 300-350°C. A systematic variation of dopants was carried out by mixing appropriate volumes of 2.85 M dopant solutions. These solutions were prepared by dissolving $InCl_3 \cdot 4H_2O$** or $SbCl_3$* in ethanol.

The spraying apparatus used was a slight modification of one developed here previously[35]. The path length and deposition area of the dispersed solution was increased in size by using a larger deposition chamber. This increase tripled the number of samples possible to prepare per deposition.

Plain glass samples required cleaning in ethanol followed by wiping prior to their placement onto the hot plate providing the heat for decomposition. Other samples having evaporated metal films had already been cleaned prior to evaporation. During the spraying, surface temperature of the substrate was reduced. To keep temperature

---

*Reagent grade, J. T. Baker Co., Philipsburg, New Jersey.

**Ventron Corporation, Alfa Products, Beverly, Massachusetts.

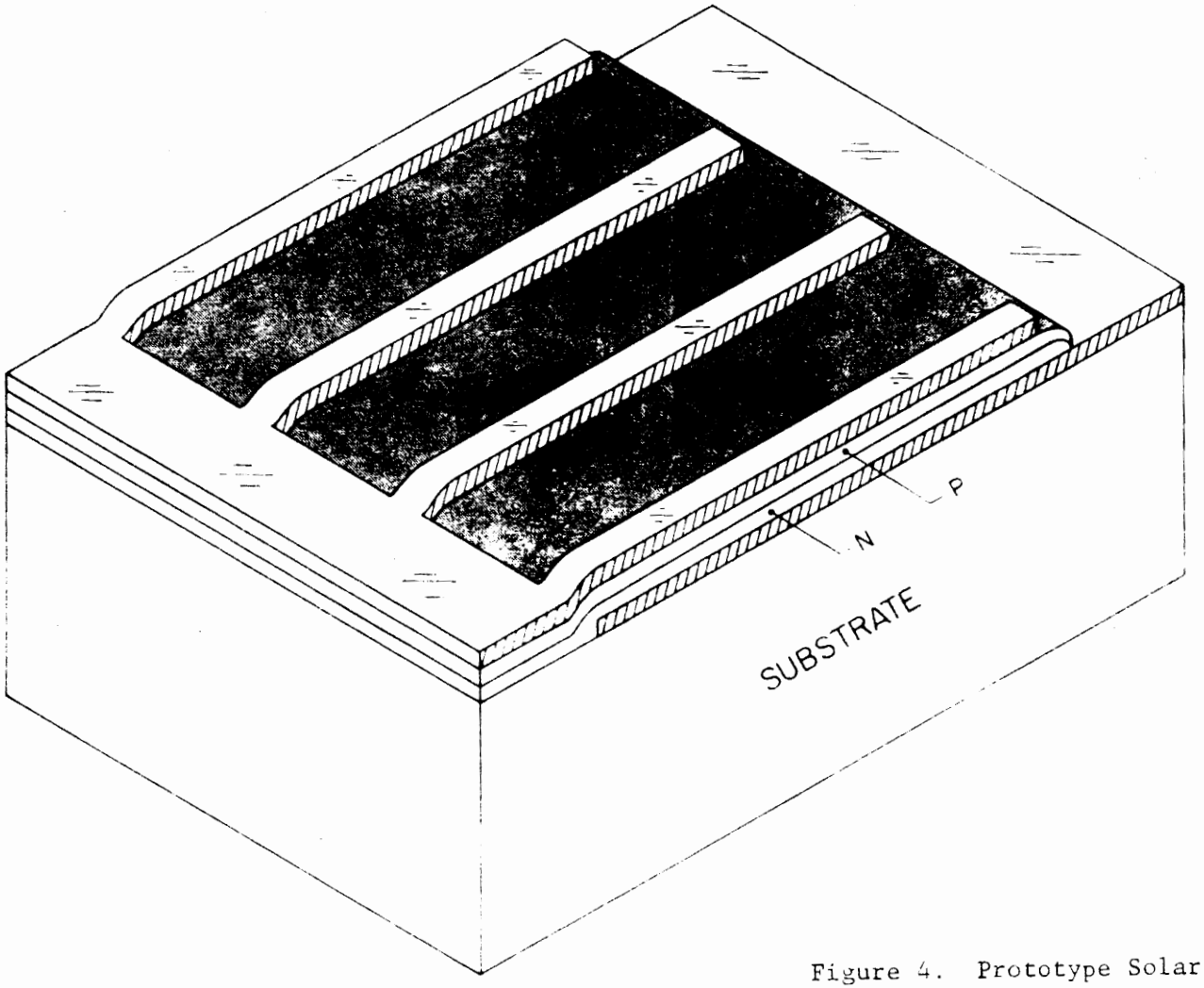

Figure 4. Prototype Solar Cell.

sufficiently high (300°C or greater) for decomposition of the hydrated tin chloride solution, one minute of spraying was alternated with one minute of reheating. The surface temperature of a typical glass slide was measured by bonding a chromel-alumel thermocouple to the upper surface of the slide which was then placed onto the hot plate.

3. Evaporation. A vacuum deposition system* having a tungsten basket filament and high current power supply was used to prepare thin film contacts and leads for electrical measurements. The procedure entailed the placement of cleaned glass slides with appropriate masking patterns into the deposition chamber, evacuation of the chamber to a pressure of less than 10^{-5} torr, and evaporation of .15 gram of nichrome which aided adhesion of .5 grams of gold deposited immediately after the nichrome. These amounts of metal were calculated to produce films having a thickness of 1,000 angstroms.

4. R. F. Sputtering. In order to prepare conductive films of cobalt oxide, a radio frequency sputtering device** was utilized. The deposition chamber of this device was evacuated to a pressure of less than 10^{-5} torr.*

This apparatus consisted of a deposition chamber having a water cooled specimen holder, entrance valves for gases, and a matching unit that provided an accelerating voltage. An alternating electrical

---

*Consolidated Vacuum Corporation, Rochester, New York.

**R. D. Mathis Co., Long Beach, California.

potential at radio frequency was applied through the matching unit to one of two pressed-sintered disks (targets) of cobalt oxide.* These disks were either pure cobalt oxide or cobalt oxide with 5 m/o lithium oxide.** They were prepared by hot pressing the oxide powders to a pressure of 3,960 p.s.i. at 500°C for 3 hours followed by sintering for 12 hours at 1500°C. Argon gas atoms were then let into the chamber at a pressure of 15 microns and ionized to Ar^+ (plasma). These ions were accelerated toward the target when it was negatively biased. The ions attained a velocity high enough to dislodge cobalt oxide molecules from the target during impact. These molecules were then free to deposit onto the substrates.

The sputtering conditions used are listed in Table I.

5. Annealing. Subsequent to pyrolytic deposition of tin oxide films a systematic study was made of the effect of annealing these in air. For this purpose an electric muffle kiln*** was used at a constant temperature of 600°C. Annealing times used were 0, 1, 10, 50, and 100 hours. The annealing atmosphere was air. A check on the effect of annealing cobalt oxide for 1 hour with the other conditions the same was also carried out.

B. Experimental Measurements

1. X-Ray Diffraction. An X-ray diffractometer**** was used to obtain diffraction patterns from the samples over a range of 20° to

*Reagent grade, J. T. Baker Co., Philipsburg, N.J.

**Atomergic Chemetals Co., Carle Place, N.Y.

***Model M10A-1A Muffle Furnace, Blue M Electric Co., Blue Island, Ill.

****Norelco Diffractometer, North American Philips, Mount Vernon, N.Y.

TABLE I

R.F. Sputtering Parameters

Condition	Plate Current (ma)	R.F. Power (KW)	Argon Pressure (μ)
Low Power	68	0.24	15
Medium Power	80	0.38	14
High Power	110	0.58	14

Distance 7.6 cm
(Target to
Sample)

60^{o} 2θ. From these crystal structure was identified and a relative measure of degree of film crystallinity was made by calculating the total peak intensity (I_T). Comparison of peak height was sufficient, as corresponding peaks in each film had similar peak breadth.

$$I_T = \sum_{1}^{4} (\text{Peak Height - Background}) \text{ cps} \tag{4}$$

where 1 to 4 signify the four tin oxide peaks observed.

Diffraction intensity at either 23^{o} or 24^{o} 2θ was recorded in order to gauge the films' thickness. This method was based on an X-ray attenuation method[36] that used the equation

$$t = \frac{\sin 2\theta \ \ln(I_u/I_c)}{2(\mu/\rho)\rho} \tag{5}$$

where t = film thickness (cm.),

I_u = diffraction intensity off uncoated glass,

I_c = diffraction intensity off coated glass,

μ/ρ = mass absorption coefficient of film (cm^2/gm)

ρ = film density (gm/cm^3)

Absorption coefficients for the compounds making up the films were calculated by taking a weighted average of the respective elemental constituents of the film.

$$(\mu/\rho)_{cpd.} = \sum_{i=1}^{n} X_i(\mu/\rho)_i \tag{6}$$

X_i is the weight fraction of element i. For a list of the diffractometer settings used, see Table II.

TABLE II

X-Ray Diffraction Conditions

	Thickness Test	Diffraction Pattern
Range	100 counts/scale	100 counts/scale
Time Constant	10	2
Range of 2θ	23^{o} or 24^{o}	20^{o} - 60^{o}
Chart Speed	7.5 in./hr.	30 in./hr.

2. SEM-EDAX. A scanning electron microscope* (SEM) with energy dispersive analysis of X-rays (EDAX) accessory was used to investigate both the morphology and the elemental composition of the films that had received varying degrees of heat treatment. This apparatus scanned a 20 KeV electron beam of primary electrons across a small rectangular area on the specimen. Upon impact these electrons were backscattered and also ejected other energetic species from the sample such as electrons (secondary electrons) and photons (X-ray and other). Synchronized scanning of either type electron output signal with the output signal of a cathode ray tube (CRT) produced an image of the sample which was photographed.** Magnification was equal to the ratio of CRT area to the area scanned on the sample. Magnifications of 500X, 2,000X, and 5,000X were used to give overview and detail micrographs respectively.

The EDAX accessory recorded the X-ray spectra given off from the samples by using a solid state detector sensitive to differences in energy. Characteristic X-ray emission lines were then correlated to these spectra to analyze the elemental components of various microstructural features of the films.

3. ESCA. Electron spectroscopy for chemical analysis (ESCA) was undertaken to investigate the Sn-O bond and chlorine impurity content in tin oxide films that had undergone differing amounts of heat treatment as previously mentioned.

---

*AR 900, Burlington, Massachusetts.

**Oscilloscope Camera C-13, Tektronix Inc., Portland, Oregon.

In this technique the sample was mounted onto a copper sample holder and placed into an evacuated chamber held at a pressure less than 10^{-5} torr. It was then subjected to a beam of AlKα X-radiation which ejected electrons of energies characteristic of elements in the sample. The kinetic energy of the photo-ejected electrons was measured in an electro-static analyzer. By subtracting this energy (K.E.) from the energy of the incident X-ray beam ($h\nu$) and accounting for energy losses due to the work function of the spectrometer (ϕ_{sp}) a measure of chemical binding energy (E_B) was obtained.

$$h_\nu - \text{K.E.} - \phi_{sp} = E_B \qquad (4)$$

The analyzer was set to scan energy intervals of 20 eV that bracketted the characteristic electron binding energies of the elements studied. The energies of interest were 542 eV for oxygen, 494 and 485 eV for tin, 202 and 200 eV for chlorine, and 451 and 443 eV for indium.

A minicomputer* was used in conjunction with the ESCA apparatus to automatically vary the energy interval and record the counts given off for each of the 200, 0.1 eV steps within each interval. Time per step was set prior to each sample run in order to give sufficient peak to background ratio for the different elements.

This accumulated data was stored on paper tape which was later fed into a high speed reader** in order to produce a display of

---

*PDP 8/e Digital Equipment Corp., Maynard, Mass.

**PDP-8/1 Digital Equipment Corp., Maynard, Mass.

results on an oscilloscope.* Photographs of these plots were taken.

4. Electrical Measurements.

a. Resistivity. To measure resistivity (ρ) of specimens a modification of the four point probe technique was used[38]. Rather than use four small point contacts, alligator clips were placed onto the four thin film strips of gold described earlier (Fig. 2). Current (I) of 10^{-4} amps was provided by a power supply** and passed through the film from the two outermost contacts. Simultaneous measurement of voltage drop (ΔV) across the center gap was achieved by using a voltmeter*** connected to the two inner strips. Resistance (R) was then calculated as $\Delta V/I$.

By definition, surface resistivity (R_s) is the resistance of any sized square of a material. It is independent of the square's size due to the fact that increased resistance caused by increased path length is compensated for by an equal decrease in resistance caused by increased path width. Since the width of the center gap (normal to the direction of the current) was one inch, it was convenient to calculate surface resistivity from measured resistance by multiplying resistance by a factor that would effectively increase gap length (L) (in the direction of the current) to one inch. This factor of 1 in./L(in.) was approximately 20.

---

*Type RM 503, Tektronix, Inc., Portland, Oregon.

**Model 865C Power Supply, Harrison Laboratories.

***1608 Digital Multimeter, Keithley Instruments Inc., Cleveland, Ohio.

The resistivity of the sample in ohm-cm was then calculated from surface resistivity in ohm/square and thickness (t) in cm. according to the following equation

$$\rho = R_s \cdot t \tag{7}$$

b. Activation Energy. Temperature dependence of resistivity of tin oxide and cobalt oxide films was studied by placing resistivity samples in a controlled temperature furnace*. Temperature was varied from room temperature to 320°C. An air circulation system reduced the maximum temperature gradient within the furnace to 1°C. Therefore, thermal gradient effect on measured voltage was negligable.

Activation energies were calculated from the slopes of Arrhenius plots of the logarithm of resistivity in ohm-cm versus reciprocal absolute temperature. The equation used is a result of the exponential dependence of resistivity on E_a and reciprocal temperature.

$$\rho = e^{E_a/kT} \tag{8}$$

$$E_a = 2.3\ kT(\log\ \rho) = 2.3\ kT(\log\ \rho)/(10^3/T)10^{-3} \tag{9}$$

where $k = 8.6 \times 10^{-5}$ eV/°K

T = Temperature Change (°K)

$\log \rho$ = Corresponding Change in $\log \rho$.

c. Hot Probe. To determine the type of semiconductivity in each film a hot probe measurement was made. The principle upon which this technique is based is the tendency of charge carriers to migrate

*MK 2300 Temperature Chamber, Delta Design Inc., LaMesa, California.

away from a heated electrical contact. A heated and an unheated contact connected to a voltmeter were placed onto the film. The resulting change in voltage enabled determination of the sign of charge carriers.

d. Rectification. The rectification sample previously described (Fig. 3) was used in conjunction with a curve tracer oscilloscope* to observe the variation of current as a function of applied voltage across the junction of a cobalt oxide film on a tin oxide film. Photographs of the oscilloscope curves were taken.

e. Solar Response. A multimeter** capable of measuring 10^{-6} volts and 10^{-9} amps was used to observe the effect of solar radiation on the solar cell sample (Fig. 4).

5. Optical Property Measurements. A recording spectrophotometer*** was used to measure absorbance and reflectance of the films as wavelength was varied from 0.3 to 2.5 microns. This range of wavelength is that portion of the spectrum accounting for the majority of solar energy reaching the earth's surface.

The recorded data were put into a computer program that converted absorbance (A) and reflectance into percent transmission (T) and percent specular reflection (R). It used the following relations:

$$\log (T) = 2 - A \qquad (10)$$

---

*Type 575 Oscilloscope, Tektronix Inc., Portland, Oregon.

**160 B Digital Multimeter, Keithley Instruments, Inc., Cleveland, Ohio.

***Cary 14, Varian Instrument, New York, New York.

$$\log (R) = A(1) - A(3) - \tfrac{1}{2}[A(1) - A(2)] \qquad (11)$$

where A(1) = Reflectance of Standard Mirror

A(2) = Reflectance of Aluminum Film

A(3) = Reflectance of Sample.

The computer program then directed the plotting of these values versus wavelength by Calcomp plotter.*

*California Computer Products, Inc., Anaheim, California.

IV. RESULTS

A. X-Ray Diffraction Results

Diffraction results of tin oxide thin films consistently followed the cassiterite pattern of tin oxide powder (Table III). Crystal orientation was found to vary from film to film and also with doping. For example, the peak at a d-spacing of 2.369Å corresponding to the (200) plane was greater in intensity for films having less than 6 m/o dopant than for the tin oxide powder pattern (Table IV). At higher dopant levels this peak had a lower intensity than that of the powder, and in the case of indium doped films it was missing altogether. There were other notable differences between the films and the powder. The peak at a d-spacing of 1.675Å in the tin oxide powder pattern was missing from every thin film pattern. The major peak in the powder occurring at a d-spacing of 3.351 was not the major peak in any of the tin oxide films. The 2.644 angstrom plane was consistently strongest for undoped tin oxide films. The 63% peak of the (211) plane was increased by all additions of antimony and was decreased by all additions of indium. No large extraneous peaks occurred. One small unidentified peak occurred at a d-spacing of 2.858Å in the film having 3 m/o antimony.

Undoped thin films having undergone 100 hours of heat treatment showed the same peaks with different orientation and more breadth.

Diffraction results of cobalt oxide powder used for the sputtering target and sputtered cobalt oxide film containing 5 m/o lithium were

TABLE III

X-Ray Diffraction Patterns for Undoped SnO_2

Sample	2θ	d	I/I_o	(hkl)
Thin Film	26.4	3.376	30	(110)
Spray 13	34.0	2.64	100	(101)
	38.0	2.37	30	(200)
	51.9	1.76	60	(211)
Thin Film	26.3	3.389	30	(110)
Spray 28	33.9	2.644	100	(101)
	38.1	2.362	80	(200)
	51.7	1.770	70	(211)
Thin Film	26.5	3.401	20	(110)
Spray 31	33.9	2.644	100	(101)
Not Heat	38.0	2.370	80	(200)
Treated	51.7	1.768	70	(211)
Thin Film	25.7	3.466	40	(110)
Spray 31	33.3	2.690	100	(101)
Heat Treated @	37.6	2.404	80	(200)
600°C for 100 hr.	51.4	1.784	50	(211)
Bulk Sample	26.6	3.351	100	(110)
Vincent[15]	33.9	2.644	90	(101)
	38.0	2.369	30	(200)
	51.5	1.775	60	(211)
	55.0	1.669	10	(220)
Powder	26.6	3.351	100	(110)
File No.	33.9	2.644	81	(101)
5-467	38.0	2.369	24	(200)
	39.0	2.309	5	(111)
	42.6	2.120	2	(210)
	51.8	1.765	63	(211)
	54.8	1.675	63	(220)
	57.9	1.593	8	(002)
Thin Film	26.6	3.351	10	(110)
CoO_x on SnO_2	33.8	2.652	15	(101)
	37.9	2.374	100	(200)
	42.4	2.132	5	(CoO Peak)
	44.5	2.036	20	(Co_3O_4 Peak)

TABLE IV

X-Ray Diffraction Patterns for Doped SnO_2 Thin Films

Sample	2θ	d	I/I_o	Total Intensity	(hkl)
1 m/o Sb	26.4	3.376	40		(110)
Spray 19	33.7	2.659	100	230.5	(101)
	37.9	2.374	50		(200)
	51.6	1.771	100		(211)
3 m/o Sb	26.5	3.363	20		(110)
Spray 19	31.3	2.858	20		
	33.7	2.659	90	290.0	(101)
	38.0	2.368	100		(200)
	51.6	1.771	80		(211)
6 m/o Sb	26.5	3.363	60		(110)
Spray 19	33.8	2.652	100	148.5	(101)
	37.9	2.374	10		(200)
	51.5	1.774	100		(211)
10 m/o Sb 20 m/o Sb Spray 19	No Pattern	No Crystal Structure			
1 m/o In	26.6	3.351	15		(110)
Spray 29	33.9	2.644	100	230	(101)
	37.9	2.374	100		(200)
	51.7	1.768	15		(211)
3 m/o In	26.2	3.401	10		(110)
Spray 29	33.7	2.659	100	120	(101)
	37.7	2.386	20		(200)
	51.6	1.771	20		(211)
6 m/o In	26.6	3.351	30		(110)
Spray 29	33.8	2.652	100	100	(101)
	51.6	1.771	50		(211)
10 m/o In	26.2	3.401	30		(110)
	33.6	2.667	100	100	(101)
	51.4	1.778	50		(211)
20 m/o In	26.4	3.376	15		(110)
	33.9	2.644	100	95	(101)
	51.6	1.771	50		(211)

similar (Table V). The film had fewer peaks than the powder. These peaks occurred at similar d-spacings and were broader. There was one exception at a d-spacing of 2.146. This was found to correspond to CoO. All other peaks corresponded to Co_3O_4. Therefore, the resulting film was a mixture of Co_3O_4 and CoO that will hereafter be designated CoO_x or "cobalt oxide".

The diffraction pattern for the cobalt oxide film heat-treated for one hour was changed. The most significant change was the disappearance of the CoO peak.

B. SEM and EDAX Results

SEM micrographs show definite changes in film morphology with increased heat treatment (Figures 5-10). The unannealed sample showed a morphology of small crystals of approximately 2.5 microns square projecting above a film which appears to be very thin (Figures 5,6). Previous experience with scanning electron micrographs of thin films indicates thicker films have coarser texture than thin ones (Figure 5). Energy dispersive analysis of X-rays of this sample indicated that tin and chlorine were present in the crystals. The film between the crystals showed the presence of tin, silicon, and calcium with tin being predominant. The film annealed for one hour had even smaller crystals of approximately one micron in length embedded in a thicker film. These smaller crystals and associated film showed no sign of chlorine while tin was evident. Continued heating brought little change until the onset of a patterning effect evident at 50 hours and well developed at 100 hours (Figures 9,10). Backscattered

TABLE V

X-Ray Diffraction Patterns for CoO_x

Sample	2θ	d	I/I_o	Corresponding Oxide	Resistivity (ohm-cm)
Powder Used	31.2	2.87	30	Co_3O_4	
In Sputtering	36.8	2.44	100	Co_3O_4	
Target	38.4	2.34	60	Co_3O_4	
	44.7	2.03	30	Co_3O_4	
Cobalt	55.8	1.65	10	Co_2NiO_4	
Oxide	59.5	1.56	45	Co_3O_4	
Thin Film	36.9	2.436	30	Co_3O_4	
CoO_x w Li	42.2	2.146	40	CoO	
Sputter	44.6	2.036	100	Co_3O_4	
No. 3	59.3	1.563	30	Co_3O_4	
Thin Film CoO_x w Li Sputter No. 3 After Anneal @ 600° for 1 hr.	36.9	2.436	20	Co_3O_4	
	44.8	2.023	100	Co_3O_4	
	59.4	1.556	30	Co_3O_4	
Thin Film CoO_x w Li Sputter No. 14 (.24 KW)	42.1	2.146	50	CoO	0.045
	44.1	2.050	100	Co_3O_4	
Thin Film CoO_x w Li Sputter No. 14 (.34 KW)	42.1	2.146	20	CoO	0.390
	44.4	2.040	100	Co_3O_4	
Thin Film CoO_x w Li Sputter No. 14 (.44 KW)	42.5	2.127	50	CoO	0.714
	44.8	2.023	100	Co_3O_4	
Thin Film CoO_x w Li Sputter No. 14 (.44 KW)	42.2	2.146	100	CoO	1.0×10^5
	44.7	2.03	60	Co_3O_4	
Thin Film CoO_x w Li Sputter No. 14 (.44KW after anneal)	44.7	2.03	100		33.0

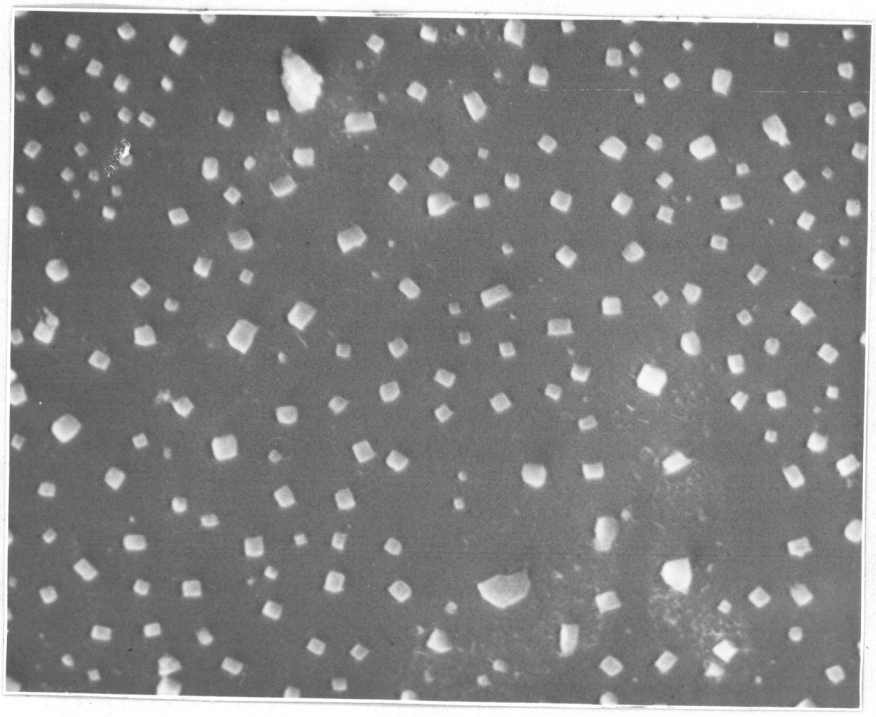

Figure 5. SEM Micrograph of Unannealed SnO_2 (2000X).

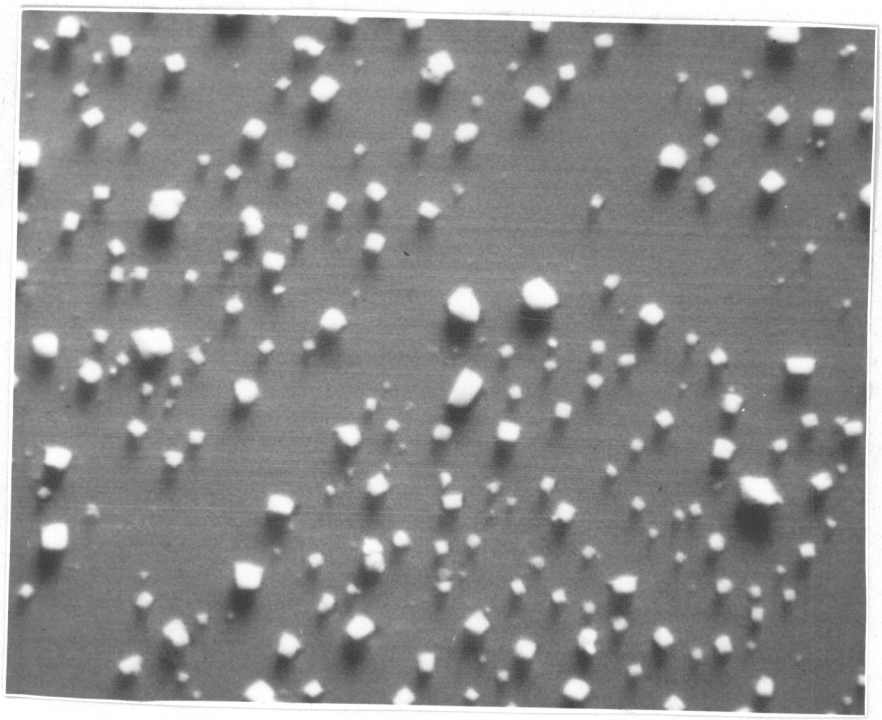

Figure 6. SEM Micrograph of Unannealed SnO_2 Backscattered Image (2000X).

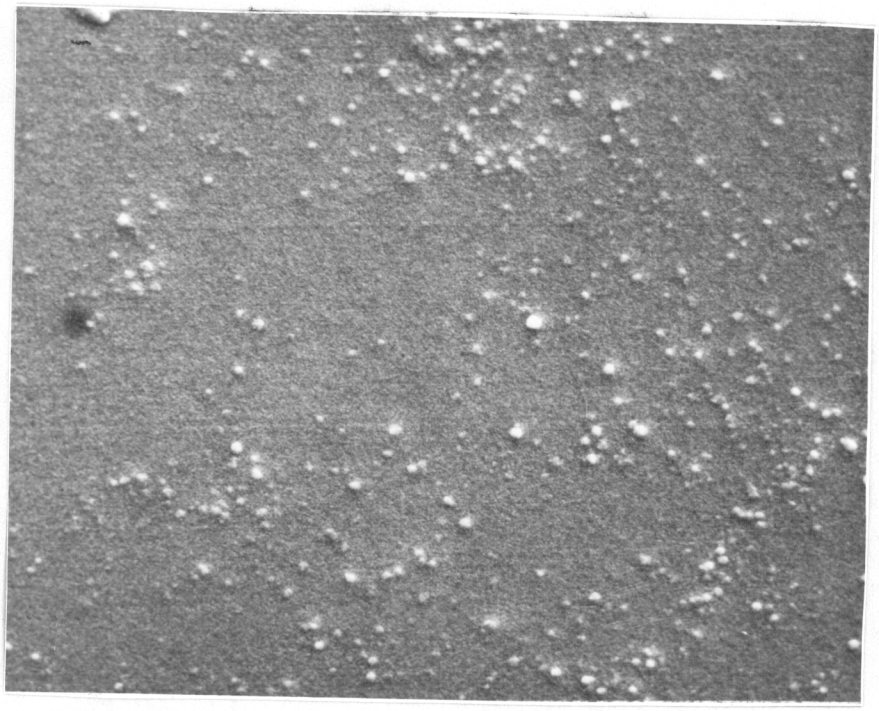

Figure 7. SEM Micrograph of SnO_2 Annealed for 1 hour (2000X).

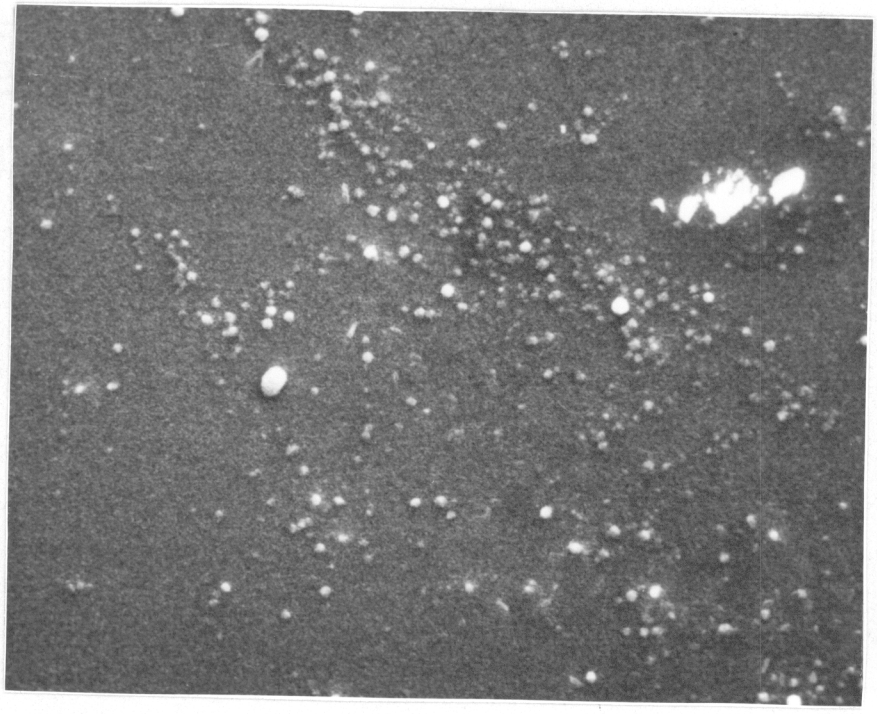

Figure 8. SEM Micrograph of SnO_2 Annealed for 10 hours (2000X).

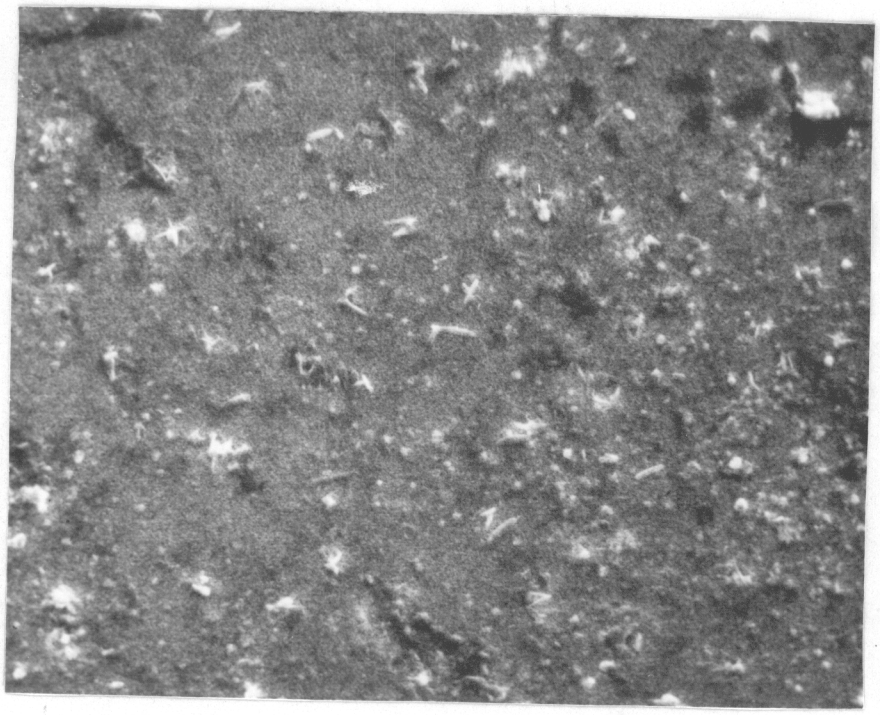

Figure 9. SEM Micrograph of SnO_2 Annealed for 50 hours (2000X).

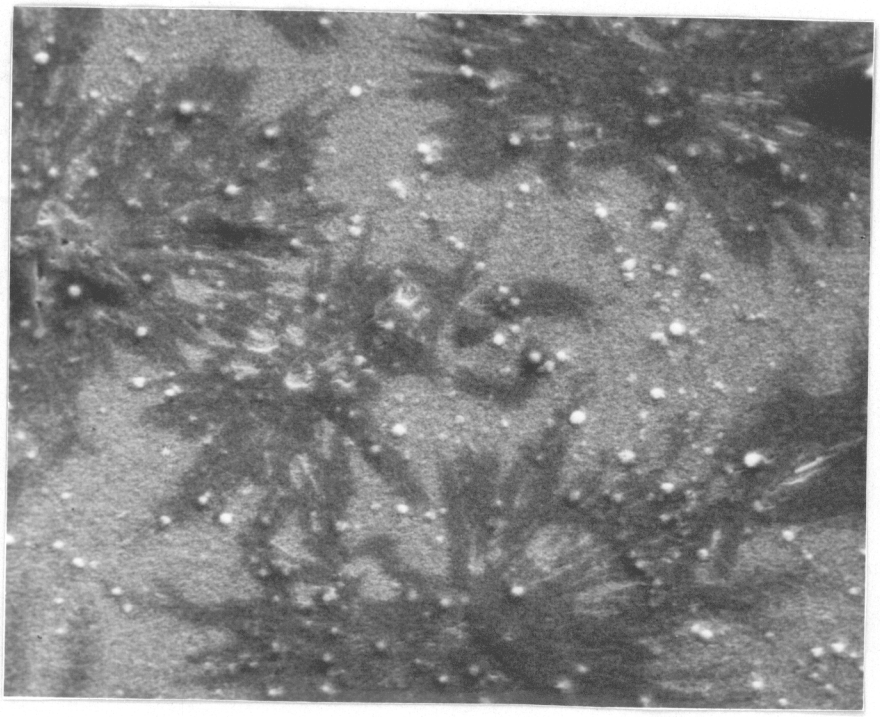

Figure 10. SEM Micrograph of SnO_2 Annealed for 100 hours (2000X).

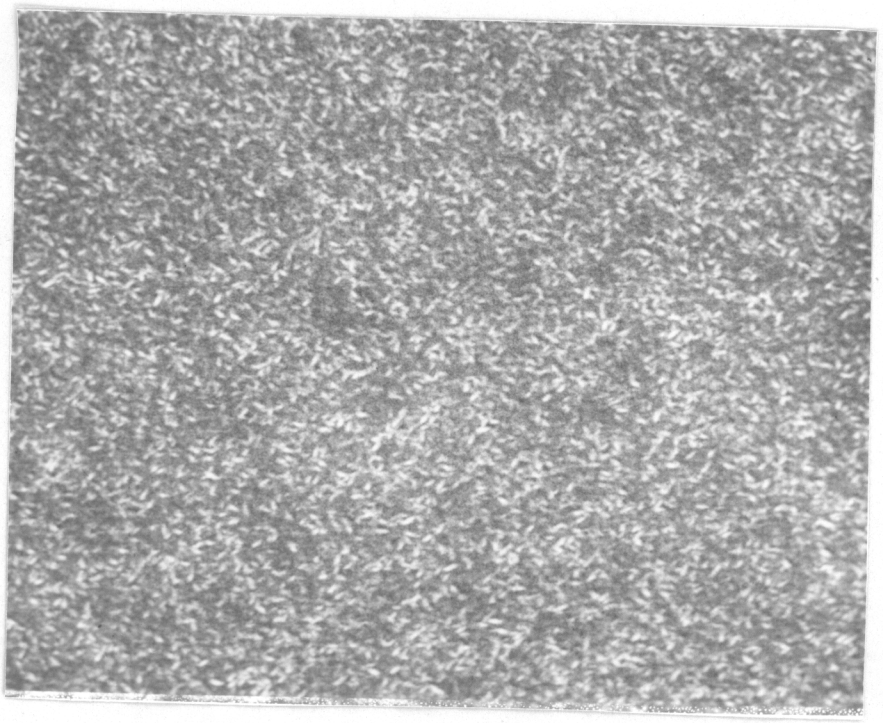

Figure 11. SEM Micrograph of Unannealed CoO_x (5000X).

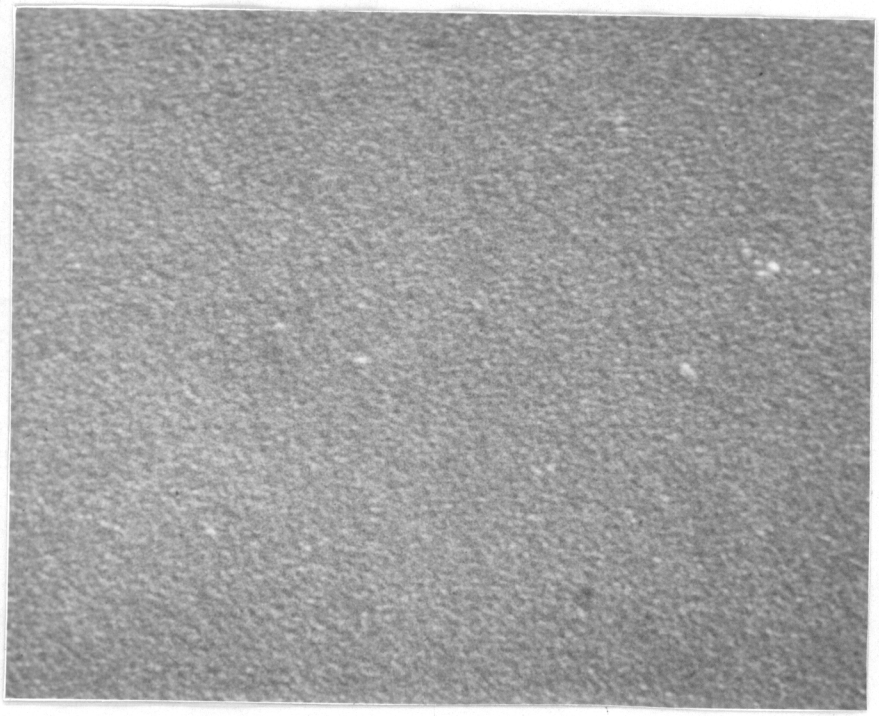

Figure 12. SEM Micrograph of CoO_x Annealed for 1 hour (5000X).

electron images indicated that these patterns did not protude above the surface. No changes in composition were observed with the advent of this effect.

A film of cobalt oxide that had been sputtered for five hours was seen to be made up of a continuous series of sub-micron sized crystallites having an acicular shape (Figure 11). This same film after one hour of annealing had crystals that were slightly smaller and less defined in shape (Figure 12).

A conductive film of cobalt oxide that had been sputtered for only one hour showed no obvious crystal structure.

C. ESCA Results

Electronic spectra of tin oxide films are shown in Figures 13-28. The peaks corresponding to tin and chlorine remained relatively unaffected for all heat treatments of the films. The indium doped sample had a greater $2p_{\frac{1}{2}}$ contribution to the chlorine double peak.

The $1s_{\frac{1}{2}}$ peak from oxygen in the films changed shape with increased anneal time and indium doping. Unannealed tin oxide films exhibited a pronounced double peak (Figure 21). This doublet characteristic diminished after one hour of annealing (Figure 22) and was absent in films of higher anneal times (Figures 23,24). Doping with indium (Figure 29) also eliminated the double peak leaving a single peak.

Table VI lists the peak to background ratios for the elements studied. The ratio steadily decreased with increased annealing for the tin peak. For the oxygen and chlorine peaks it increased after

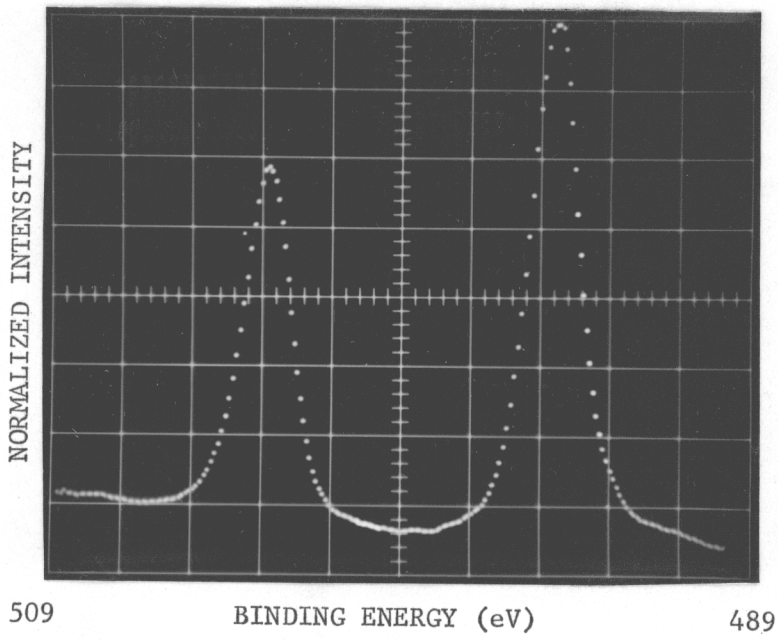

Figure 13. Electronic Spectrum of Tin ($3d_{3/2}$, $3d_{5/2}$). Unannealed SnO_2 Sample.

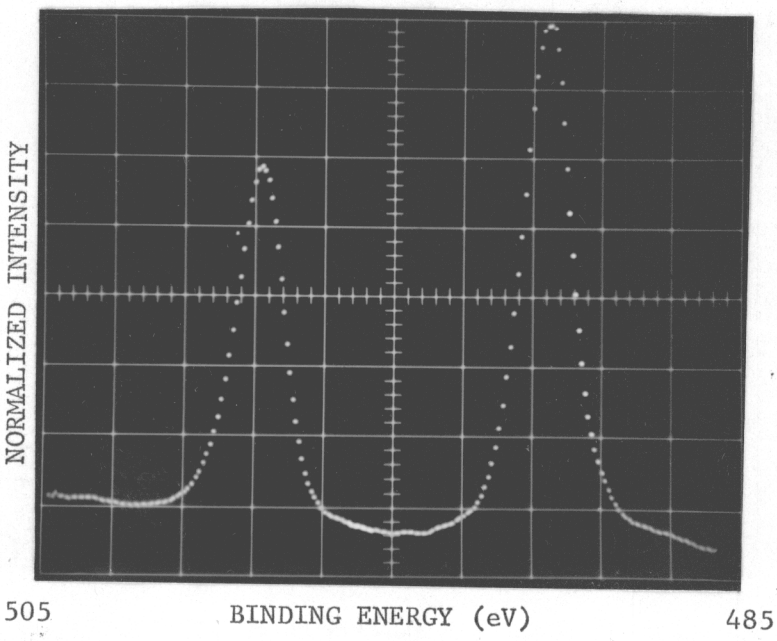

Figure 14. Electronic Spectrum of Tin ($3d_{3/2}$, $3d_{5/2}$). SnO_2 Sample.

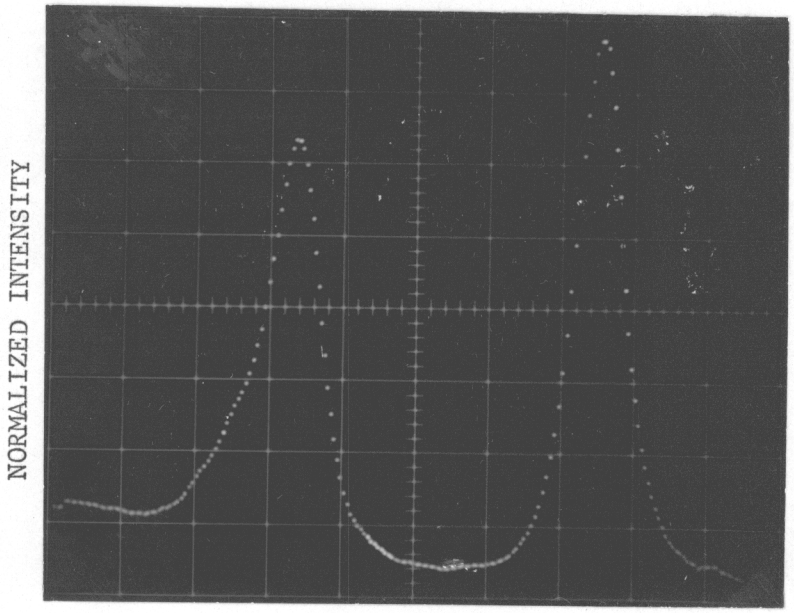

Figure 15. Electronic Spectrum of Tin ($3d_{3/2}$, $3d_{5/2}$). SnO_2 Sample Annealed for 50 hours.

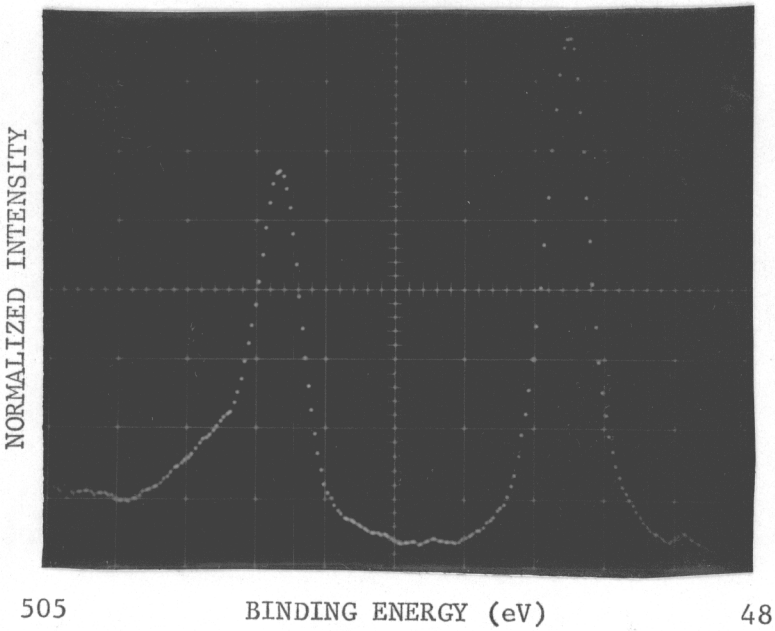

Figure 16. Electronic Spectrum of Tin ($3d_{3/2}$, $3d_{5/2}$). SnO_2 Sample Annealed for 1 hour.

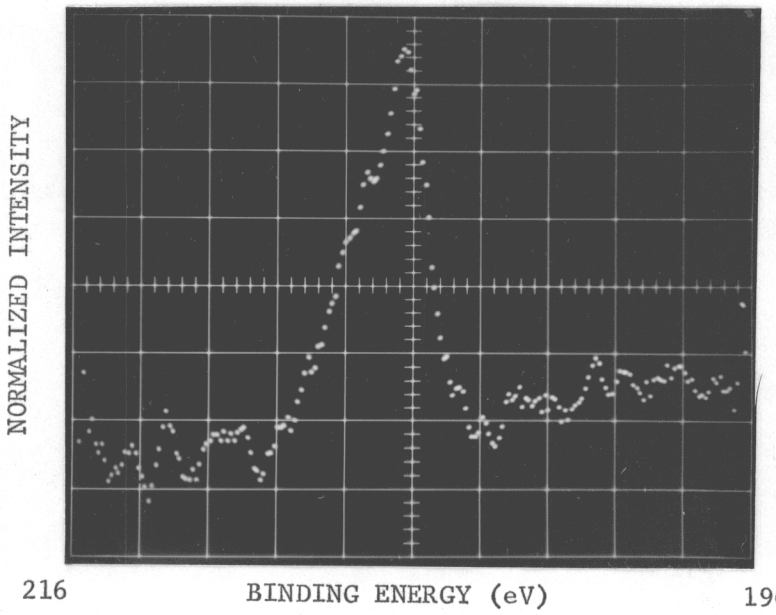

Figure 17. Electronic Spectrum of Chlorine ($2p_{1/2}$, $2p_{3/2}$). Unannealed SnO_2 Sample.

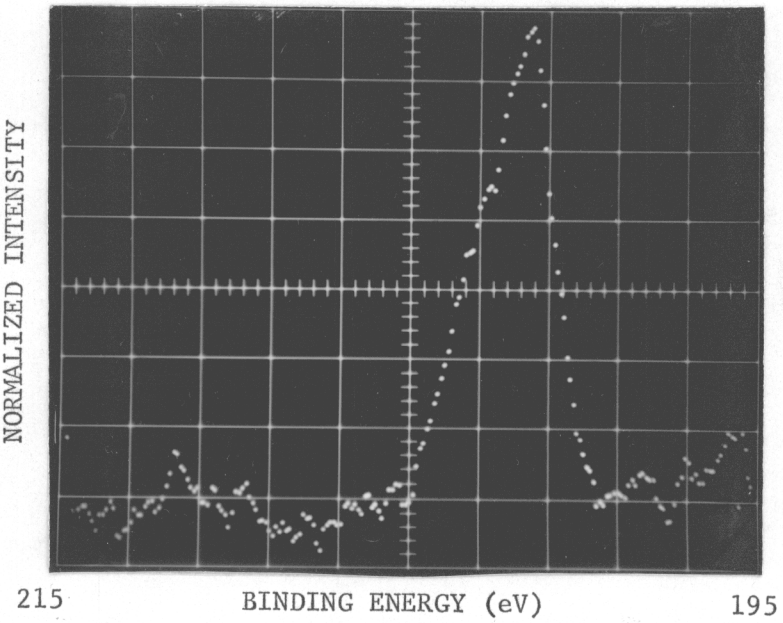

Figure 18. Electronic Spectrum of Chlorine ($2p_{1/2}$, $2p_{3/2}$). SnO_2 Sample Annealed for 1 hour.

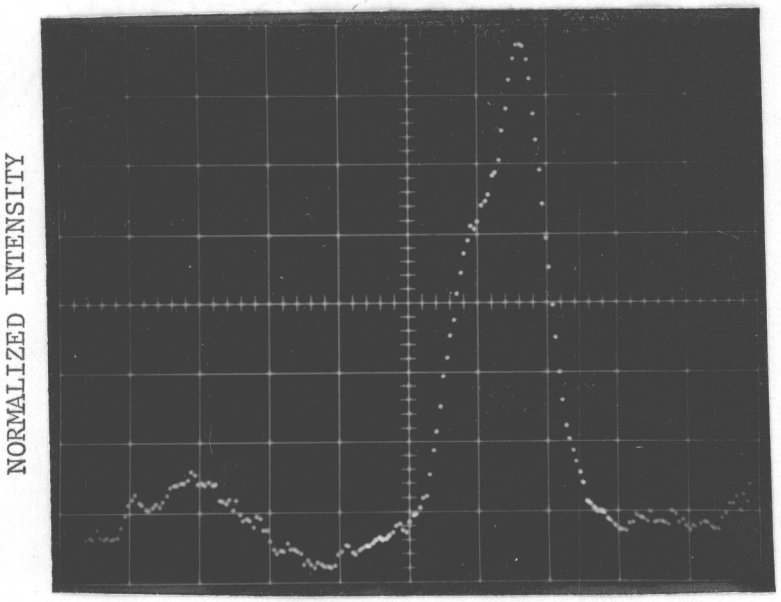

Figure 19. Electronic Spectrum of Chlorine ($2p_{1/2}$, $2p_{3/2}$). SnO_2 Sample Annealed for 50 hours.

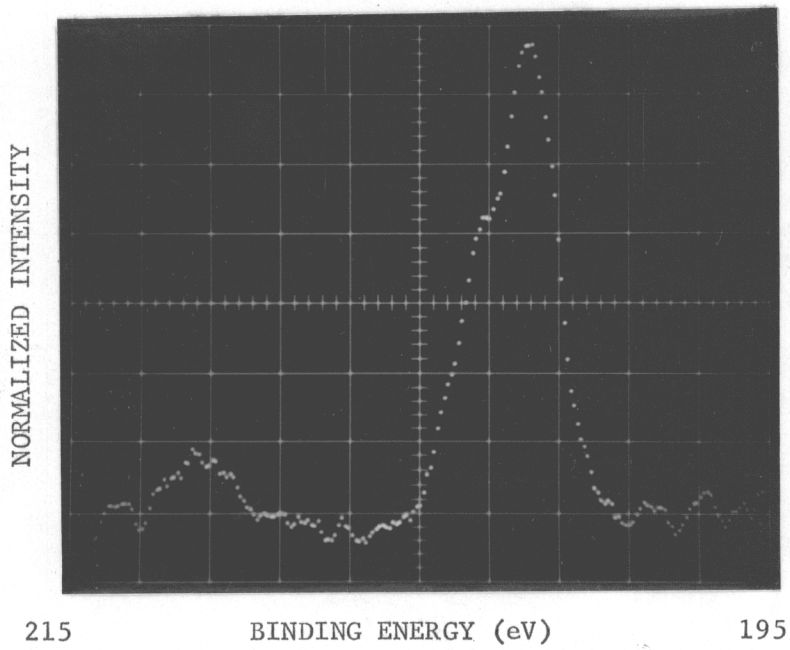

Figure 20. Electronic Spectrum of Chlorine ($2p_{1/2}$, $2p_{3/2}$). SnO_2 Sample Annealed for 100 hours.

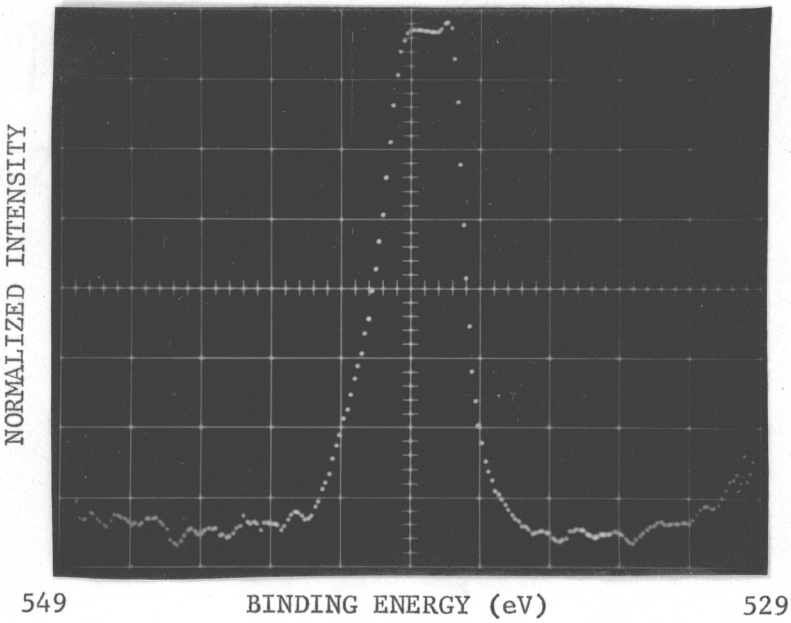

Figure 21. Electronic Spectrum of Oxygen ($1s_{1/2}$). Unannealed SnO_2 Sample.

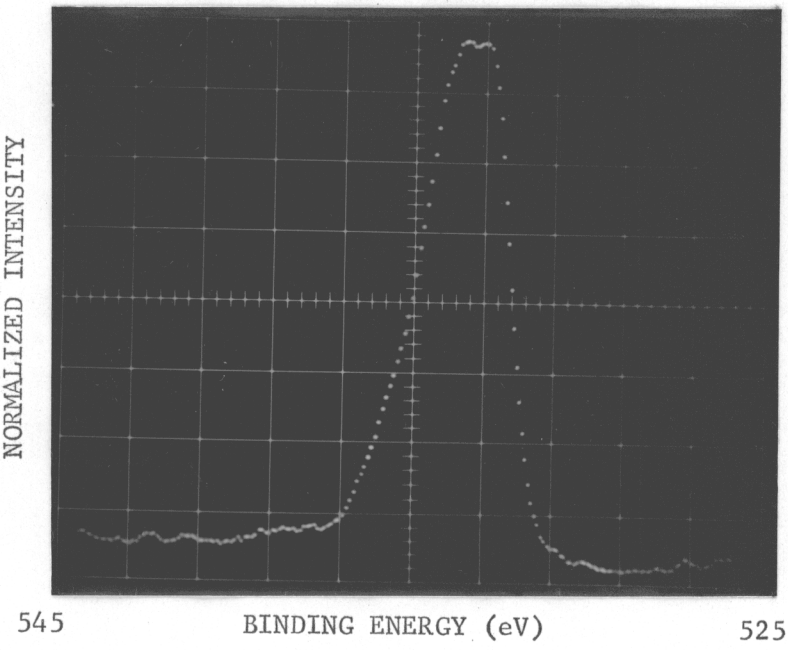

Figure 22. Electronic Spectrum of Oxygen ($1s_{1/2}$). SnO_2 Sample Annealed for 1 hour.

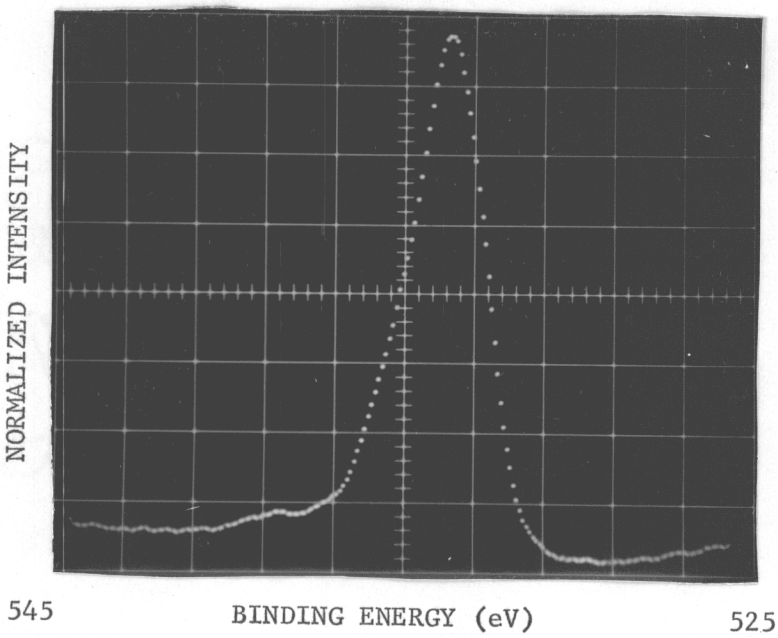

Figure 23. Electronic Spectrum of Oxygen ($1s_{1/2}$) SnO_2 Sample Annealed for 50 hours.

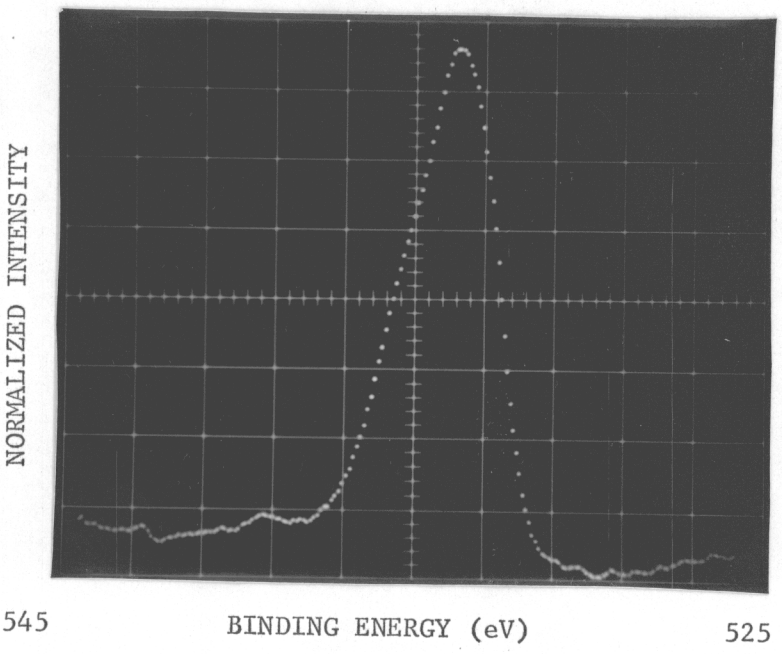

Figure 24. Electronic Spectrum of Oxygen ($1s_{1/2}$) SnO_2 Sample Annealed for 100 hours.

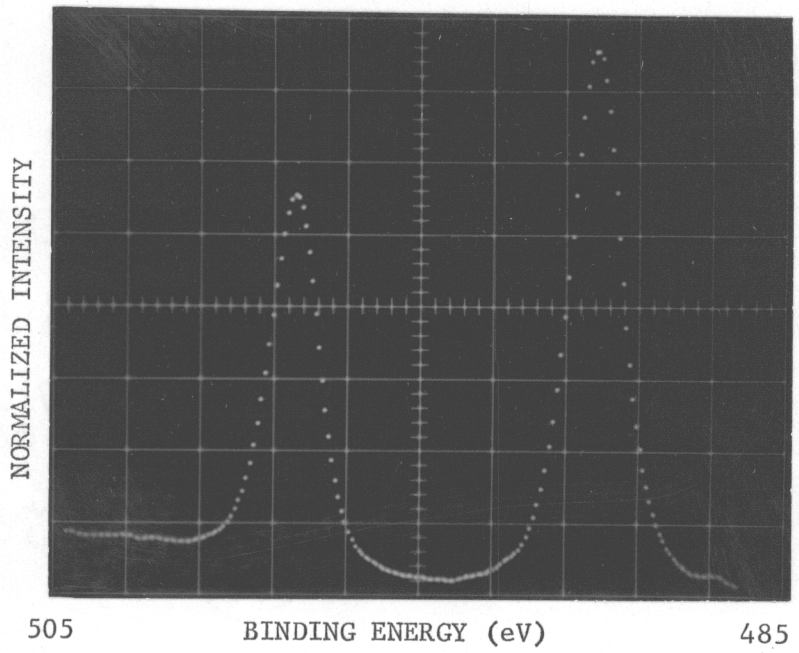

Figure 25. Electronic Spectrum of Tin ($3d_{3/2}$, $3d_{5/2}$) Unannealed SnO_2 with 3m/o In.

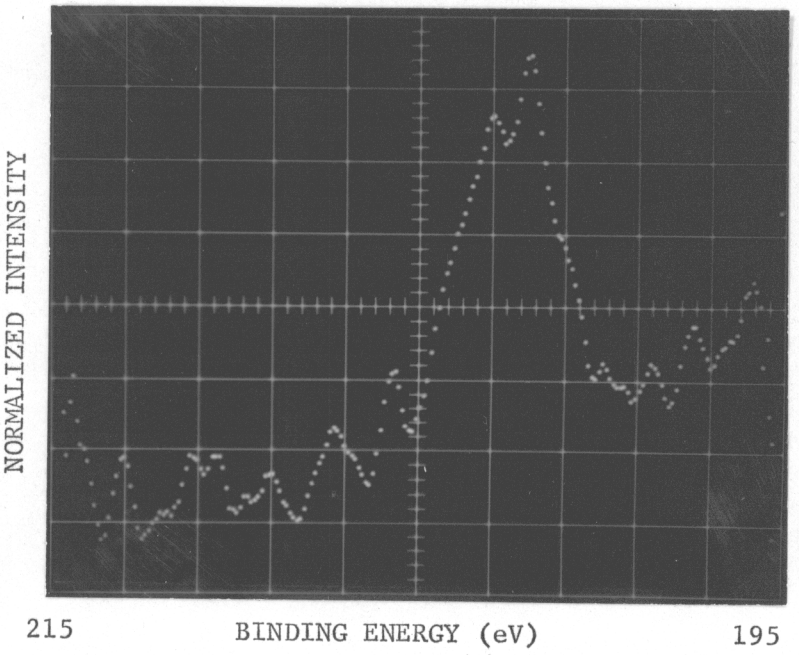

Figure 26. Electronic Spectrum of Chlorine ($2p_{1/2}$, $2p_{3/2}$) Unannealed SnO_2 with 3m/o In.

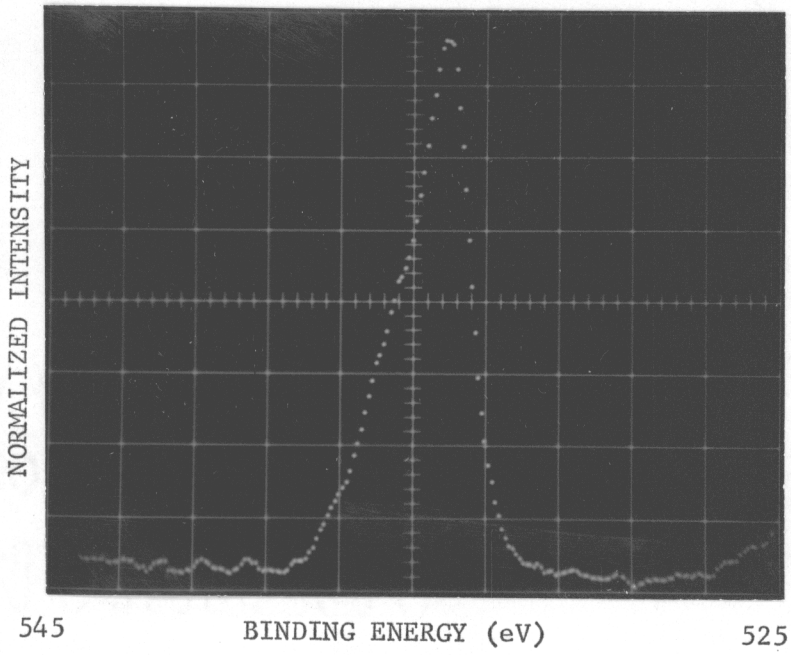

Figure 27. Electronic Spectrum of Oxygen ($1s_{1/2}$) Unannealed SnO_2 with 3m/o In.

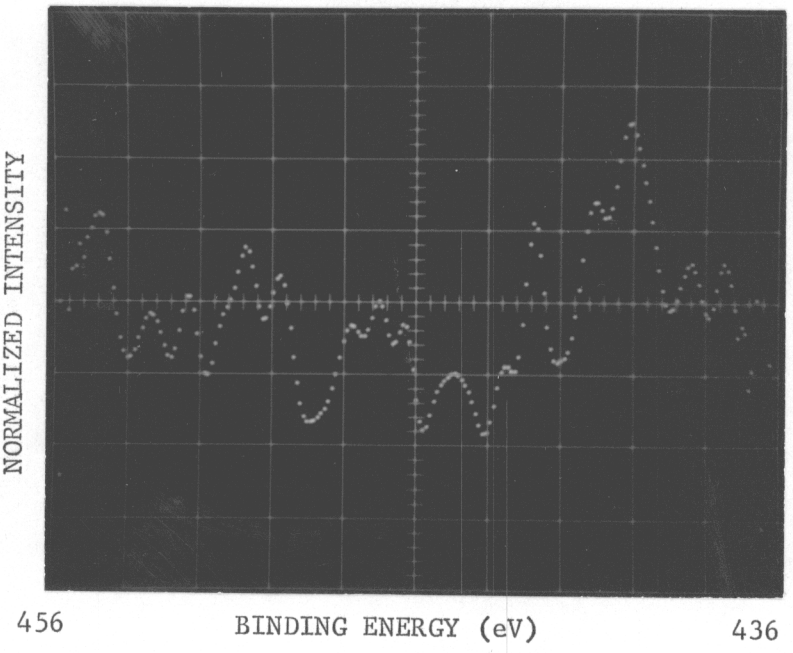

Figure 28. Electronic Spectrum of Indium ($3d_{3/2}$, $3d_{5/2}$) Unannealed SnO_2 with 3m/o In.

TABLE VI

Peak to Background Ratios for Electronic Spectra of Thin Film SnO_2

Sample	Sn	O	Cl	No. Scans
Spray No. 31 0 Hr. Anneal	15.89	0.62	0.28	10
Spray No. 31 1 Hr. Anneal	8.54	2.321	0.43	11
Spray No. 31 50 Hr. Anneal	5.34	2.37	0.41	43
Spray No. 31 100 Hr. Anneal	3.91	1.76	0.43	32
Spray No. 29 0 Hr. Anneal 3 m/o In	12.16	1.46	0.21	12

one hour of annealing and remained relatively unchanged from then on. Doping with indium had little effect on the ratios for tin and chlorine, but it doubled that of oxygen.

Binding energies for the unannealed sample are shifted approximately 4.5 eV above those for the other samples. This inconsistency was due to an increased work function of film electrons due to positive charging of the sample.

D. Electrical Results

Resistivity for both tin oxide and cobalt oxide samples is listed in Table VII along with approximate thickness, activation energy, and keys to the location of corresponding logarithmic resistivity versus reciprocal temperature curves (Figures 29,30,35) and optical property figures. The effect of doping tin oxide films with antimony and indium on film resistivity is shown in Figures 31 and 32.

The effect of varying annealing time is shown in Figures 33 and 34. Figure 33 shows resistivity versus time with dotted lines indicating a region for which only one measurement was made per data point. Figure 34 shows temperature dependence of resistivity for samples having undergone 0, 1, and 10 hours of heat treatment. Further heat treatment destroyed the gold contacts making measurements impossible on the films heat treated for 50 and 100 hours.

This data showed that both resistivity and activation energy were increased with anneal time and addition of indium. Addition of 1 m/o antimony decreased resistivity and activation energy slightly.

TABLE VII

Comprehensive Table of Data

	Spray No.	Film Thickness (Å)	Room Temp. ρ (ohm-cm)	ρ vs. T^{-1} (Fig.)	E_a (eV)	Low Temp. E_a (eV)	Opt. Props. (Fig.)
Undoped SnO_2	13	6,600	0.71×10^{-2}	29	2.0×10^{-2}	0	
	14	9,000	1.10×10^{-2}	29	4.4×10^{-2}	0	
	16	9,000	0.87×10^{-2}	29	1.3×10^{-2}	0	
	20	4,500	1.61×10^{-2}	29	4.6×10^{-2}	0	
	21	12,500	1.41×10^{-2}	29	10.7×10^{-2}	1.6×10^{-2}	
	28	15,000	2.49×10^{-2}				37
	31	9,600	2.37×10^{-2}				38
	32	6,900	1.47×10^{-2}				
Sn w Sb							
1 m/o	18	9,000	1.75×10^{-2}				
	21	15,000	0.80×10^{-2}	29	3.2×10^{-2}	1.0×10^{-3}	39
3 m/o	18	15,000	2.13×10^{-2}	29	0	0	
	21	14,000	1.94×10^{-2}		0	0	40
6 m/o	19	6,800	7.10×10^{-2}	29	7.5×10^{-2}	1.6×10^{-2}	
	22	7,800	1.05×10^{-1}	29	7.9×10^{-2}	2.0×10^{-2}	41
10 m/o	19	4,000	5.35	29	6.0×10^{-2}	2.3×10^{-2}	
	22	5,700	1.43×10^{1}	29	1.1×10^{-1}	8.2×10^{-2}	42
20 m/o	19	4,500	1.99×10^{3}				
	20	5,000	4.99×10^{3}				
	22	5,400	Beyond Measure				43
Sn w In							
1 m/o	17	7,000	7.7×10^{-2}	30	2.0×10^{-2}	4.0×10^{-3}	
	29	12,400	2.0				44
3 m/o	23	6,900	4.01	30	1.5×10^{-1}	4.3×10^{-2}	
	29	11,900	5.45				45
6 m/o	17	6,700	4.10	30	1.1×10^{-1}	3.1×10^{-2}	46
	23	8,600	4.70				
	29	9,200	2.10				
10 m/o	17	5,000	1.76	30	1.5×10^{-1}	2.0×10^{-2}	
	23	9,600	2.84	30	2.8×10^{-1}	5.9×10^{-2}	47
20 m/o	17	4,000	1.65	30	1.7×10^{-1}	3.0×10^{-2}	48

TABLE VII (Cont.)

	Sputter No.	Film Thickness (Å)	Room Temp. ρ (ohm-cm)	ρ vs. T^{-1} (Fig.)	E_a (eV)	Low Temp. E_a (eV)	Opt. Props. (Fig.)
CoO_x							
5 m/o Li	1	1,300	8.2	35	1.8×10^{-1}	8.0×10^{-2}	49
Undoped	2	1,500	208.0	35	8.3×10^{-1}	2.9×10^{-1}	50
5 m/o Li	3	15,000	147.0				51 & 52
5 m/o Li	4	2,600	0.2				53
5 m/o Li	5	3,900	0.1				
5 m/o Li	6	4,400	403.0				
5 m/o Li	7	4,400	265.0				
5 m/o Li	14(.24 KW)	4,100	0.05				
5 m/o Li	14(.34 KW)	6,300	0.39				
5 m/o Li	14(.44 KW)	4,100	0.71				
5 m/o Li	14(.44 KW)	4,500	1.0×10^{5}				
5 m/o Li	15(.44 KW) (Annealed)	4,500	3.3×10^{1}				

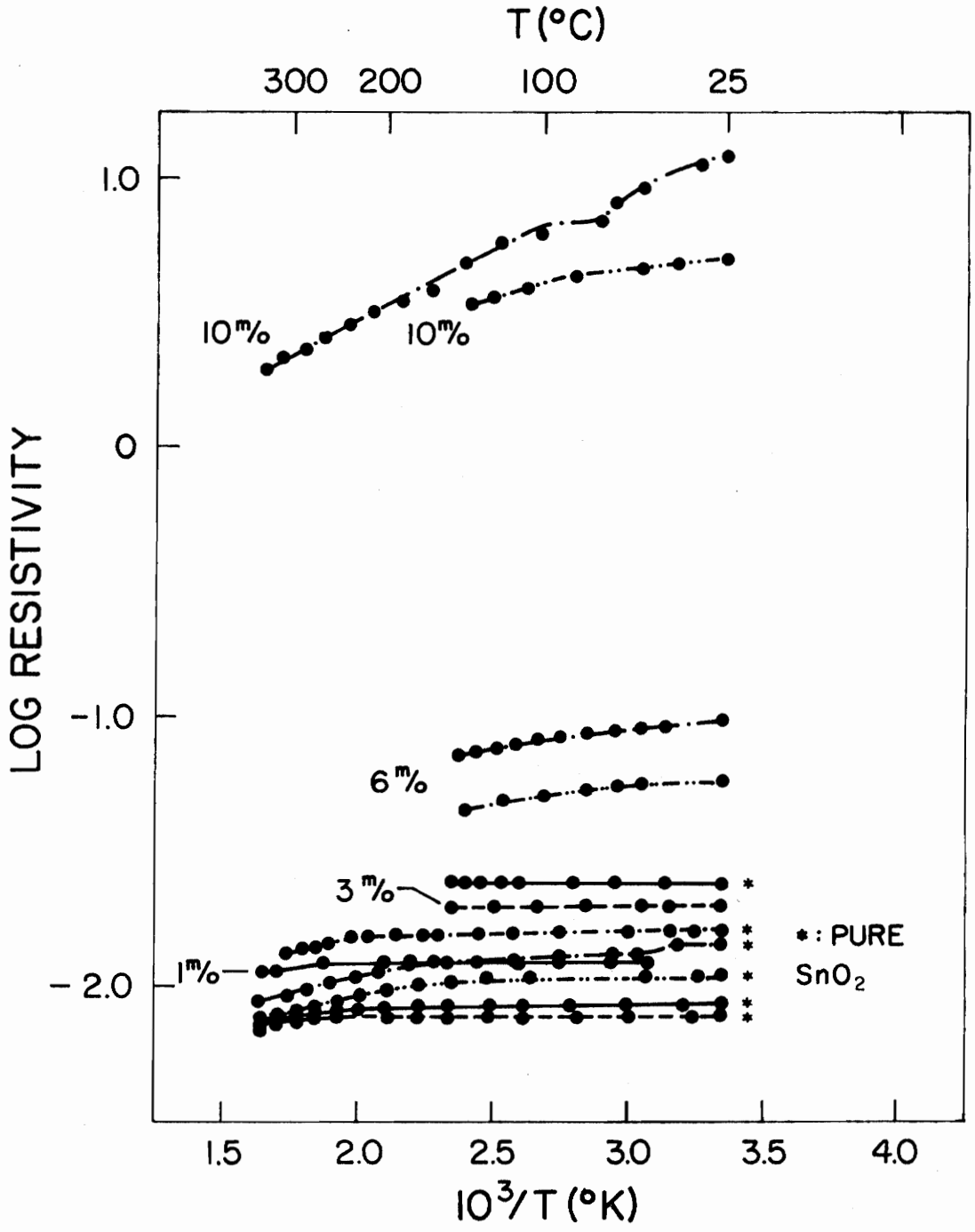

Figure 29. Temperature Dependence of Resistivity for Antimony Doped SnO_2 Films.

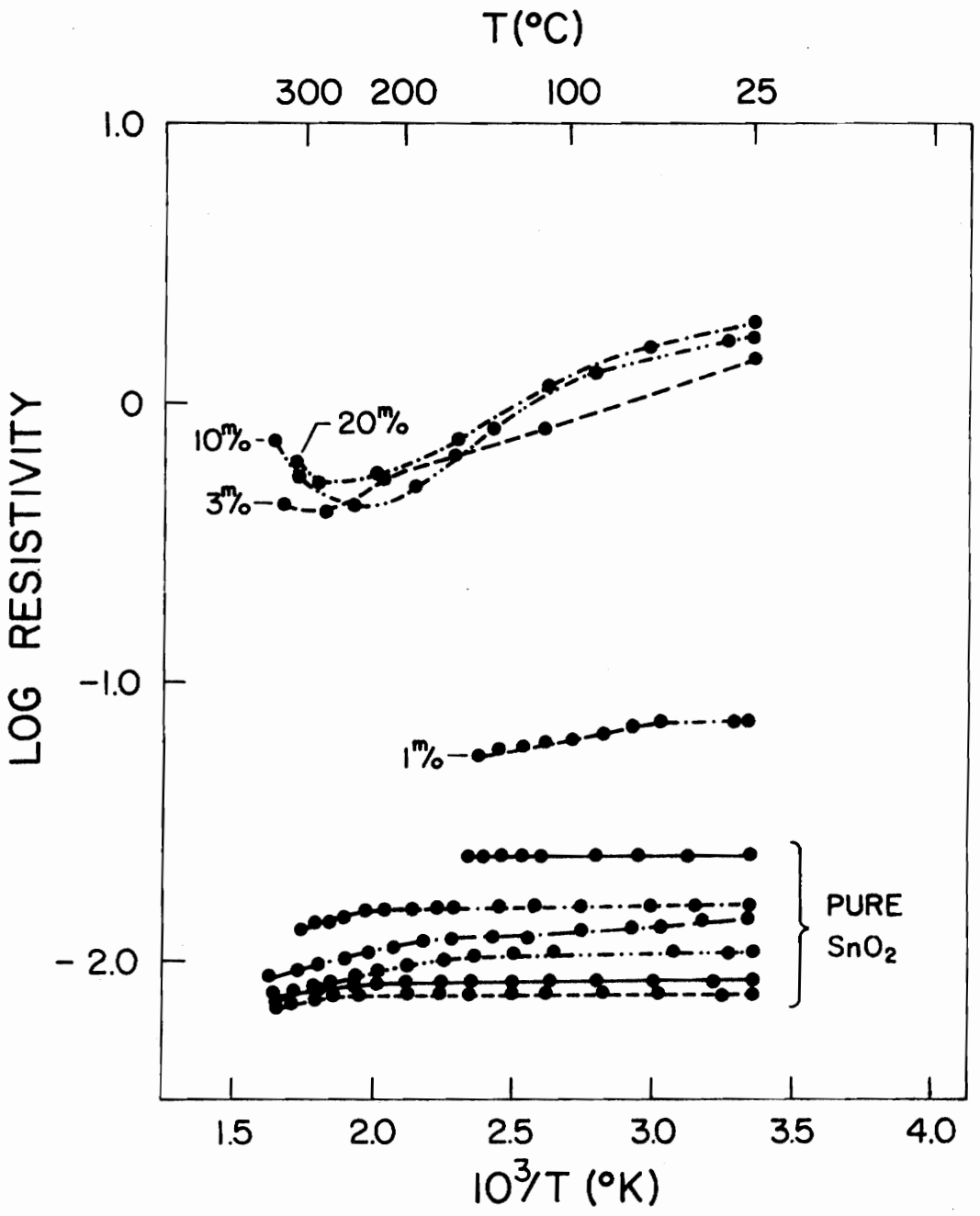

Figure 30. Temperature Dependence of Resistivity for Indium Doped SnO_2 Films.

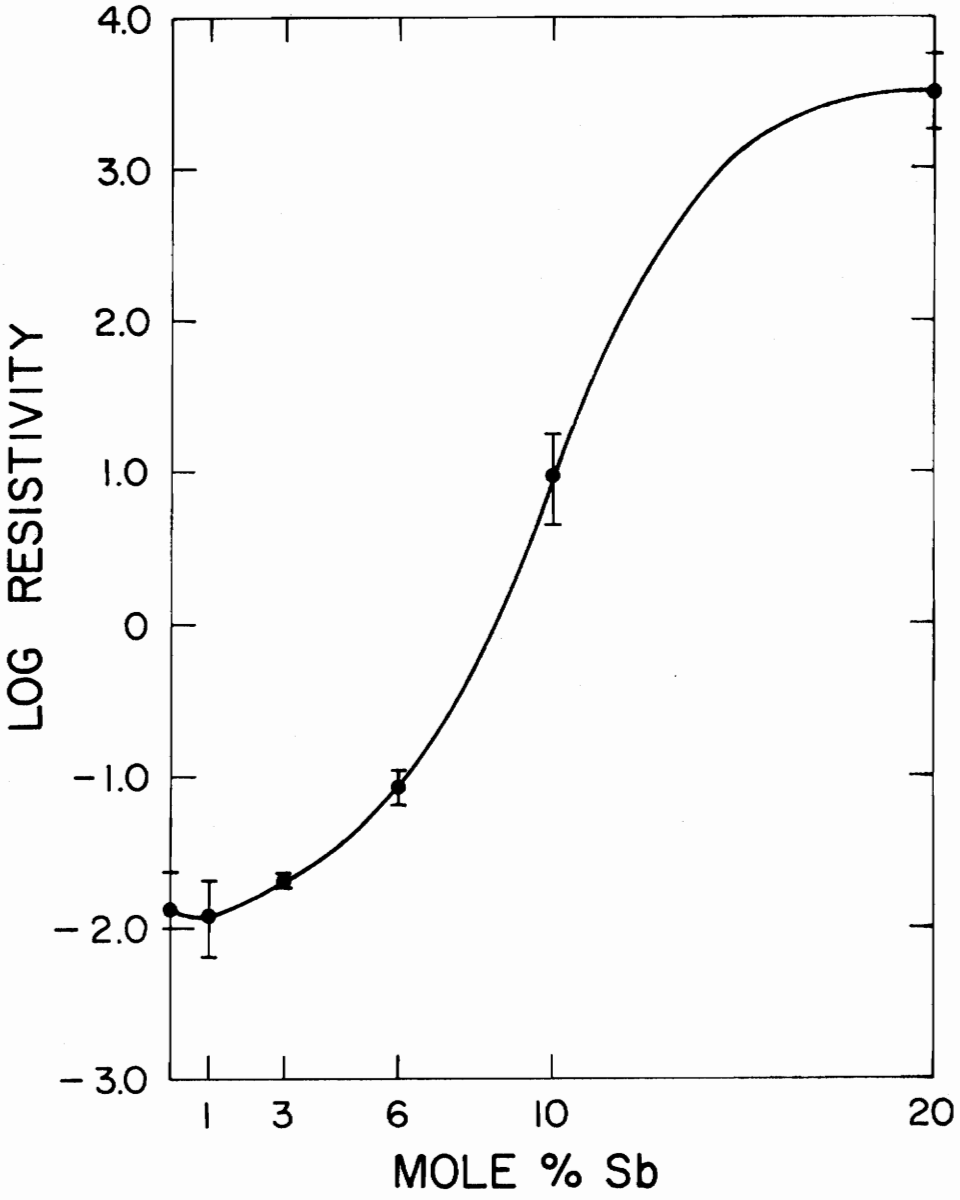

Figure 31. Resistivity of Antimony Doped SnO_2 Films.

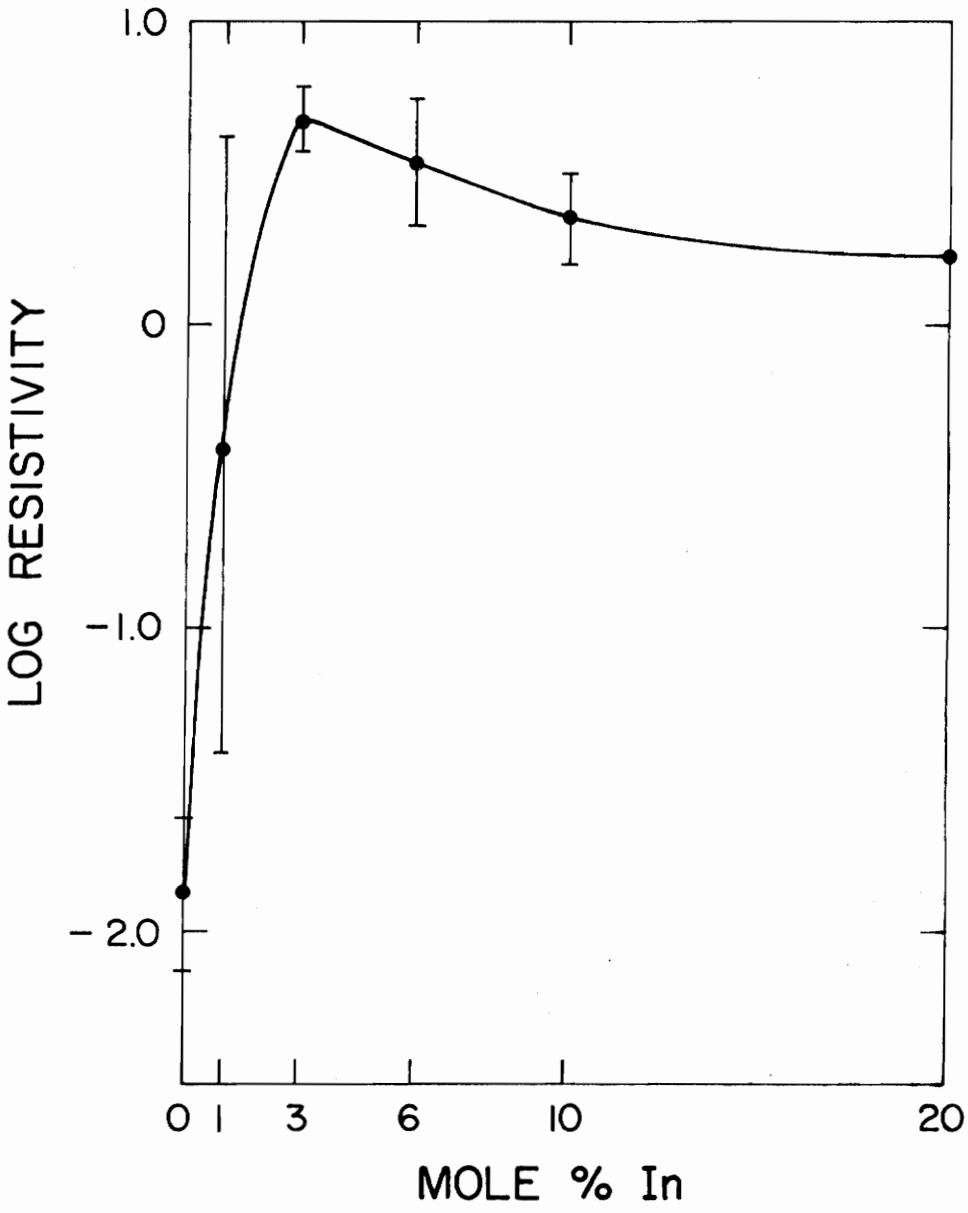

Figure 32. Resistivity of Indium Doped SnO_2 Films.

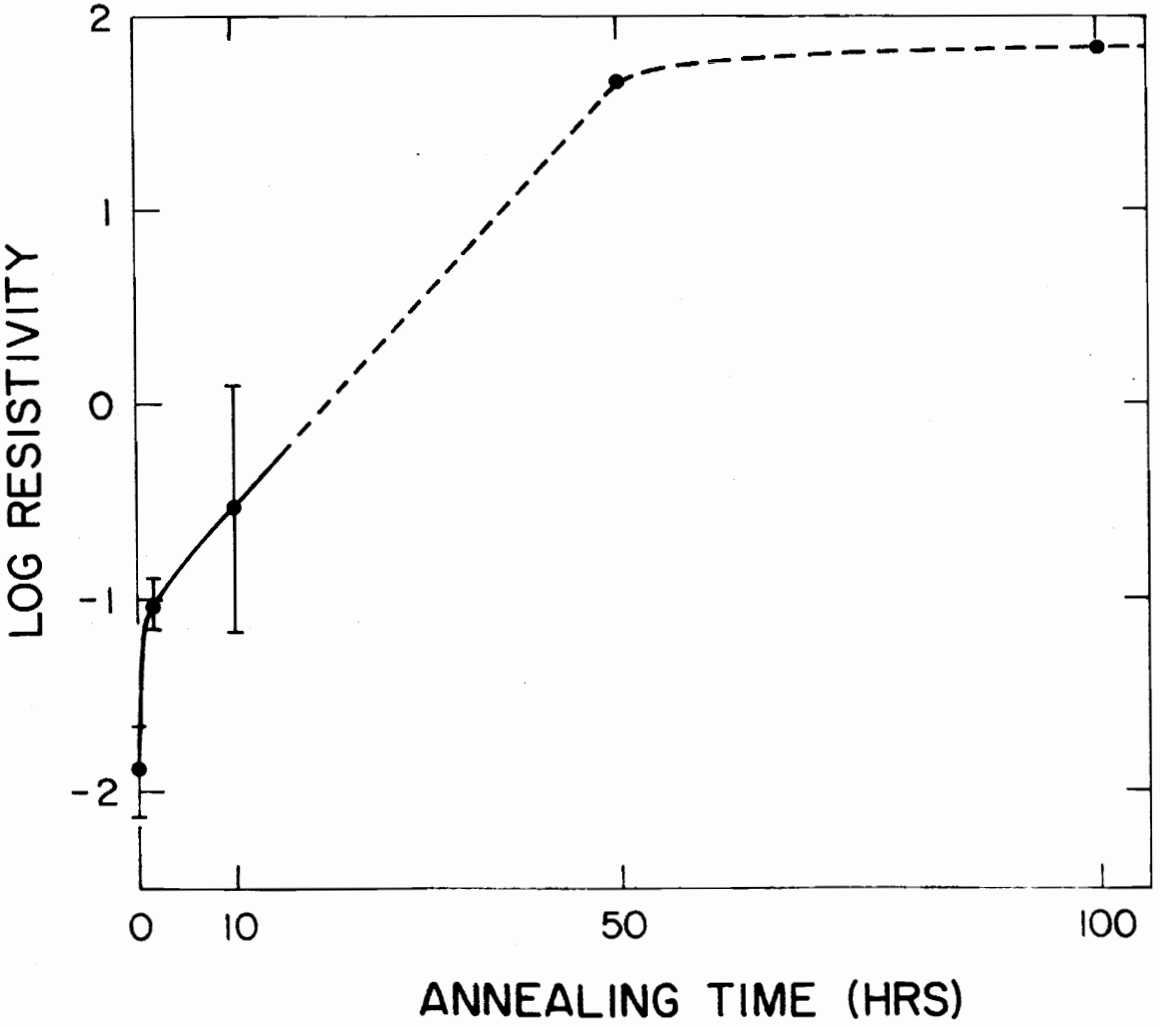

Figure 33. Resistivity of Annealed SnO_2 Films.

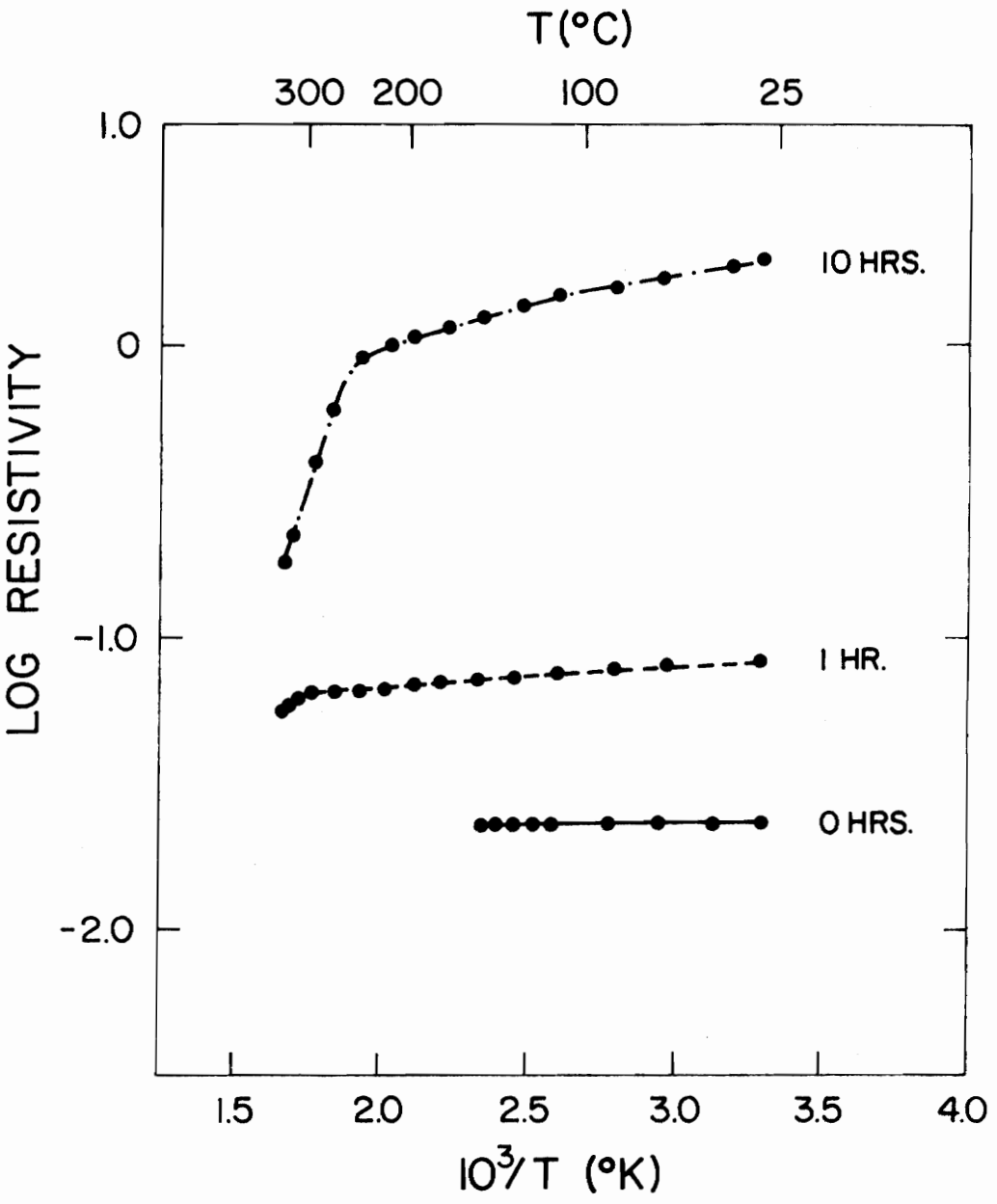

Figure 34. Temperature Dependence of Resistivity for Annealed SnO_2 Films.

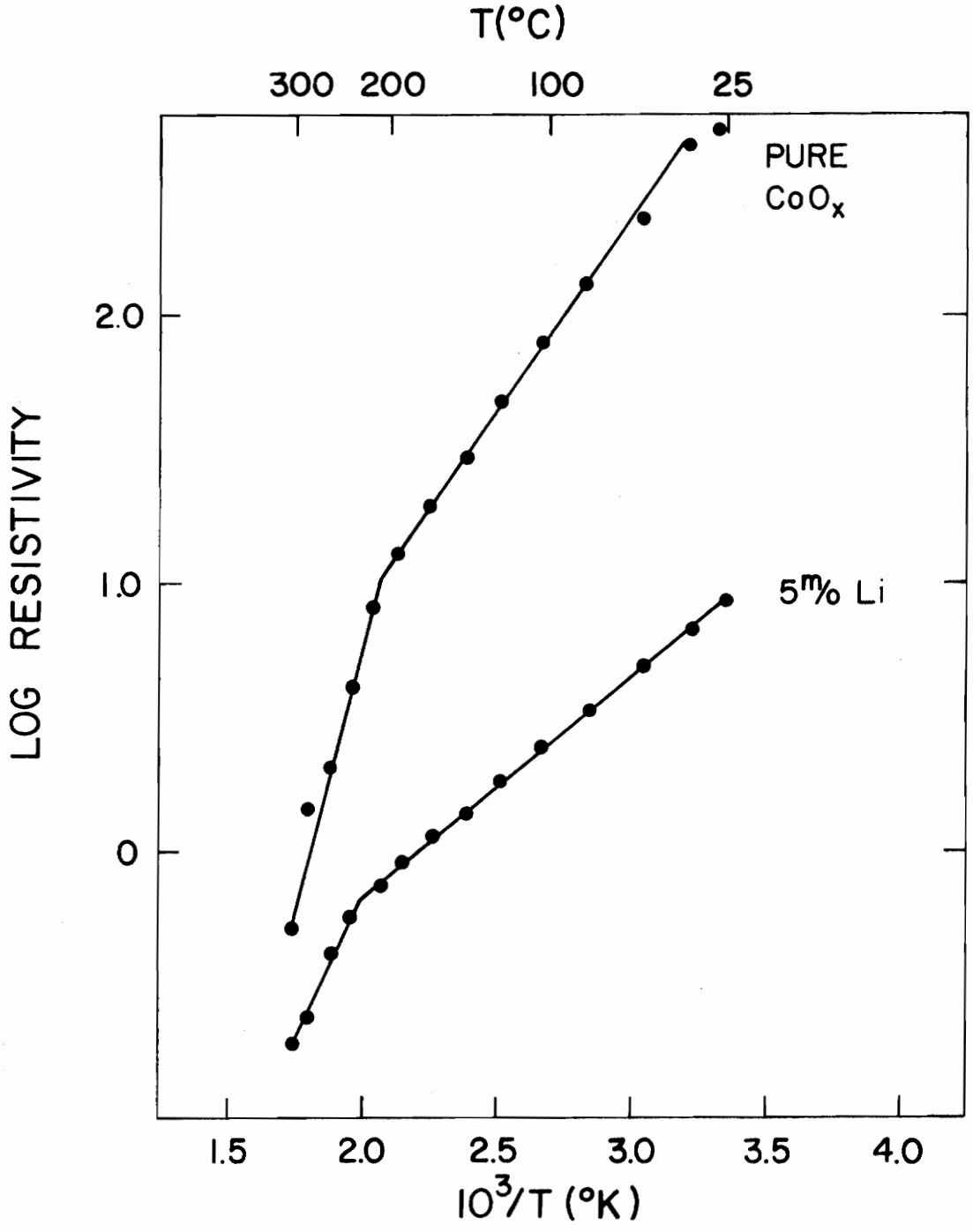

Figure 35. Temperature Dependence of Resistivity for Pure and Lithium Doped CoO_x films.

Additions of 3 m/o antimony caused little change, and additions of greater than 6 m/o increased these properties.

Hot probe tests indicated that all tin oxide films were n-type and all cobalt oxide films were p-type.

Figure 36 shows the current-voltage characteristic of a cobalt oxide film sputtered onto a tin oxide film.

E. Optical Results

Figures listed in Table VII according to film composition show changes in reflection, absorption, and transmission (in percent) as wavelength is varied from 0.3 microns to 2.5 microns. Reflection is plotted from the top of the graph, transmission is plotted from the bottom, and absorption is the remaining portion of total incident energy.

All films tended to absorb light more so than reflect it. Films of tin oxide absorbed more at 2.5 microns than at visible wavelengths while cobalt oxide films showed greater absorption in the visible part of the spectrum. Undoped and indium doped tin oxide films were transparent. Antimony doped tin oxide films had a blue coloration. Additions of 6 m/o antimony or less increased absorption at 2 microns from a value of 45% for undoped films to 90% at 1 m/o antimony, 95% at 3 m/o, and 60% at 6 m/o (Figures 39-41). Addition of 10 m/o or 20 m/o antimony decreased absorption at 2 microns to 15% (Figures 42,43). All additions of indium decreased absorption to a range from 15% to 10% (Figures 44-48). Films with 1 m/o antimony showed maximum infrared reflection of 15%.

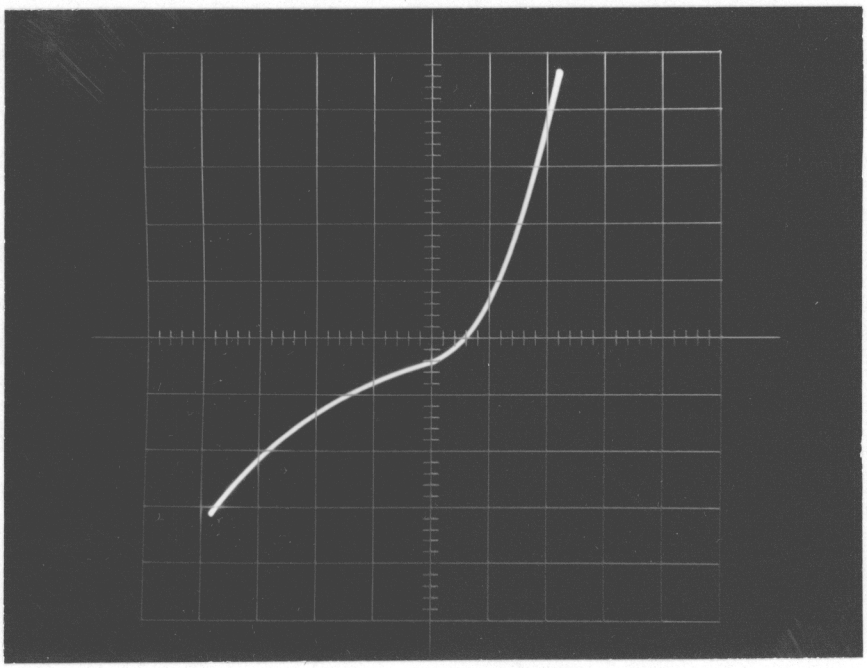

Figure 36. Rectification Through Heterojunction of CoO_x Thin Film on SnO_{2-x} Thin Film.
Vertical Scale: 1.0 ma/Div.
Horizontal Scale: 0.5 V/Div.

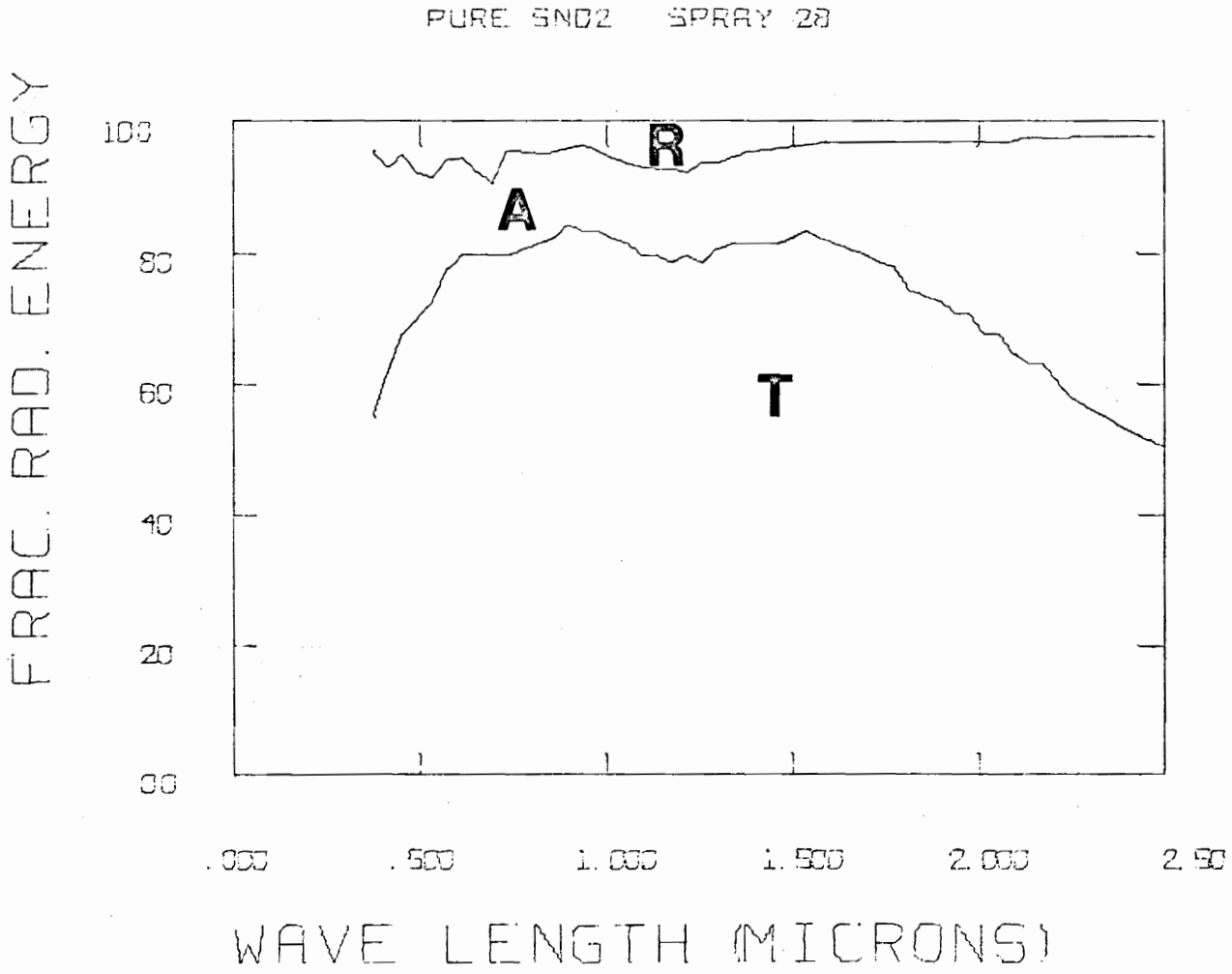

Figure 37. Change in Reflection (R), Absorption (A), and Transmission (T) of Light with Wavelength for Thin Film of SnO_2 - Spray 28.

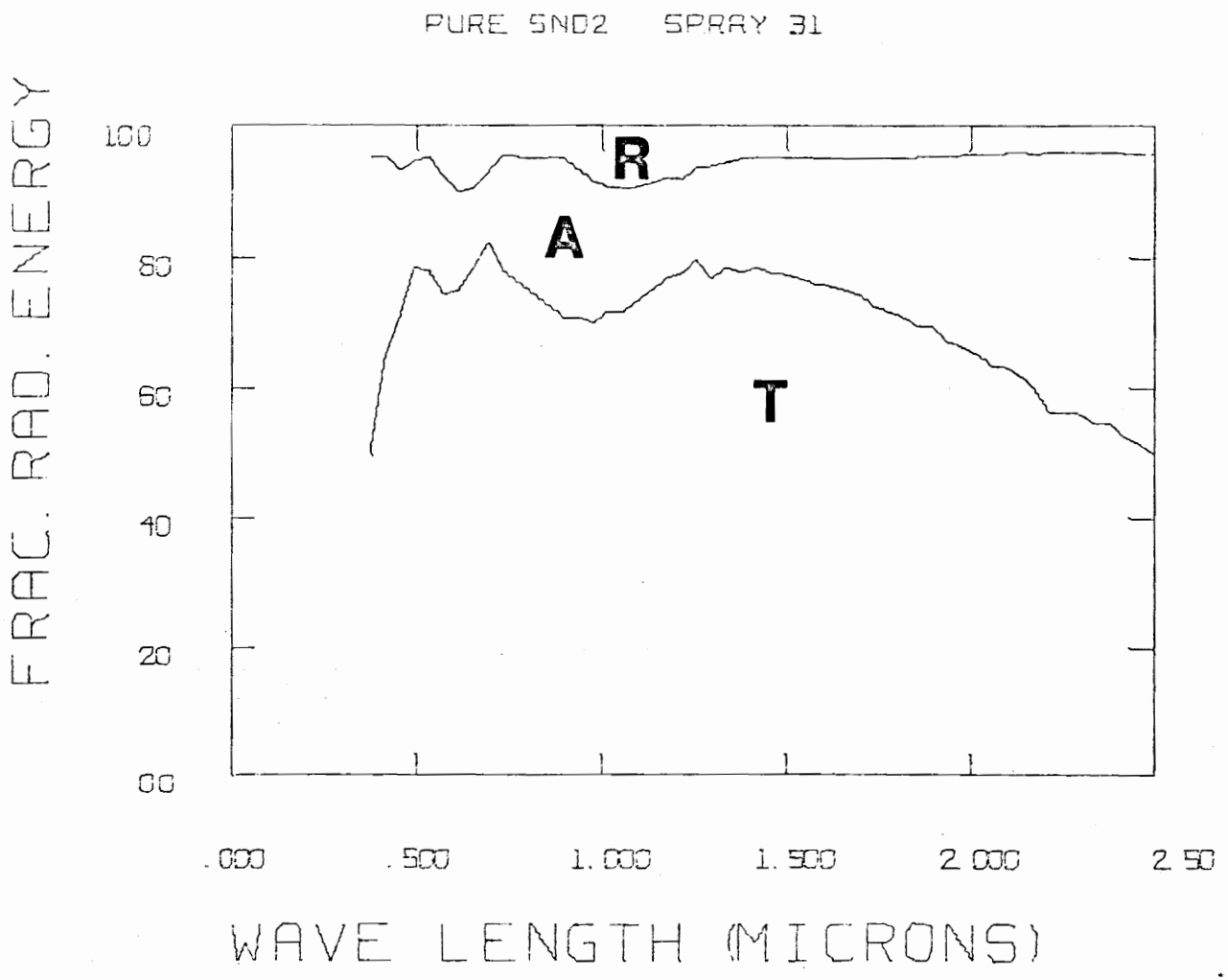

Figure 38. Change in Reflection (R), Absorption (A), and Transmission (T) of Light with Wavelength for Thin Film of SnO_2 - Spray 31

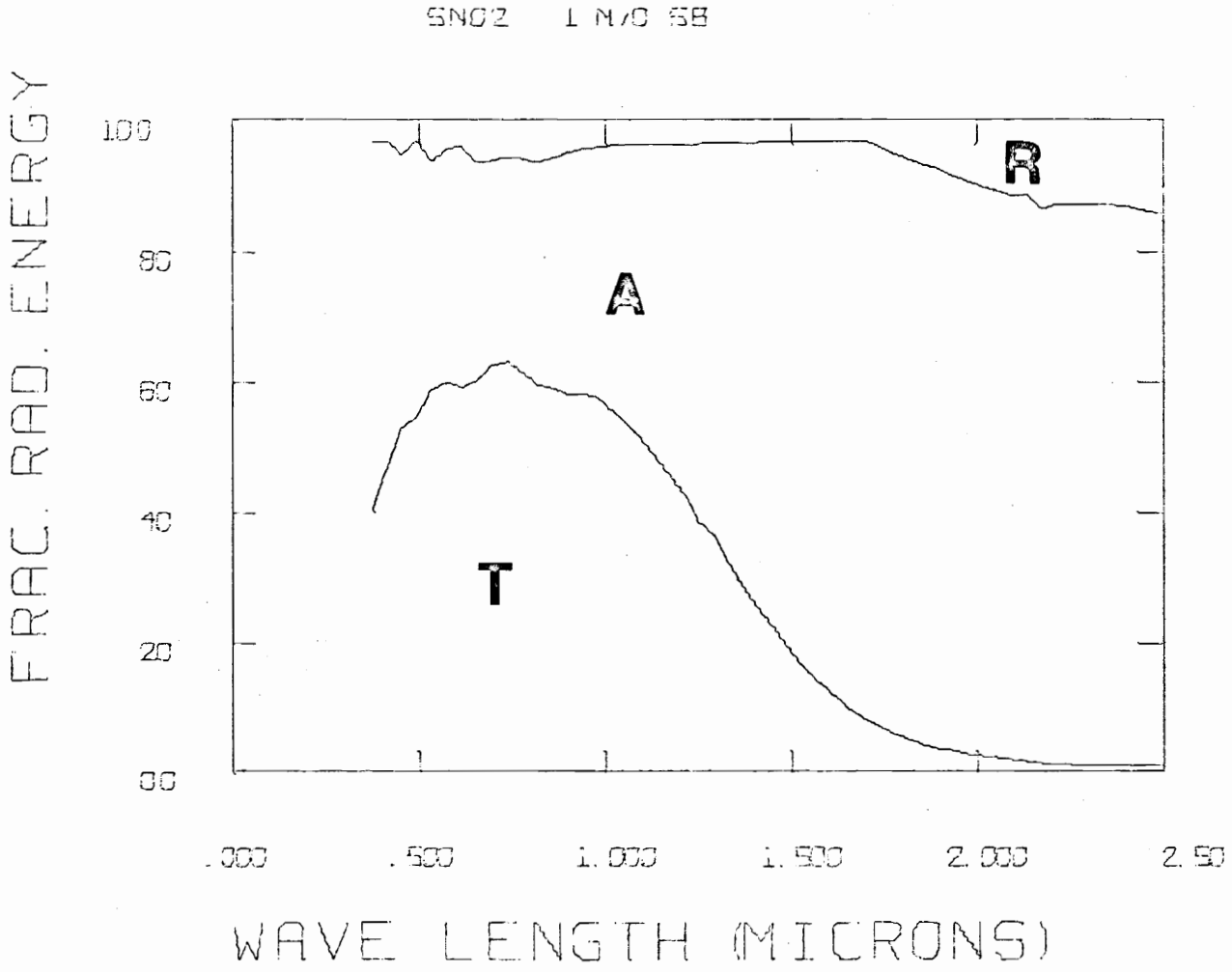

Figure 39. Change in Reflection (R), Absorption (A), and Transmission (T) of Light with Wavelength for Thin Film of SnO_2 with 1 m/o Sb - Spray 21.

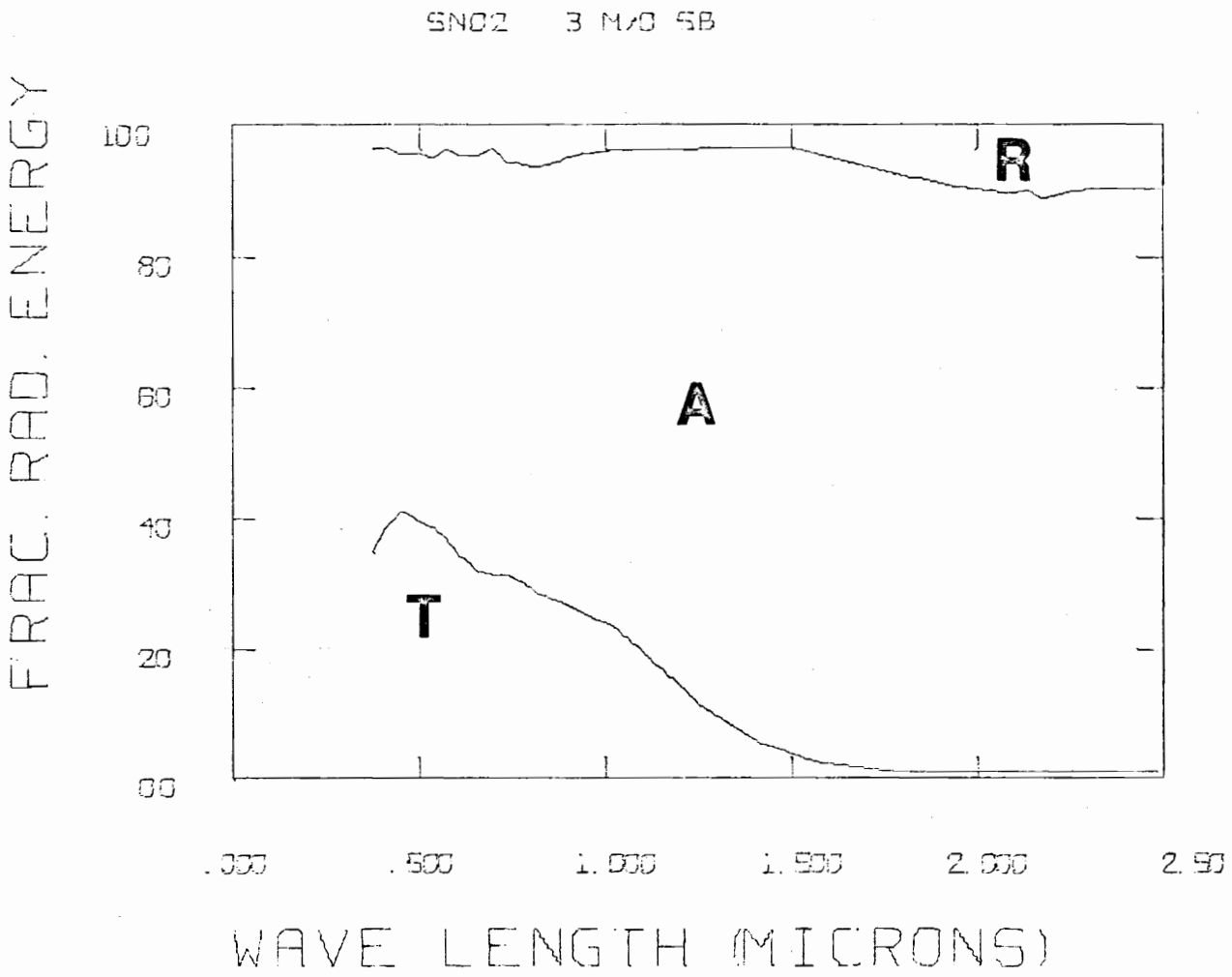

Figure 40. Change in Reflection (R), Absorption (A), and Transmission (T) of Light with Wavelength for Thin Film of SnO_2 with 3 m/o Sb - Spray 21.

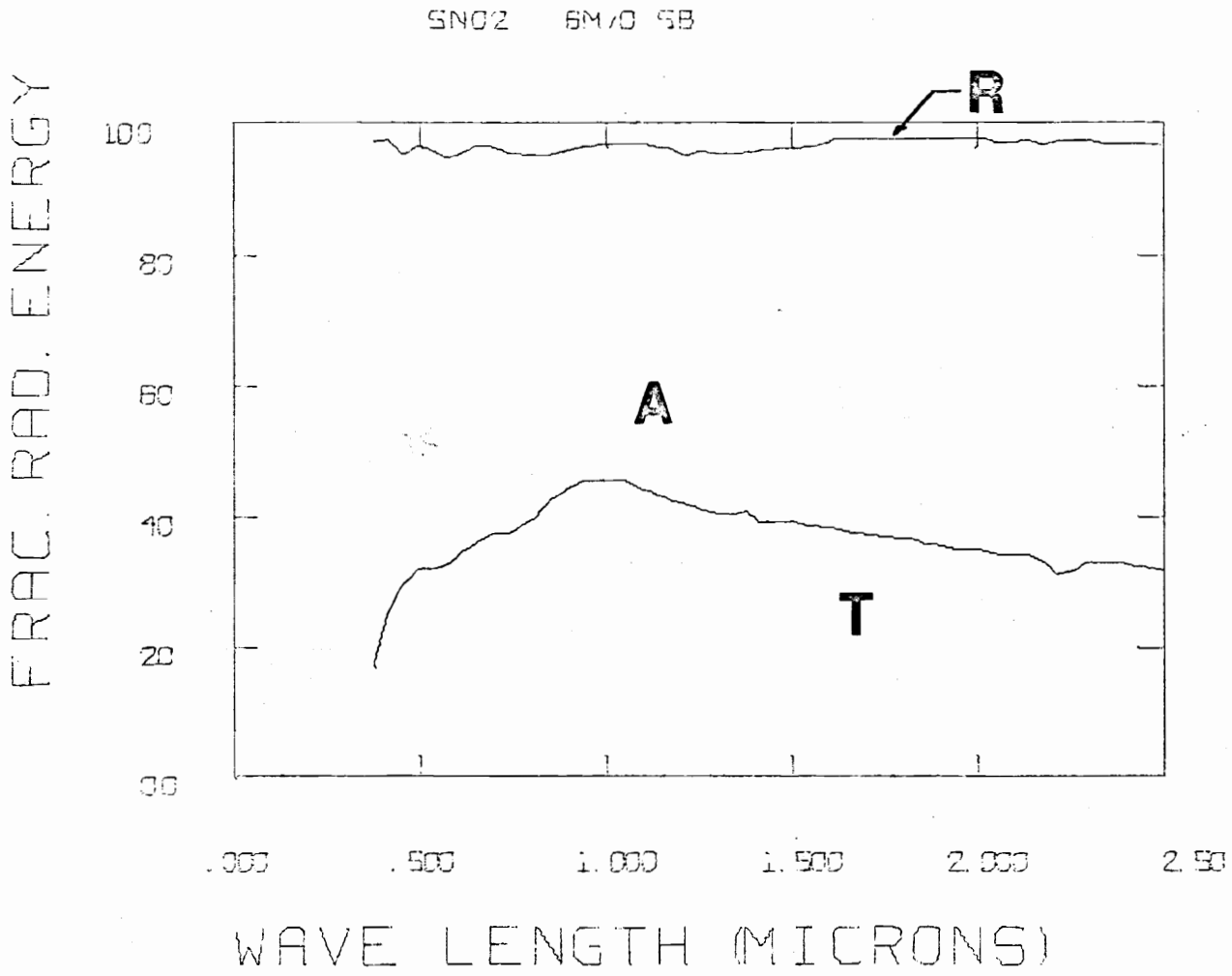

Figure 41. Change in Reflection (R), Absorption (A), and Transmission (T) of Light with Wavelength for Thin Film of SnO_2 with 6 m/o Sb - Spray 22.

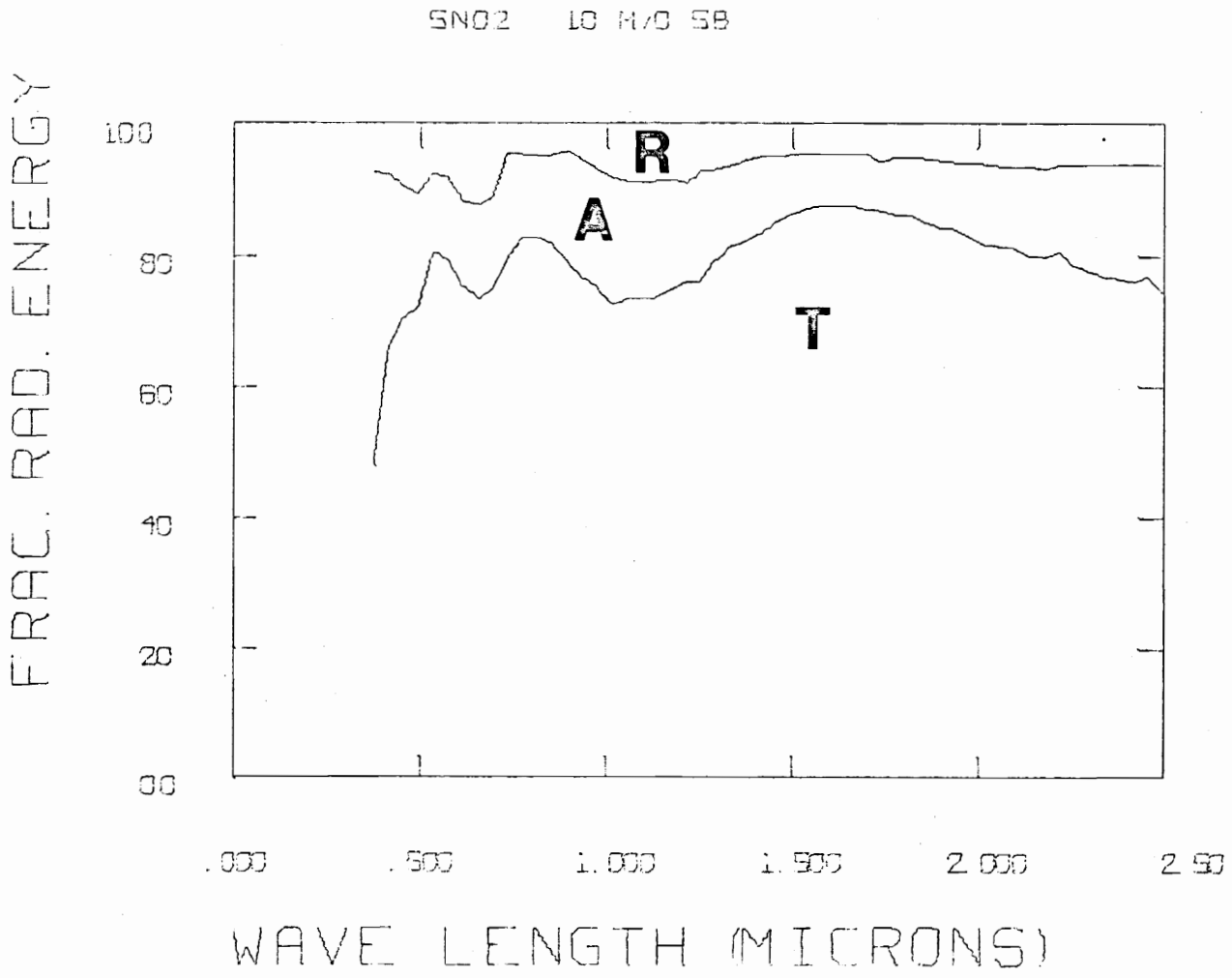

Figure 42. Change in Reflection (R), Absorption (A), and Transmission (T) of Light with Wavelength for Thin Film of SnO_2 with 10 m/o Sb - Spray 22.

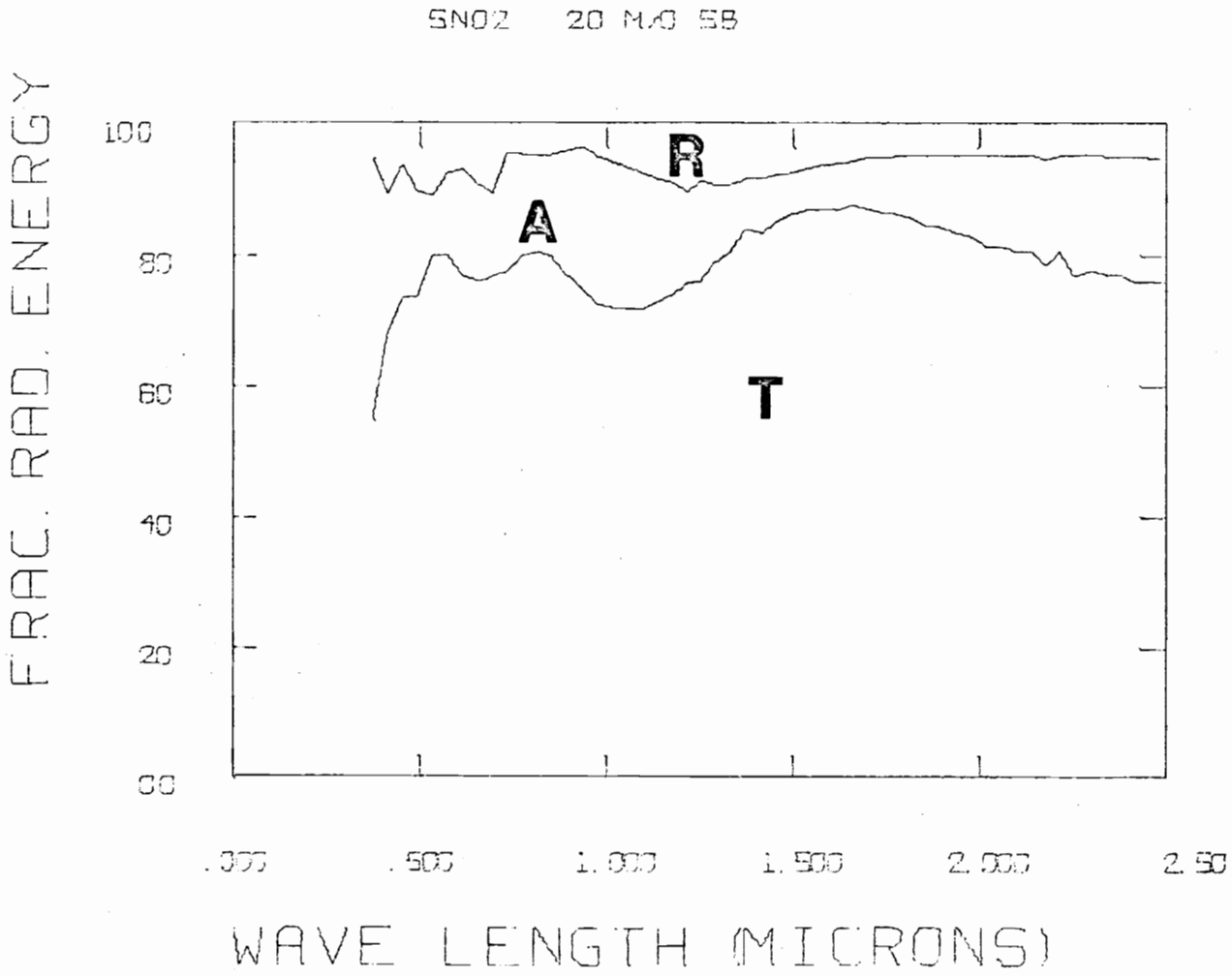

Figure 43. Change in Reflection (R), Absorption (A), and Transmission (T) of Light with Wavelength for Thin Film of SnO_2 with 20 m/o Sb - Spray 22.

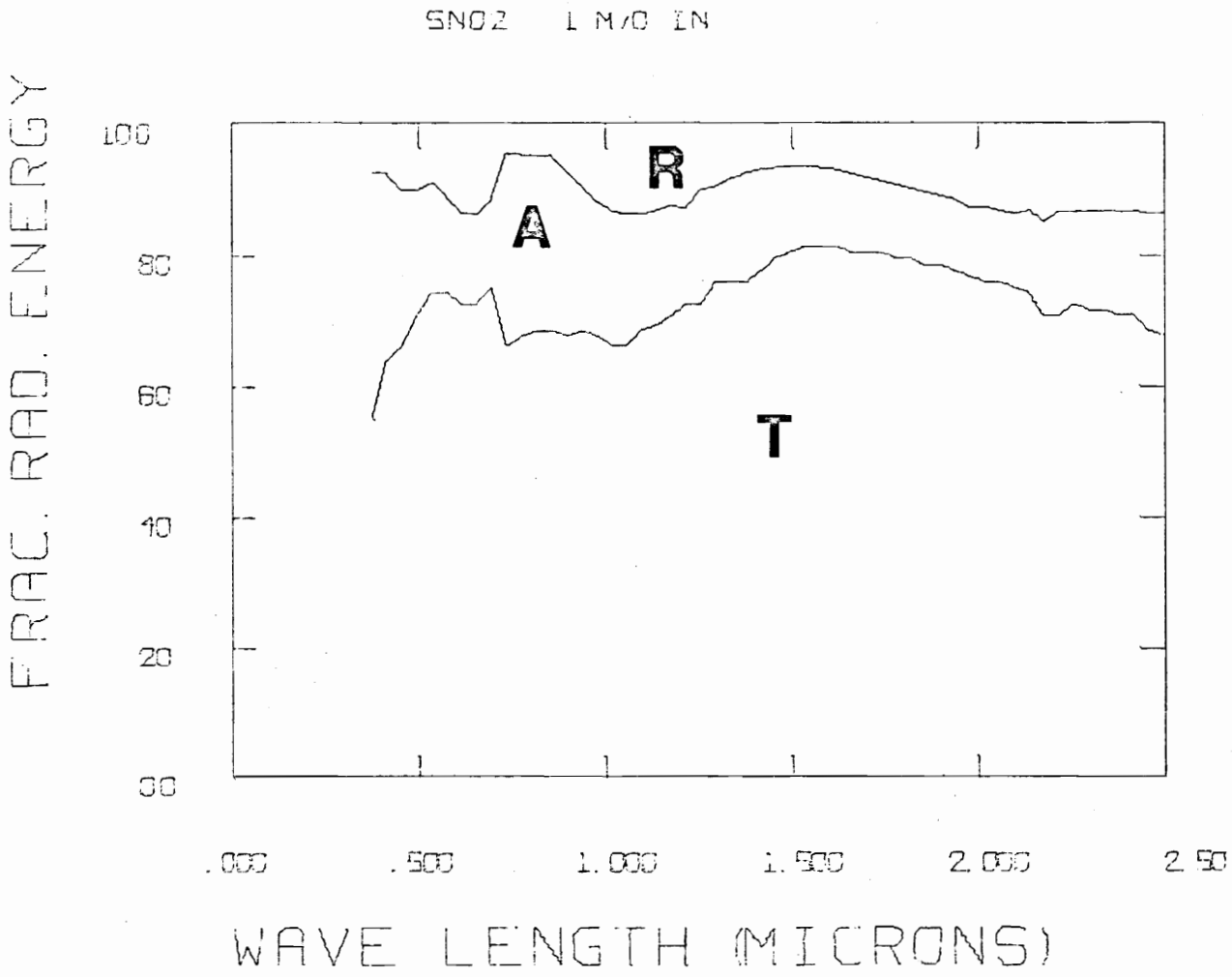

Figure 44. Change in Reflection (R), Absorption (A), and Transmission (T) of Light with Wavelength for Thin Film of SnO_2 with 1 m/o In - Spray 29.

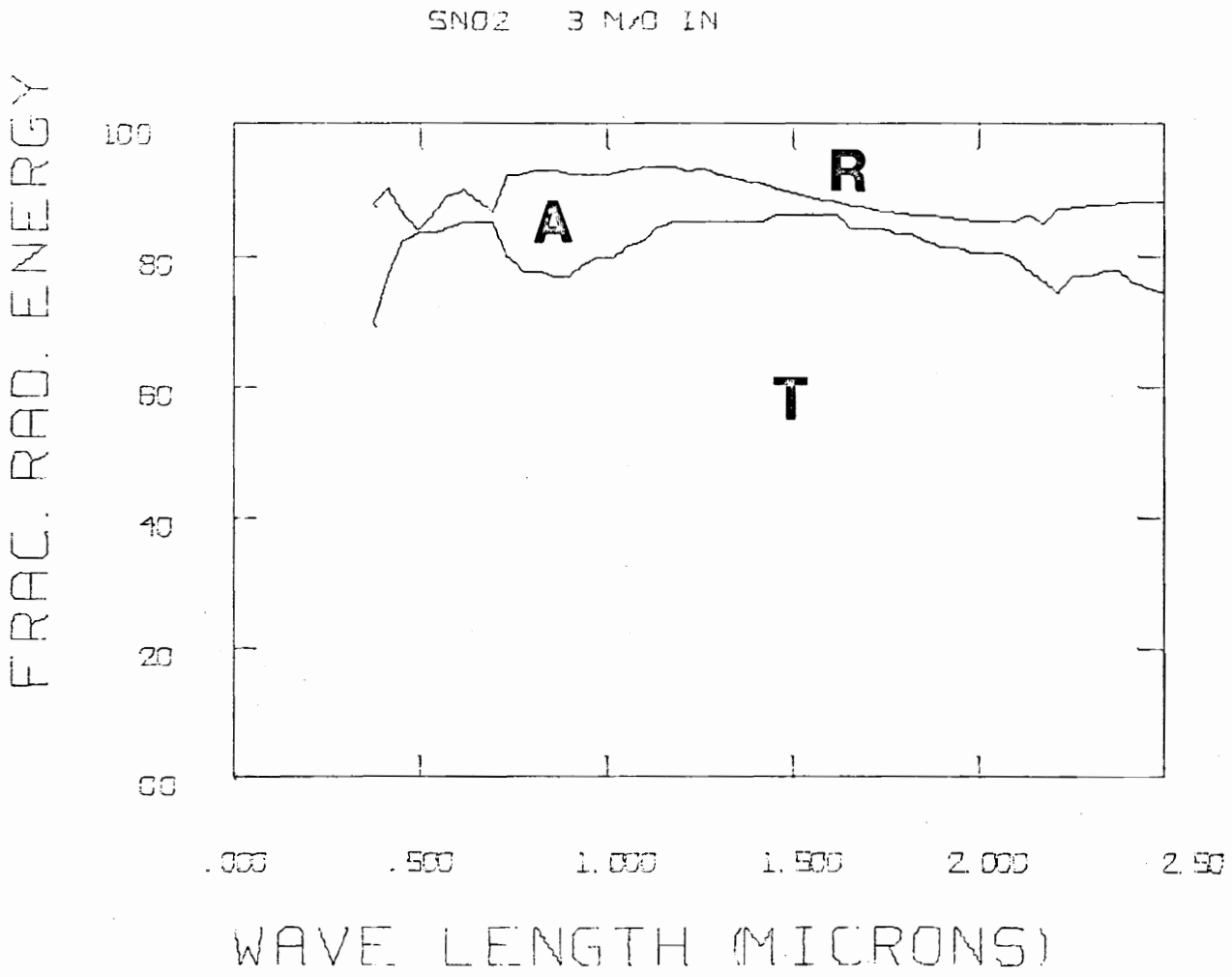

Figure 45. Change in Reflection (R), Absorption (A), and Transmission (T) of Light with Wavelength for Thin Film of SnO_2 with 3 m/o In - Spray 29.

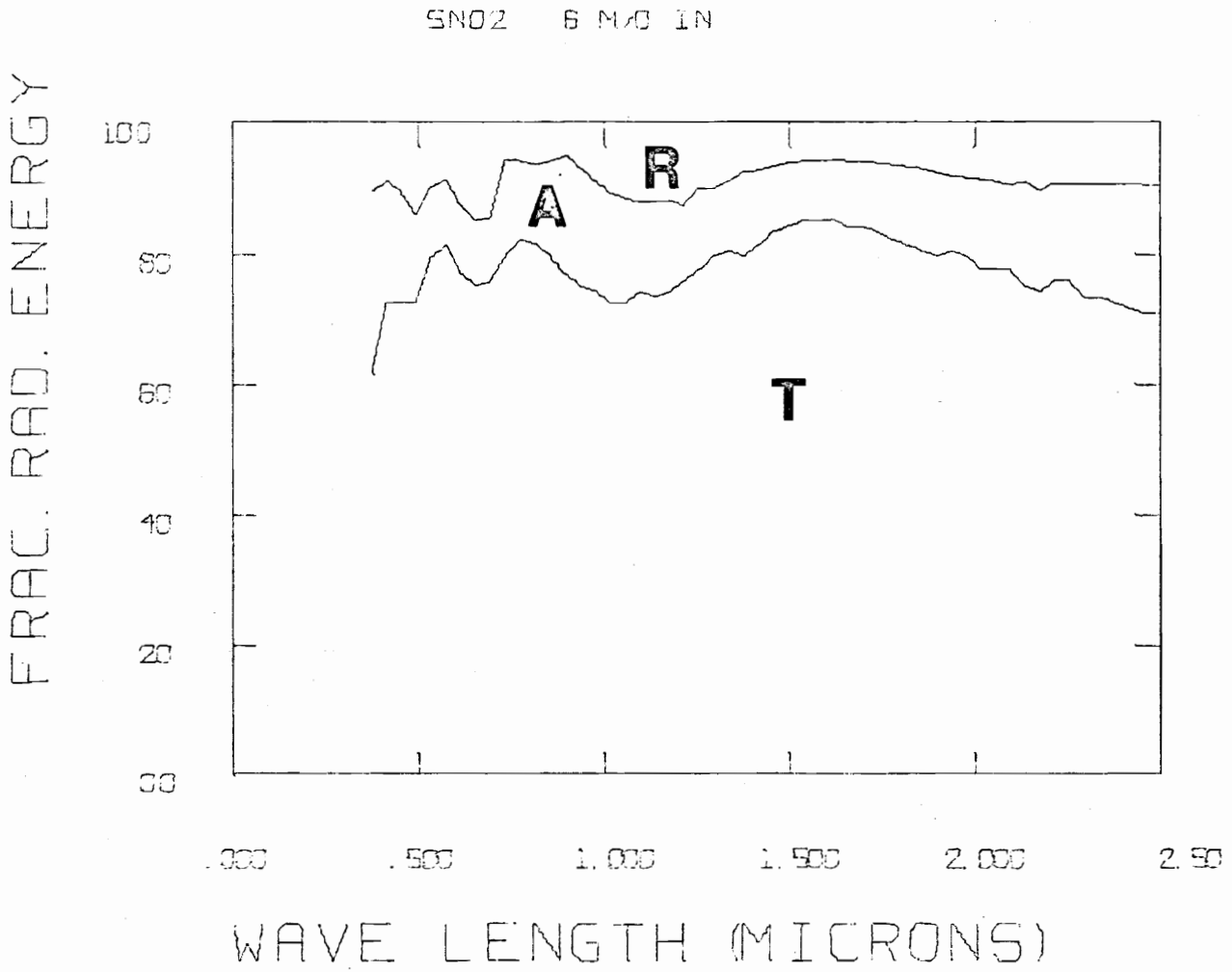

Figure 46. Change in Reflection (R), Absorption (A), and Transmission (T) of Light with Wavelength for Thin Film of SnO_2 with 6 m/o In - Spray 17.

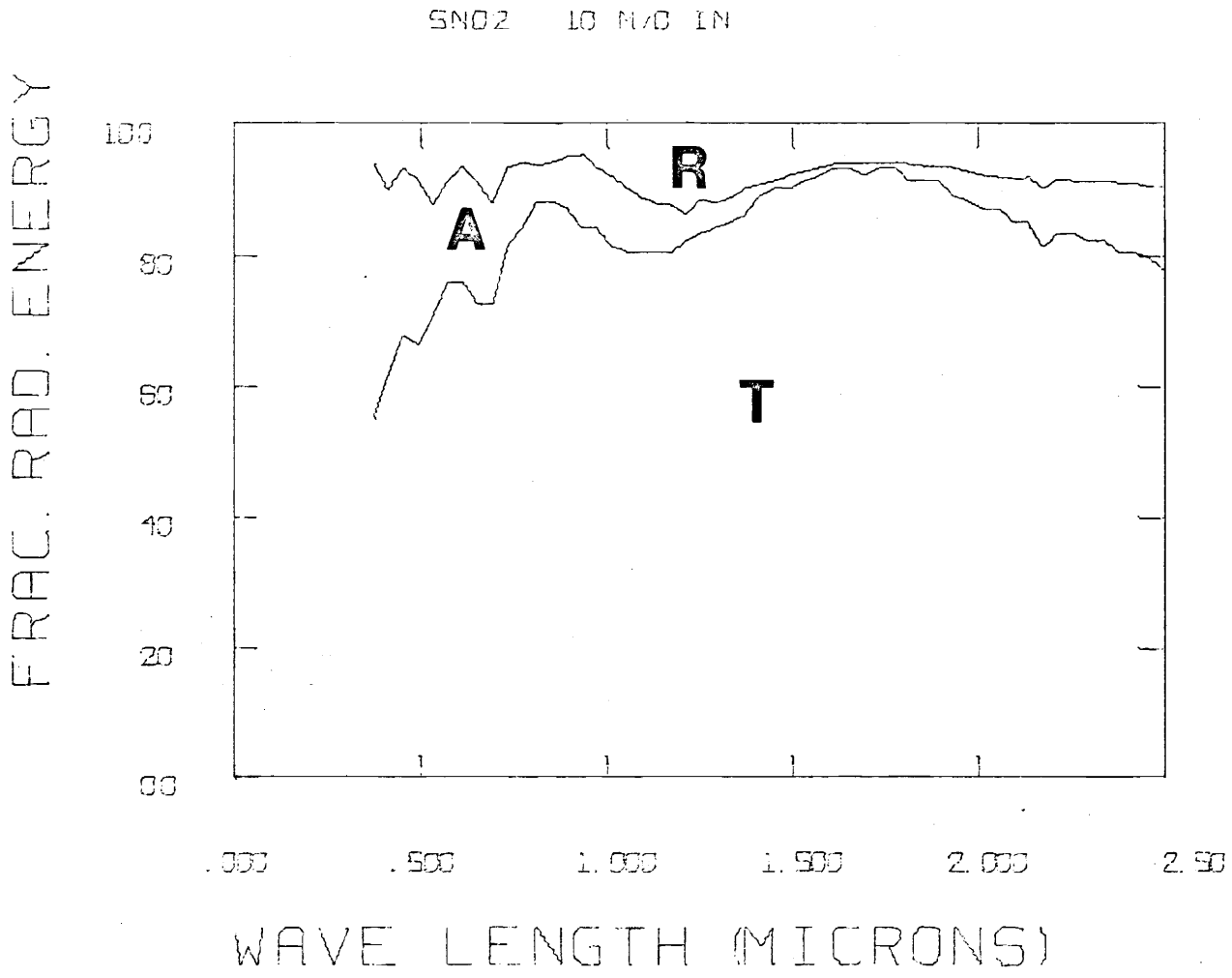

Figure 47. Change in Reflection (R), Absorption (A), and Transmission (T) of Light with Wavelength for Thin Film of SnO_2 with 10 m/o In - Spray 17.

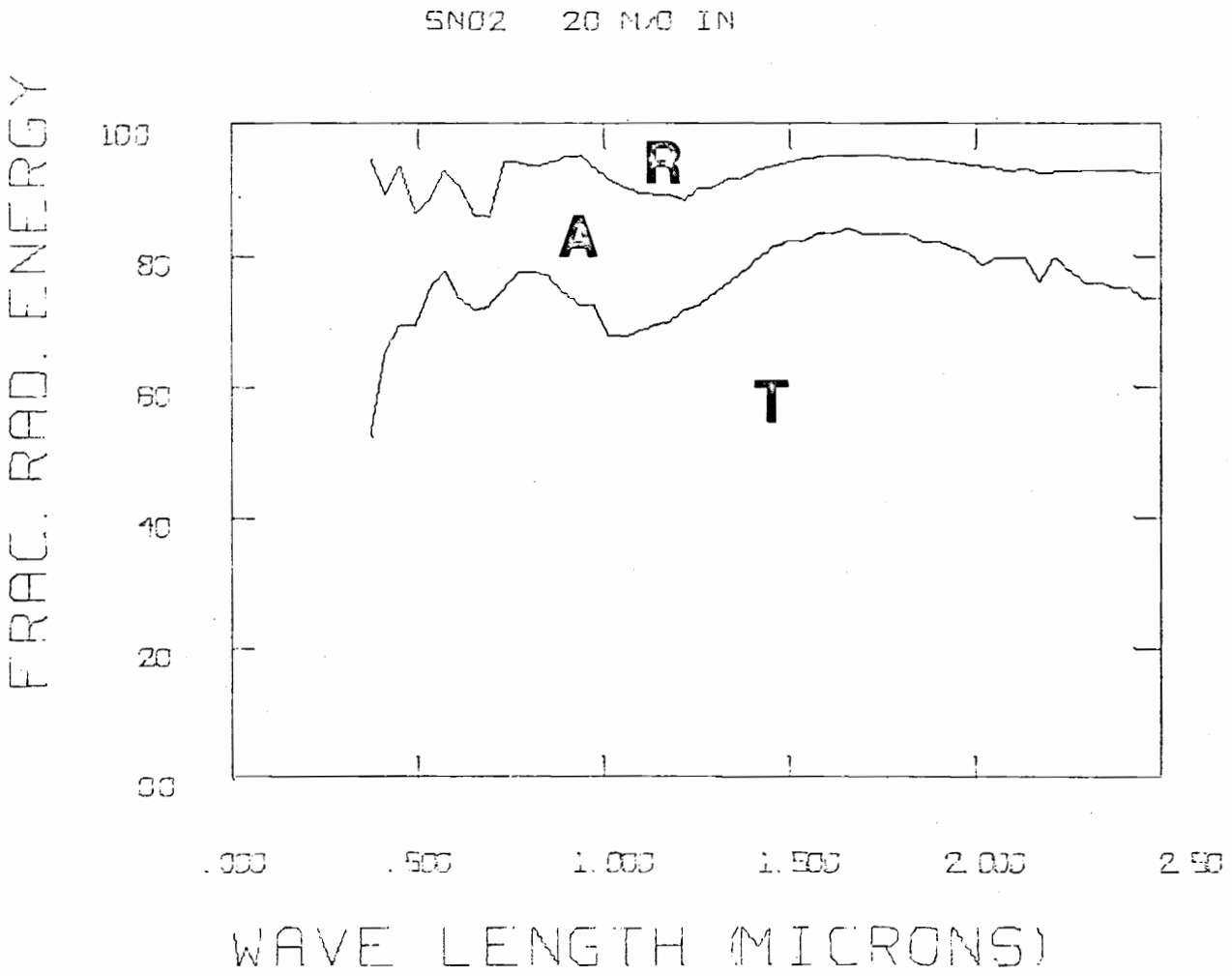

Figure 48. Change in Reflection (R), Absorption (A) and Transmission (T) of Light with Wavelength for Thin Film of SnO_2 with 20 m/o In - Spray 17.

Cobalt oxide films generally showed higher reflectivity than tin oxide films (Figures 49-53). This was especially the case for visible light where a maximum reflection of 22% was recorded. Heat treatment of one film (sputter run 3) reduced its reflectivity. All cobalt oxide films had a green-brown tint that deepened with film thickness.

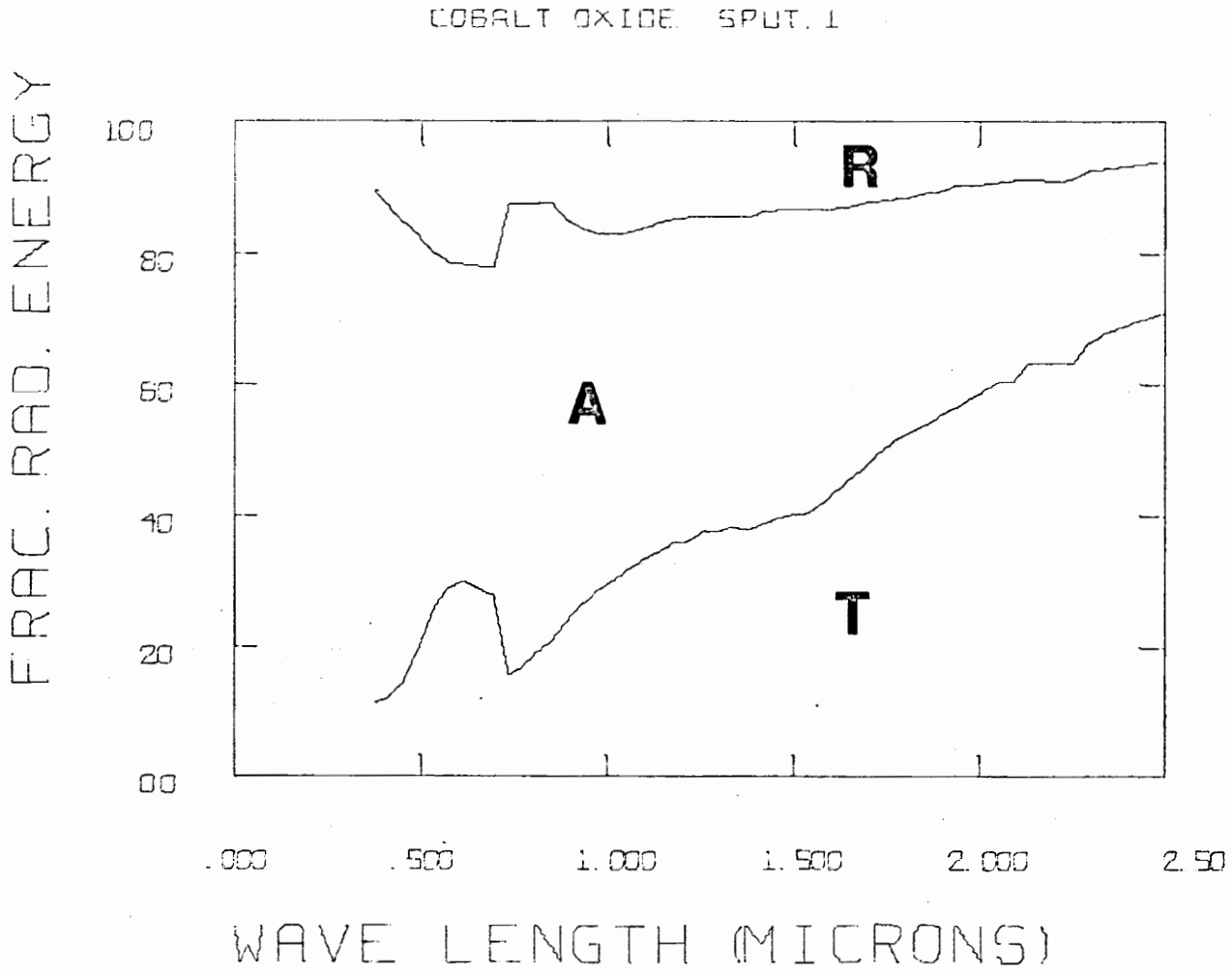

Figure 49. Change in Reflection (R), Absorption (A), and Transmission (T) of Light with Wavelength for Thin Film of CoO_x - Sputter No. 1.

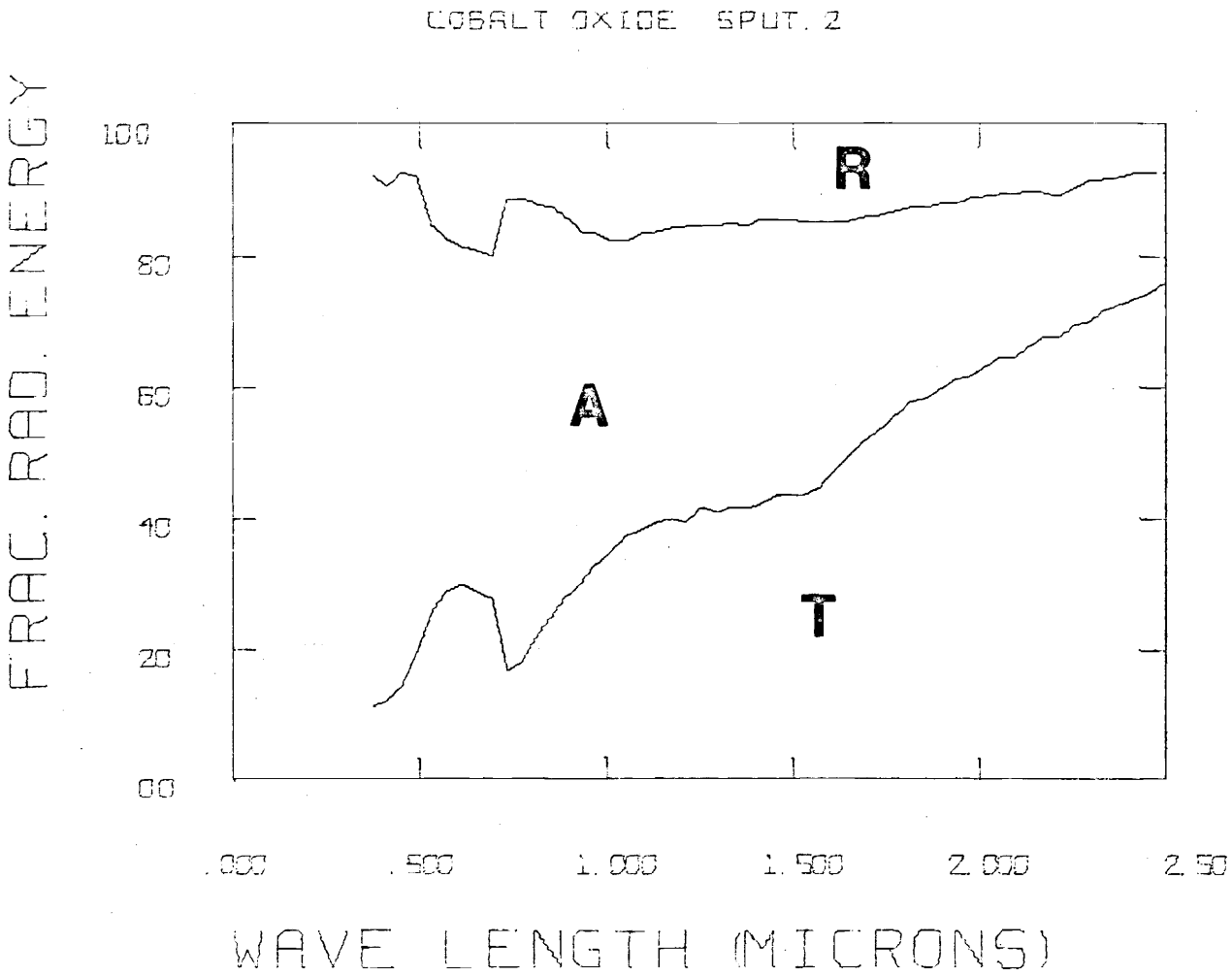

Figure 50. Change in Reflection (R), Absorption (A), and Transmission (T) of Light with Wavelength for Thin Film of CoO_x - Sputter No. 2.

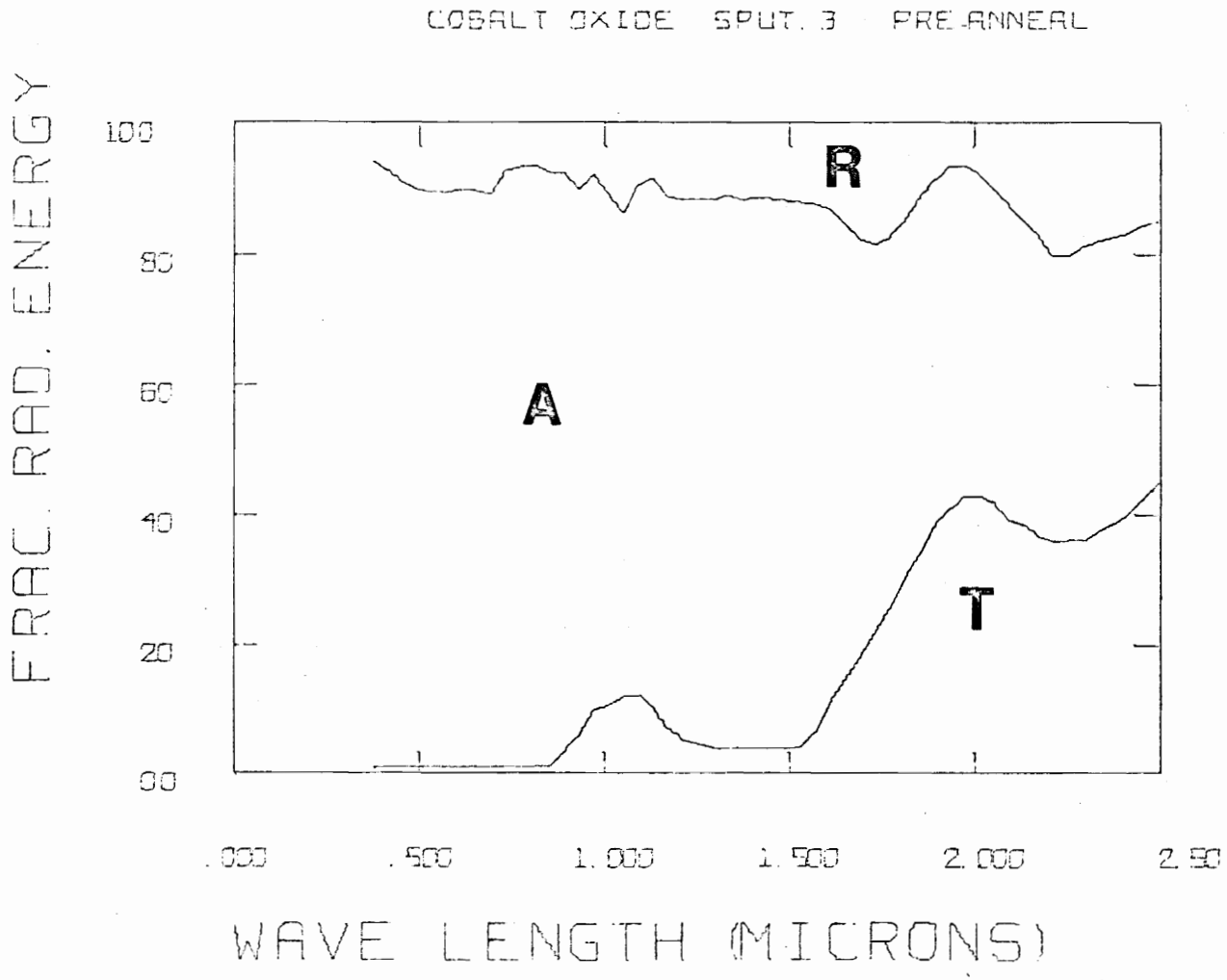

Figure 51. Change in Reflection (R), Absorption (A), and Transmission (T) of Light with Wavelength for Thin Film of CoO_x - Sputter No. 3.

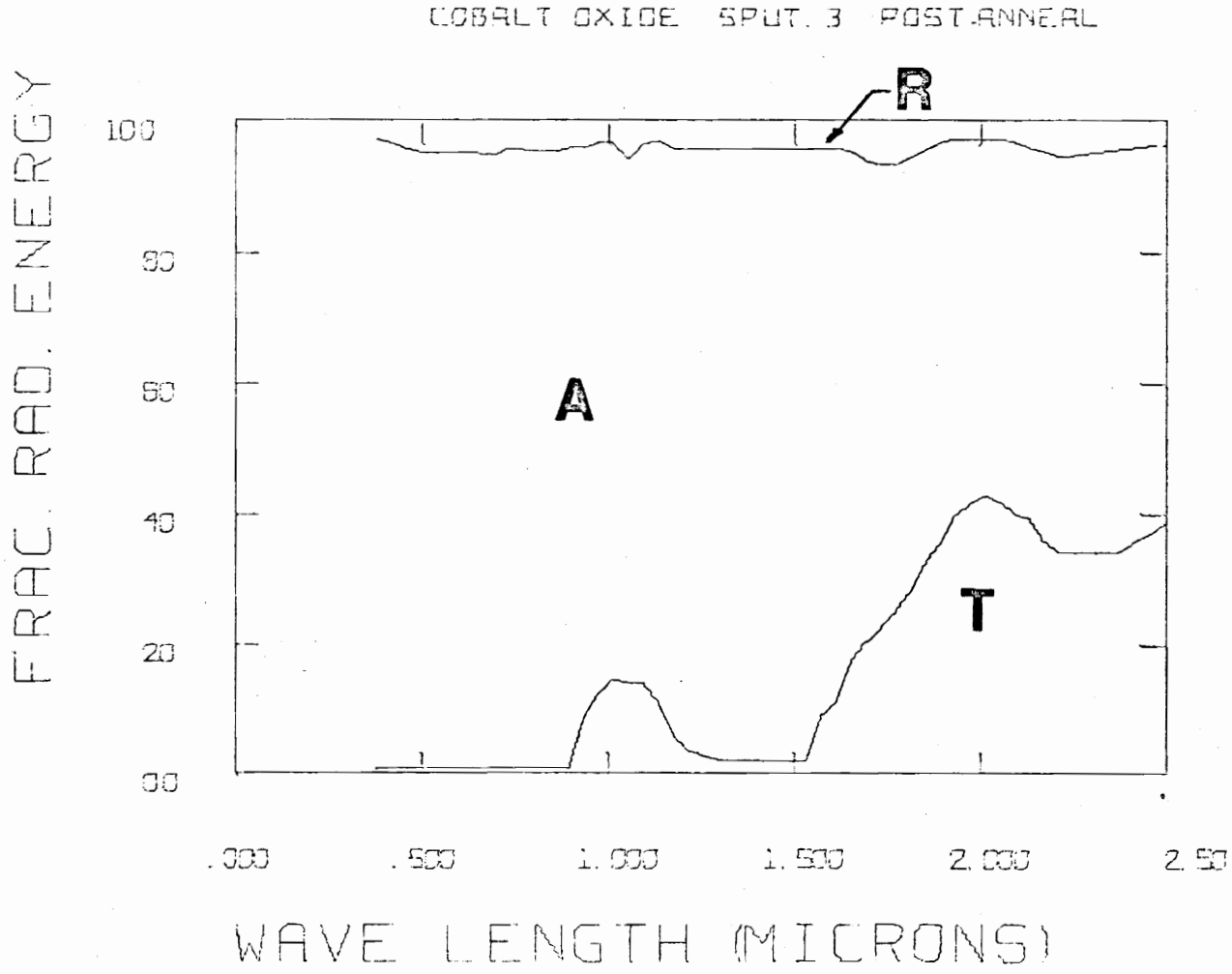

Figure 52. Change in Reflection (R), Absorption (A), and Transmission (T) of Light with Wavelength for Thin Film of CoO_x - Sputter No. 3 (annealed).

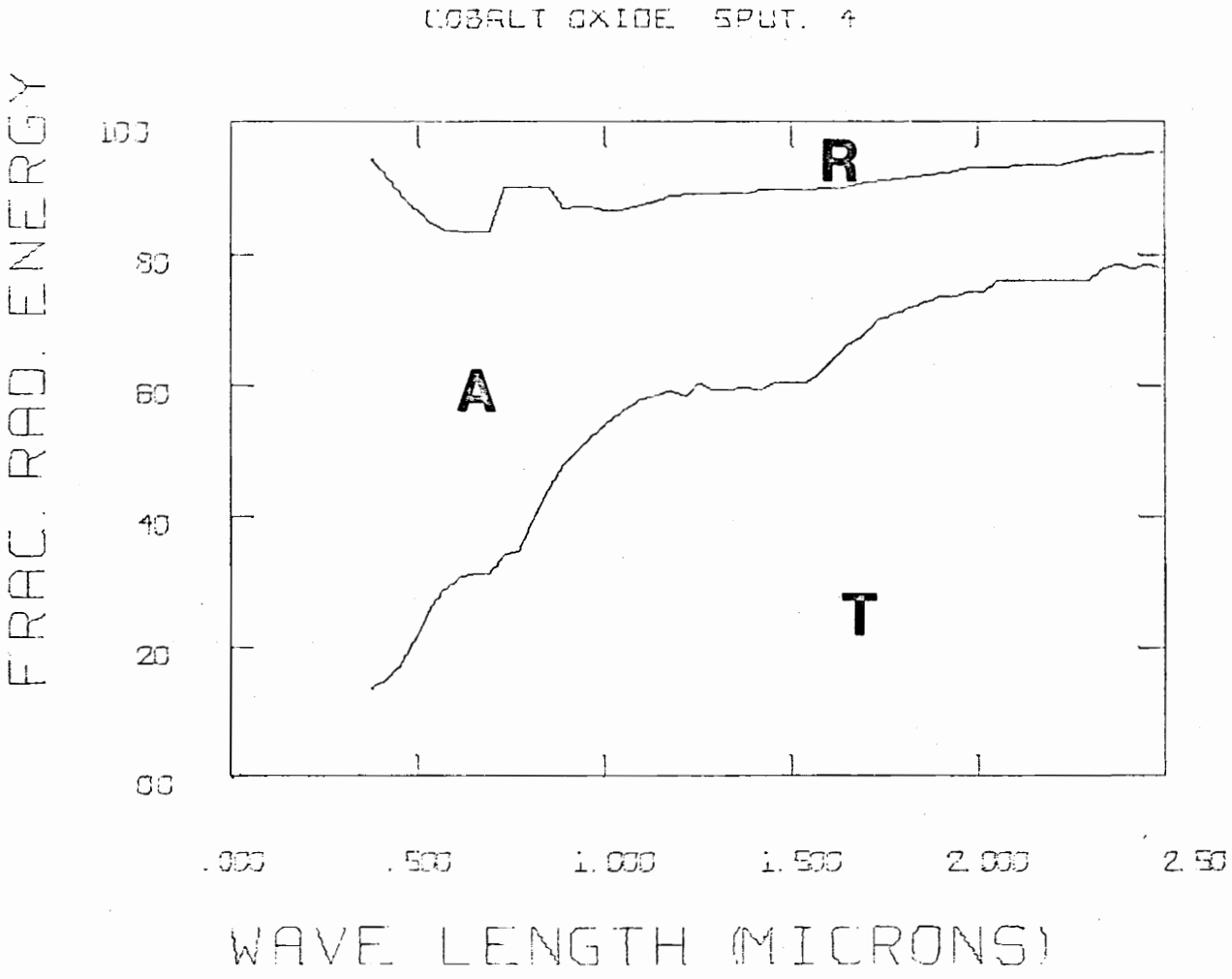

Figure 53. Change in Reflection (R), Absorption (A), and Transmission (T) of Light with Wavelength for Thin Film of CoO_x - Sputter No. 4.

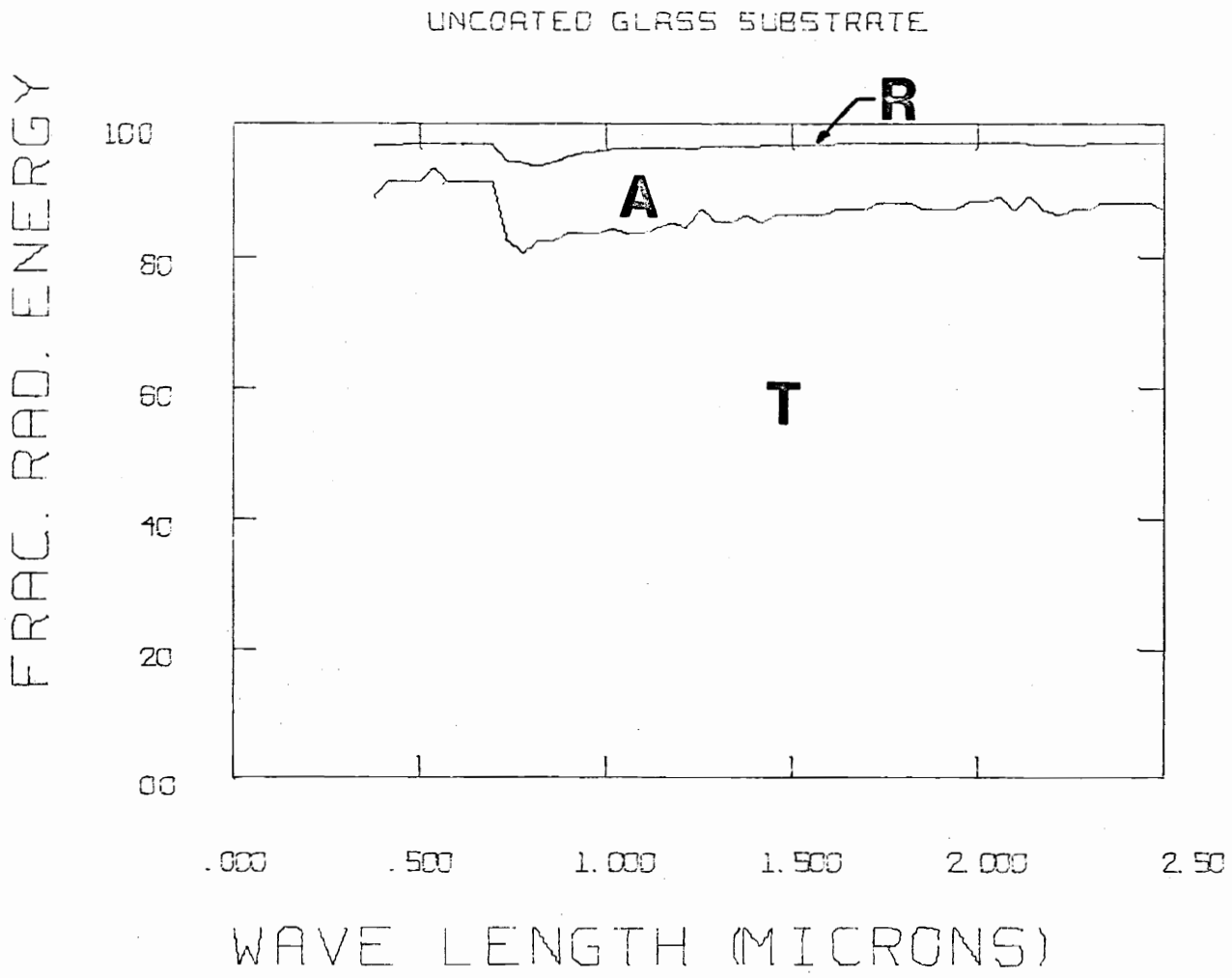

Figure 54. Change in Reflection (R), Absorption (A), and Transmission (T) of Light with Wavelength for Uncoated Glass Substrate.

V. DISCUSSION

Both n-type and p-type semiconducting oxide films were prepared in this study with tin oxide films being n-type and cobalt oxide films being p-type. The brief attempt to form solar cells from these extrinsic semiconductors did not result in an observable voltage, but current rectification was observed in some of the p-n junctions. This behavior will be discussed in a later part of this section since the prime objective of this work was to characterize the tin oxide and cobalt oxide films in an effort to understand their electrical and optical characteristics. This understanding will be helpful in future utilization of these materials in applications involving p-n junctions. The tin oxide will be discussed first followed by discussion of cobalt oxide.

A. Conductivity Mechanism of Tin Oxide

The temperature dependence of resistivity in undoped tin oxide thin films revealed that the films were extrinsic semiconductors with two sets of donor levels (Figure 29). The independence of resistivity at temperatures below 150°C indicated that one set of donor levels overlapped to form a band, similar to an impurity band in a heavily doped semiconductor, whose uppermost energy existed within the conduction band of the tin oxide. At temperatures greater than 150°C, activation energies of about 0.02 eV (Table V) indicated that a second different donor species existed in the film.

It is mentioned in the literature review that both residual chlorine and oxygen vacancies have been suspected to be responsible for extrinsic semiconduction in tin oxide thin films. This work suggests that in these films deposited at low temperatures, both species are present. The presence of chlorine indicates an incomplete chemical reaction during the pyrolytic thin film formation process in which the hydrated tin chloride solution is expected to completely decompose to form tin oxide.

A comparison of tin oxide films prepared in this study with those of a previous one that deposited the tin chloride solution at a higher temperature (600^{o}C) shows how incomplete decomposition affected film properties. The decomposition reaction of the previous study was most likely more advanced. Evidence of the large quantity of chlorine remaining in the films of this study is given by a comparison of chlorine and indium ESCA peaks for the indium doped sample. The indium showed no peak at the 3 m/o level while the chlorine gave an appreciable peak (Figures 26,28).

The greater residual chlorine concentration in films of the present study than films of the previous study could possibly account for the different effect that doping had on film resistivity. In Figure 55 the resistivity of tin oxide as a function of antimony content is plotted for films of both this study and the previous one. In region I very little effect is observed for films of this study whereas films of the previous study showed a decrease in resistivity as was seen by others.[4,7] Films of this study with their higher

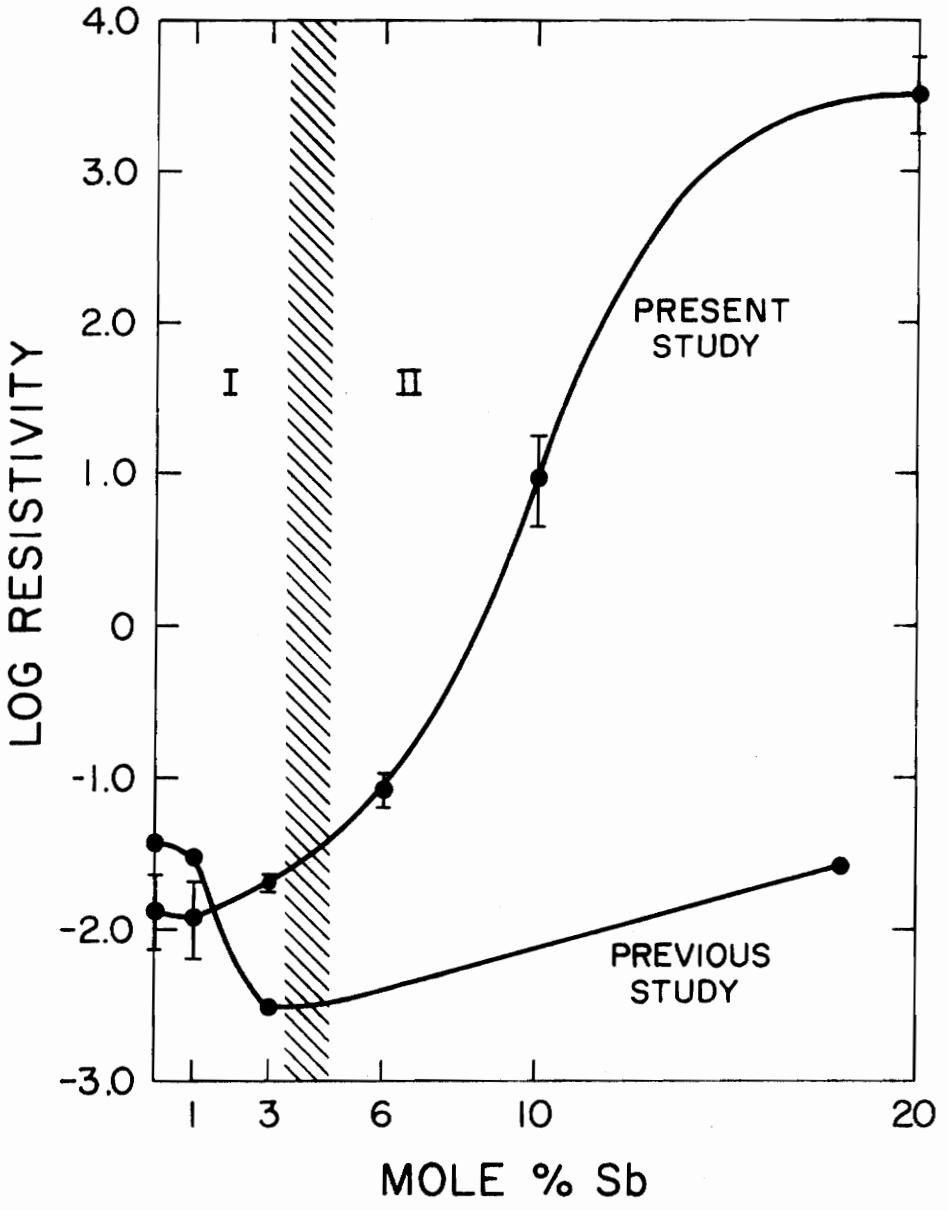

Figure 55. Comparison of Resistivity of Antimony Doped Films of this Study with Corresponding Films Prepared by Rohatgi[11].

chlorine content may have had such a high concentration of conduction electrons that the effect of adding antimony was diminished. The increased resistivity caused by adding of indium was also reduced for films of this study as opposed to those in the previous one. The added indium attracted free electrons as it substituted for Sn^{4+} as In^{3+}. Once the electrons were trapped the In^{3+} became In^{4+}. Some of these electrons were supplied by electrons originating from oxygen vacancies. Evidence of this was a change in the ESCA oxygen peak (Figure 27). It had only one major peak which corresponded to oxygen bonded to Sn^{4+}. A shoulder on the oxygen peak occurred at a binding energy about 1 eV greater than that of the peak itself. This could be due to an increase in binding energy of oxygen in the vicinity of the In^{4+} where In-O bonding would exist. Other electrons were supplied by the chlorine. Since there were more of these electrons available due to more chlorine for films of this study, the film resistivity increased to a lesser extent.

Large additions of both antimony and indium did not continue the initial effects observed in film resistivity. This can be best understood in terms of the structural effects introduced by these additives at the low temperature conditions employed in this study. In region II of Figure 55 the resistivity of SnO_2 films rises with an increasingly steeper slope. In Table II the tin oxide X-ray diffraction shows an increase in crystal disorder with increased antimony to the extent of the total loss of crystallinity at 10 m/o antimony and above. These two observations taken together show

the large rise in resistivity at 10 m/o to be due to the amorphous nature of the film.

This effect was caused by the fact that antimony oxide is a glass former.[31] The low deposition temperature had the effect of quenching the film into the glassy state. The lower rate of resistivity increase for films of the previous study was due to the fact that this quenching did not occur and disorder introduced into the crystal by the antimony never reached the point of glass formation. Once amorphous the films behaved as intrinsic semiconductors in that semiconducting glasses can accommodate impurities without sensing any appreciable electronic effect.[43] This accommodation entails the insertion of impurity atoms between the interconnected glass network without the need for substitution in the network of primary bonds that would disturb the energy states of the bonding electrons.

Indium oxide and tin oxide are not glass formers. Therefore, the low temperature deposition did not cause these to form as glass. However, large additions of indium in the tin oxide of 6 m/o or greater reduced the tin oxide crystallinity somewhat as indicated by the loss of a diffracted peak and reduction of total intensity (Table IV). These large additions of indium did not increase resistivity further than the maximum resistivity obtained for films containing 3 m/o indium (Figure 32). The indium must be entering the crystal as In^{4+} in order for this lack of change to occur.

The fact that antimony tends to form a glass can be used to interpret region I of Figure 55 in a different way from the previous

discussion which considered chlorine content. One can observe in X-ray data (Table IV) and optical data (Figures 39 and 40) that the initial additions of antimony alter the films' crystallinity and optical absorption. Films of the previous work showed similar optical effects for films having larger additions of antimony of 8.65 m/o. Increased antimony content up to 3 m/o increased optical absorption in this study to a maximum value of 90% at 2 microns while films having 8.65 m/o antimony in the previous study had absorption of 75%. This indicates that films with 3 m/o antimony of this study behaved like films having slightly more than 8.65 m/o antimony of the previous study. Therefore, low temperature deposition of tin oxide with antimony must cause greater disruption of the crystalline order normally formed in deposition of undoped tin oxide. This tendency toward amorphous structure could enable the crystal to accommodate the antimony in a manner analogous to a glass in which added impurities would not disturb the electronic status quo. It should be noted that the appreciable conductivity of the films would then be due to impurities other than antimony such as chlorine or oxygen vacancies that were already within the crystal structure prior to adding the antimony. Chlorine acted as a donor by substituting for oxygen. Its -1 valence allowed one electron that would normally be bound to oxygen to be free to move.

The increase in resistivity and activation energy that accompanied annealing of undoped tin oxide films (Figures 33 and 34) was not a result of the removal of chlorine as suggested by Miloslavski and Vincent.[9,15] Electronic spectra from the chlorine in these films

(Figures 17-20 and Table VI) are relatively unaffected by annealing. The peak to background ratio for chlorine actually increased by a factor of 1.5 after one hour of annealing. The schematic depiction of annealing effects in Figure 56 shows how this increased detection of chlorine could be attributed to its segregation to the surface of the film where ESCA senses chemical species and their bonding.

Tin content was shown to steadily decrease with annealing while oxygen content increased rapidly in the first hour and remained relatively unchanged thereafter (Table VI). Earlier work done on tin oxide films[11] indicated that silicon and sodium from the underlying glass entered the film after one hour of annealing. Considering this, it is probable that films annealed for times greater than one hour experienced a greater degree of diffusion of these glass components.

The crystal defect structure was also affected by annealing. Electronic spectra of oxygen show a gradual progression from a double peak for unannealed tin oxide to a single peak after 50 hours of annealing. The portion of the convoluted peak that gradually disappears is the lower energy portion. Oxygen bonded at lower energy corresponds to oxygen in the vicinity of oxygen vacancies. Therefore, the loss of the low energy part of the oxygen doublet would be due to elimination of oxygen vacancies by oxidation of the film. After 100 hours of annealing the oxygen peak was broadened due to convolution of a second peak at higher energy (by 1 eV) with the peak corresponding to the $O\text{-}Sn^{4+}$ bond. It is possible that the silicon that had entered

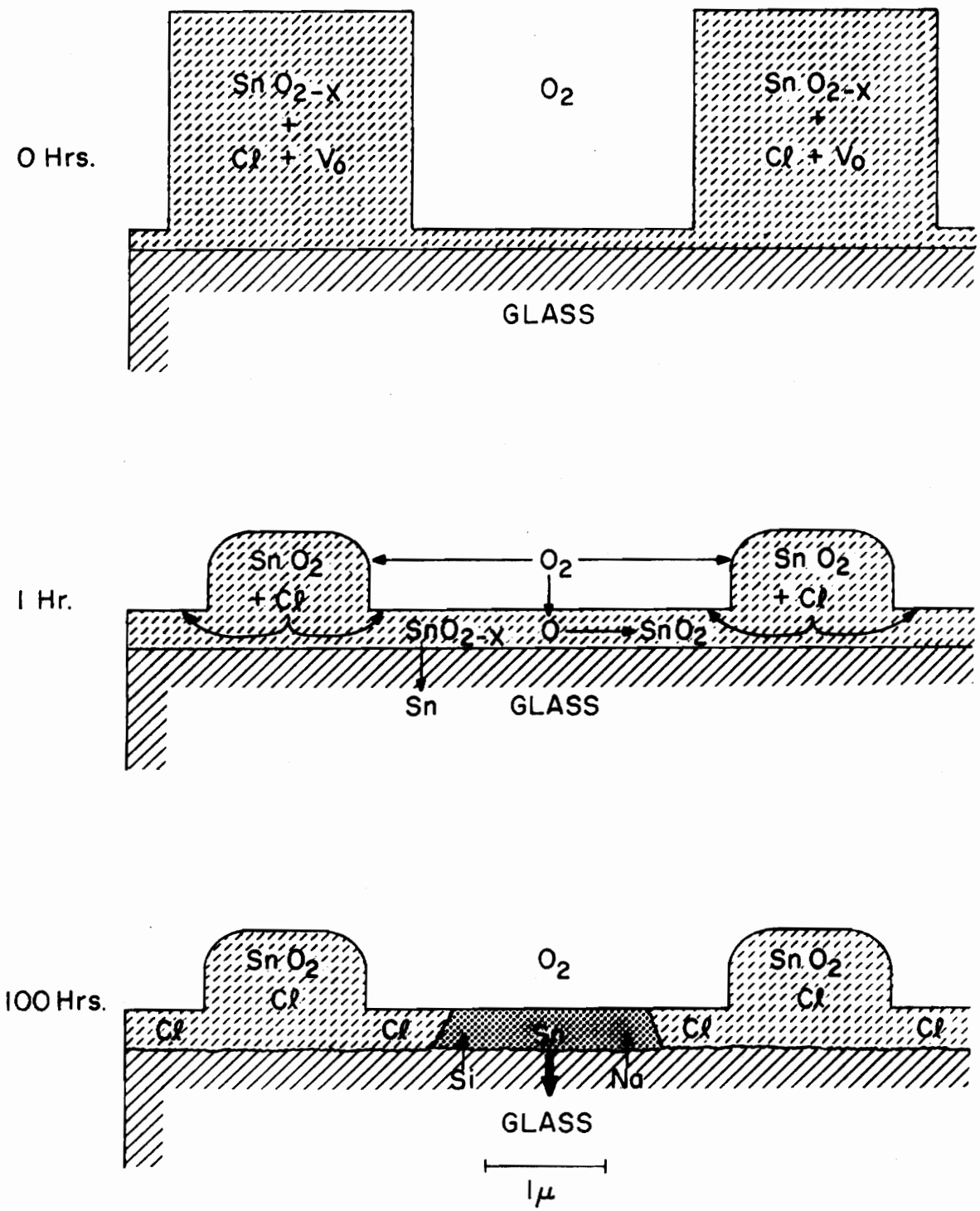

Figure 56. Schematic Representation of Changes in Morphology of SnO_2 Films with Annealing.

the film from the substrate had formed a slightly stronger bond to oxygen atoms in its vicinity.

Annealing had an immediate effect on film morphology as seen by comparing micrographs of the unannealed film and the film annealed for one hour (Figures 5 and 7). The film appeared to be spreading out as large crystals lost their definite shape and size and form a thicker film (Figure 56). This would explain X-ray peak broadening. This must have occurred as a result of the adsorption of atmospheric oxygen onto the film surface followed by its incorporation into the crystal[39]. This initial change in the film can be summarized as the oxidation of the film that eliminated many oxygen vacancies and caused a spreading out of film morphology. This loss of oxygen vacancies reduced the concentration of free electrons and thereby increased resistivity. The majority of free electrons still existant were supplied by the chlorine.

Further heat treatment brought no more spreading out and only a small increase in oxygen content (Table VI, Figures 9,10). There was a continued reduction in tin content as interdiffusion of the tin with components of the glass substrate proceeded. The introduction of these insulating materials into the film can be seen as the formation of dark branch-like shapes in the micrograph of the 100 hour sample (Figure 10). Darkening indicates the ejection of fewer secondary electrons from that portion of the film. This would be due to the stronger bonding of electrons to the insulating silicon and sodium oxides than to the semiconductive tin oxide.

The increased resistivity with increased anneal time of Figure 33, for time greater than the first few hours, must have been caused by these diffused glass components. Evidence for this would be the absence of further oxidation after one hour (Table VI) and the similar morphologies of films having undergone heat treatment for one hour or more (Figures 8-10).

B. Conductivity Mechanism of Cobalt Oxide

Sputtered films of cobalt oxide exhibited extrinsic p-type semiconductivity. These films were more resistive and had higher activation energies than the tin oxide films. Cobalt vacancies acted as acceptors for electrons from the valence band of the cobalt oxide. In the case of cobalt oxide containing 5 m/o lithium, the added lithium also acted as an acceptor.

The abrupt increase in activation energy that occurred at temperatures of approximately 220°C can be accounted for by an increasing ionization of defects.[29,30] Increased thermal energy at higher temperature caused the cobalt vacancies to gain an extra effective negative charge.

$$V_{Co}' \rightarrow V_{Co}'' + h^{+} \qquad (12)$$

This would free an extra positive hole from the V_{Co}' for conduction in the cobalt oxide valence band.

Another factor influencing cobalt oxide resistivity was the film's constitution. X-ray diffraction patterns of the films showed peaks corresponding to CoO and Co_3O_4 (Table V). The Co_3O_4 phase was the

more conductive of the two as seen by simultaneous increases in conductivity and Co_3O_4 content on annealing in air at 600°C. Apparently the annealing process increased the concentration of holes by increasing the excess oxygen in CoO_{1+x} with the final effect of converting the CoO to Co_3O_4.[28]

Forming conditions also affected cobalt oxide film constitution. The starting material in the sputtering target had no appreciable CoO phase (Table V). In the sputtering process some of the oxide molecules dislodged from the target were dissociated into elemental cobalt and oxygen as they passed through the high energy plasma to the substrate. The recombining of these elements at the substrate tended to form CoO due to the reducing effect of the argon atmosphere in the sputtering chamber. Therefore, high power conditions which dissociated more of the Co_3O_4 molecules given off from the target along with a higher oxygen evacuation-argon refill rate that removed oxygen tended to form more CoO in the resulting film. Films formed at low power were much less resistive due to the greater concentration of the Co_3O_4 phase (Table V). The low resistivity of Co_3O_4 arises from the fact that it has the spinel crystal structure. In this structure electrons are readily exchanged from Co^{2+} ions to Co^{3+} ions.[32]

The morphology of the film was affected slightly by 1 hour of annealing at 600°C. A continuous series of 0.5 micron crystals with definite relief spread out upon being heated and lost their relief somewhat. The extent of interdiffusion with the glass was not large enough to increase film resistivity indicating that film integrity was still intact after this limited heat treatment.

C. Applications

To be able to utilize these films in solar energy applications the basic characteristics of electrical conductivity and optical absorption of each film need to be considered.

For use as heterojunctions the cobalt oxide and tin oxide both fulfill the requirement of semiconducting films having opposite charge carrier type. Their optical absorption properties indicate that cobalt oxide appears to have an absorption edge in the visible part of the spectrum near a wavelength of 0.4 microns. The tin oxide shows no indication of this. An absorption edge arises from excitation of electron-hole pairs. These electron-hole pairs are needed for the photovoltaic effect to be possible in a junction device. Even if no intrinsically excited charge carriers were produced in the combined films, the electric contact potential at the junction caused by equalization of fermi-levels could rectify currents passing through the combined films. Formation procedures need to be optimized in order to protect this junction from deterioration by diffusion or micro-flaws.

The preliminary combinations of these films produced a few cases where rectification was observed (Figure 36). These rectifying junctions were formed by sputtering cobalt oxide onto tin oxide. When tin oxide was sprayed onto cobalt oxide, no rectification was observed due to the 350^{o}C deposition temperature of the tin oxide. At this temperature thermal energy was sufficient to cause some interdiffusion of tin oxide and cobalt oxide. This diffusion

increased the width of the transition region between the films. Therefore, there was little junction behavior.

Temperatures of the sputtering process were found to cover a range of $80^{\circ} \pm 20^{\circ}C$. Temperature increased with sputtering power. The heat provided at these temperatures was not large enough to cause deleterious amounts of interdiffusion. The low power - low temperature conditions of 0.24 KW - $60^{\circ}C$ were used to produce the most rectifying junction as seen in Figure 36.

Lack of rectification most likely was not due to formation of abrupt junctions. If abruptness were responsible for failure to rectify, the films having been heated most would have shown the best rectification.

This rectification indicates that the photovoltaic effect is possible for these films. The prototype solar cells did not show any photovoltage or photocurrent. This lack of results was probably due to large energy gaps of each film. Therefore, high energy photons such as X-rays would be needed to produce electron-hole pairs in them. If electron-hole pairs were formed, their failure to be transferred across the junction would have been due to recombination of minority carriers with majority carriers at impurity sites. These impurity sites have a high density of charge and therefore are the most probable locations for recombination. They are called electron traps or hole traps.

In the area of solar energy collectors, the cobalt oxide and antimony doped tin oxide would have the most potential as absorbing

materials. In fact, the addition of small amounts of antimony such as 1 or 3 m/o completely altered the optical behavior of the tin oxide thin films. The infrared transmission was totally cancelled by a large absorption and appreciable reflection.

The films showed little reflection of light with average percent reflection being 5%. Addition of 1 m/o antimony increased this to approximately 15%.

VI. CONCLUSIONS

Techniques used in the preparation of the thin film semiconductors of this study had a great effect on the final electrical properties of the films.

In the case of tin oxide films the low temperature pyrolytic deposition ($350^{o}C$) allowed large quantities of chlorine present in the spray solution to remain in the film. This residual chlorine impurity contributed to the extrinsic semiconduction behavior of the tin oxide.

The resistivity of tin oxide films exhibited two activation energies with activation energy of zero below $150^{o}C$ and a small activation energy of 0.04 eV $\pm$ 0.03 eV due to two different species acting as electron donors. These species were the residual chlorine and oxygen vacancies. One of these had donor energy levels overlapping the low energy boundary of the tin oxide conduction band.

The tin oxide film retained the chlorine impurity throughout all stages of annealing. The increases in resistivity caused by annealing were found to be caused by both oxidation of the film which eliminated oxygen vacancies and interdiffusion of the film with the glass substrate which introduced insulating Si-O bonds into the film.

Doping of the tin oxide with antimony produced little decrease in resistivity due to either the initially high defect concentration in undoped films or to a reduction of the films' crystal order. Large additions of antimony disrupted the crystalline nature of the film to the extent that the films formed in an amorphous state.

Doping with indium produced a monotonic increase in resistivity as indium concentration was increased up to 3 m/o. This increase in resistivity was less pronounced than for films formed at higher temperatures. High residual chlorine content was responsible. At concentrations greater than 3 m/o resistivity was nearly constant. This plateau effect of resistivity vs. indium suggested that a change occurred in the way in which indium was incorporated into the film. At doping levels under 3 m/o the indium acted as electron acceptors whereas higher additions may have entered the tin oxide as tetravalent indium that behaved similarly to tetravalent tin.

Films of cobalt oxide were also sensitive to preparation conditions. In this case the power of the r. f. sputtering unit affected film composition and properties. High power conditions dissociated some of the Co_3O_4 units in transit from the target to the substrate. The elemental cobalt and oxygen recombined as CoO. The resulting film was a combination of CoO and Co_3O_4. Films with more Co_3O_4 due to either sputtering conditions or annealing showed more conductivity due to electron exchange in its multi-valence spinel structure.

Cobalt oxide films formed by sputtering with a Co_3O_4 target doped with 5 m/o Li_2O had substantially lower resistivities than undoped cobalt oxide films. The lithium atoms acted as electron acceptors.

Two activation energies in both doped and undoped films of cobalt oxide were caused by an increase in the ionization of the cobalt vacancies from V_{Co}' to V_{Co}''. Thermal energy excited cobalt

oxide valence electrons which then ionized the cobalt vacancy acceptor to an effective charge of -2.

In some samples of cobalt oxide deposited onto tin oxide rectification was observed (Figure 36). Rectification was not observed in other samples in which tin oxide had been deposited onto cobalt oxide. The fact that this formation sequence subjected the combined films to more heating indicated that interdiffusion of films was responsible for deterioration of the junction. The photovoltaic effect was not observed in any prototype solar cell. This must have been caused by lack of electron-hole pairs or by recombination of these at electron or hole traps.

The films exhibited considerable optical absorption in the case of tin oxide doped with antimony, and both undoped and lithium doped cobalt oxide. Due to this, these films could serve as either solar absorbers or solar transmitters depending on thickness and degree and type of doping.

Optical reflection for the films was generally low at approximately 5%. Tin oxide films containing 1 m/o antimony showed the highest reflection of the films studied. This reflection of 15% at wavelengths of 2.1 to 2.5 microns is unique in that many other oxides do not show any appreciable infrared reflection.

VII. FUTURE WORK

Studies of the basic properties and applications of semiconducting oxide thin films can be continued. These investigations would entail:

1. Study of electronic spectra of oxygen bonded to indium, silicon, and other glass components. This investigation would be helpful in gaining a clearer understanding of the nature of oxygen bonding in oxide films.
2. Study of electronic spectra of chlorine bonded to tin, indium, antimony, and glass components. This would give a clearer picture of the bonding of residual chlorine in tin oxide films.
3. Determination of direct band gap energies of semiconducting oxide thin films by optical absorption and photoconductivity measurements.
4. Follow up band gap measurements by carrying out a systematic combination of those materials having band gaps of energies that fall within the solar spectrum.
5. Investigation of an alternative means of forming a hetero-junction by diffusion of vacuum deposited metals into oxide thin films.
6. Study of metal-semiconductor contacts. This would enable the proper selection of a particular metal for use as either an ohmic contact to semiconducting films or as a part of metal semiconductor junction.

REFERENCES

1. R. Gomer,"Preparation and Some Properties of Conducting Transparent Glass," Rev. Sci. Instru., 24 993 (1953)

2. R G. Livesay, E. Lyford, and H. Moore,"A Technique for the Production of Transparent Electrically Conducting SnO_2 Films on Glass Substrates," J. Sci. Instru., 1 (1) 947 (1968)

3. R.F. Bortholomew and H.M. Garfinkle,"Preparation of Thick Crystalline Films of Tin Oxide and Porous Glass Partially Filled with Tin Oxide," J. Electrochem. Soc., 116 (9) 1205 (1969)

4. D. Elliot, D.L. Zellmer, and H.A. Laitinen,"Electro-Chemical Properties of Polyctystalline Tin Oxide," J. Electrochem. Soc., 117 (11) 1343 (1970)

5. K. Kajiyama and Y. Furukawa,"Electrical and Optical Properties of SnO_2-Si heterojunctions," Jap. J. Appl. Phys., 6 905 (1967)

6. K. Ishiguro, and others, "Optical and Electrical Properties of Tin Oxide Films," J. Phys. Soc. Japan, 13 (3) 296 (1958)

7. T. Arai,"The Study of the Optical Properties of Conducting Tin Oxide Films and their Interpretation in Terms of a Tentative Band Scheme," J. Phys. Soc. Japan, 15 (5) 916 (1960)

8. V.K. Miloslavski,"Infrared Absorption of Thin Films of Tin Dioxide," Opt. Spectr. (USSR) 7 154 (1959)

9. V.K. Miloslavski and A.P. Lyashenko,"Optical and Electrical Properties of Thin Films of Tin Dioxide," Opt. Spectr. (USSR) 8 455 (1960)

10. T. Ingaki, N. Yasuro, and S. Hajme,"Negative Magnetoresistance in Tin Oxide Films," Jap. J. Appl. Phys. 8 (5) 625 (1969)

11. A. Rohatgi, M.S. Thesis,"Semiconducting Thin Films on Glass," Virginia Polytechnic Institute and State University, (1973)

12. A.V. Sheklein,"The Microoptical Structure of Selective Semiconducting Films on Glass," Geliotekhnika, 3 (1) 21 (1967)

13. D.B. Fraser and H.D. Cook,"Highly Conductive, Transparent Films of Sputtered $In_{2-x}Sn_xO_{3-y}$," J. Electrochem. Soc., 119 1368 (1972)

14. S. Yamanaka and T. Oohashi,"Preparation of SnO_2 Films by D.C. Glow Discharge Sputtering," Jap. J. Appl. Phys., 8 1058 (1969)

15. C.A. Vincent and D.G.C. Weston,"Preparation and Properties of Semiconducting Polycrystalline Tin Oxide," J. Electrochem. Soc., 119 (4) 518 (1972)

16. K. Niwa, I. Yamai, and T. Wada,"A Study of Tin Oxides by X-Ray Diffraction Method," Bull. Chem. Soc. Japan, 31 725 (1958)

17. E.W. Grieske, and others,"A Proton Magnetic Resonance and Electron Diffraction Study of the Thermal Decomposition of Tin(IV)Hydroxides," Inorganic Chem., 6 1294 (1967)

18. C.A. Vincent,"The Nature of Semiconductivity in Polycrystalline Tin Oxide," J. Electrochem. Soc., 119 (4) 515 (1972)

19. J. Whitney and N. Davidson,"Spectrophotometric Investigation of the Interaction Between Ions of Different Oxidation States of an Element," J. Amer. Chem Soc., 69 2076 (1947)

20. E.D. Adirovich, Y.U.M. Yuabov, and G.R. Yagudaev,"Thin Film Structures with nCdS-pCdTe Heterojunction," International Conference on the Physics and Chemistry of Semiconductor Heterojunction and Layer Structures. Proceedings, 2 (1971)

21. J.F. Jordan,"Development of Low Cost Solar Cells," Session IV Proceedings of Photovoltaic Conversion of Solar Energy for Terrestrial Applocations Workshop, 2 NSF, Cherry Hill, N.J., 182 (1973)

22. Fillard, and others,"SnO_2-Semiconductor Heterojunction, Electrical Properties of a Particular MOS Structure," Jap. J. Appl. Phys. 9 (8) 1012

23. L.J. VanRuyven, J.M.P. Papenhuijzen, and A.C.J. Verhoeven,"Optical Phenomena in Ge-GaP Heterojunctions," Solid State Electronics, 8 631 (1965)

24. I.I. Borisova and O.K. Botvinkin,"Investigating the Conditions for the Formation of Cobalt Oxide Coatings on Glass," Steklo i Keramika, 22 (5) 15 (1965)

25. O.K. Botvinkin, I.I. Borisova, and V.A. Ryabov,"New Type of Sun Protective Glass," Steklo i Keramika 21 (5) 7 (1964)

26. H.B. Sachse and G. Nichols,"Determinations of Stoichiometric Variations in Sputtered Oxide Films," J. Appl. Phys., 41 (10) 4237 (1970)

27. P.A. Urick and M.R. Notis,"Final Stage Densification During Pressure Sintering of CoO," J. Amer. Cer. Soc. 11 570 (1973)

28. W.K. Chen and R.A. Jackson,"Self Diffusion in Undoped and Doped Cobaltous Oxide," J. Phys. Chem. Solids, 30 1309 (1969)

29. J.T. Cox and C.M. Quinn,"Conductivity Measurements on Cobalt and Nickel Oxides in Highly Enriched Oxygen Atmospheres," J. Mater. Sci., 4 (1) 33 (1962)

30. B. Fisher and D.S. Tannhauser,"Electrical Properties of Cobalt Monoxide," J. Chem. Phys., 44 (4) 1663

31. B. Fisher and J.B. Wagner,Jr.,"Thermogravimetric and Seebeck Effect Measurements on Li-Doped CoO at High Temperatures," J. Appl. Phys. 38 (10) 3838 (1967)

32. W.D. Kingery, Introduction to Ceramics, John Wiley and Sons, Inc., New York, (1967)

33. R.R. Heikes and W.D. Johnston,"Mechanism of Conduction in Li-Substituted Transition Metal Oxides," J. Chem. Phys., 26 (3) 582 (1957)

34. H. Ichimura and W. Komatsu,"Distribution of Various Dopant Cations (Li^{+}, Al^{3+}, Ga^{3+}, and In^{3+}) in Cobalt Spinel," Nippon Kagakukai Nippon Kagoku Kaishi, 4 690 (1972)

35. C.W. Pratt,Jr. and R. Coehlo, "Optical Absorption of CoO and MnO Above and Below the Neel Temperature," Phys. Rev. 116 (2) 281 (1959)

36. T. Viverito, E. Rilee, and L.H. Slack,"Oxide Film Deposition by an Improved Pyrolitic Decomposition Process," Bull. Amer. Cer. Soc. 54 (2) (1975)

37. D.L. Evans and G.R. Fischer,"X-Ray Determination of Film Thickness Using the Glassy Halo," Bull. Amer. Cer. Soc. 52 (6) 510 (1973)

38. L.B. Valdez,"Resistivity Measurements on Germanium for Transistors," Proc. I.R.E., 42 420 (1954)

39. G. Bliznakov and D. Klissurski,"Adsorption of Oxygen on Co_3O_4," Bulgarian Academy of Sciences, 2 (2) 165 (1969)

40. Ad Hoc Committee on the Fundamentals of Amorphous Semiconductors, Fundamentals of Amorphous Semiconductors, National Academy of Sciences, Washington, D.C., 41 (1972)

41. K. Sieghban, and others,"Electron Spectroscopy for Chemical Analysis," Technical Report AFML-TR-68-189 NTIS (1968)

42. K. Sieghban, and others, ESCA Applied to Free Molecules, American Elsevier Publishing Co., Inc., New York, 13 (1969)

43. Powder Diffraction File, Joint Committee on Powder Diffraction Standards, Swarthmore, Pa.

VITA

The author was born on June 17, 1952 in Westwood, New Jersey. He spent all of his childhood in Westwood attending its public schools until June of 1970 at which time he graduated from Westwood High School.

In the Fall of 1970 the author entered Rutgers College of Engineering in New Brunswick, New Jersey. While there he studied Ceramic Science and became a member of Tau Beta Pi and Keramos honorary societies. He graduated with a Bachelor of Science Degree and highest honors in May of 1974.

During the summer of 1974 he worked for Materials Research Corporation in the quality control department of the Ceramic Products Division.

He began his work leading to a Master of Science Degree in Ceramic Engineering at Virginia Polytechnic Institute and State University in the Fall of 1974.

Alan F. Carroll

SEMICONDUCTING TIN OXIDE AND COBALT OXIDE FILMS FOR FUTURE SOLAR ENERGY APPLICATIONS

by

Alan F. Carroll

(ABSTRACT)

Increased need for alternative energy sources has instigated much interest in conversion of solar energy to other useful forms of energy. Semiconducting oxide thin films have potential applicability in photovoltaic conversion of solar energy to electrical energy and thermal energy collection or reflection.

Pyrolytic thin films of SnO_{2-x} and r. f. sputtered thin films of CoO_x were prepared in this study and analyzed for electrical, optical, and structural characteristics. The experimental techniques used for this investigation were X-ray diffraction, visible and infrared spectrometry, electron spectroscopy for chemical analysis, scanning electron microscopy, heat treatment, and electrical resistivity measurement carried out at different temperatures.

The information obtained from this investigation has shed new light on the cause for conductivity in SnO_{2-x}. Chlorine impurity atoms were found to remain in the film due to incomplete pyrolytic decomposition. Of great interest was the finding that this chlorine was not affected by annealing of the films. Resistivity increases caused by annealing were shown to arise from film oxidation and interdiffusion of film with glass substrate. Resistivity increases

caused by large additions of antimony were found to arise from formation of amorphous SnO_{2-x} films.

Causes for variability in resistivity of CoO_x were investigated in order to obtain reproducible films for use in heterojunctions with SnO_{2-x}. The major cause for variation was determined to be the degree of oxidation of the CoO phase in the film. As the CoO was oxidized to form Co_3O_4 resistivity decreased due to the increased number of defects (V_{Co}).

SEMICONDUCTING TIN OXIDE AND COBALT OXIDE FILMS FOR SOLAR ENERGY APPLICATIONS

by

Alan F. Carroll

(ABSTRACT)

Increased need for alternative energy sources has instigated much interest in conversion of solar energy to other useful forms of energy. Semiconducting oxide thin films have potential applicability in photovoltaic conversion of solar energy to electrical energy and thermal energy collection or reflection.

Pyrolytic thin films of SnO_{2-x} and r. f. sputtered thin films of CoO_x were prepared in this study and analyzed for electrical, optical, and structural characteristics. The experimental techniques used for this investigation were X-ray diffraction, visible and infrared spectrometry, electron spectroscopy for chemical analysis, scanning electron microscopy, heat treatment, and electrical resistivity measurement carried out at different temperatures.

The information obtained from this investigation has shed new light on the cause for conductivity in SnO_{2-x}. Chlorine impurity atoms were found to remain in the film due to incomplete pyrolytic decomposition. Of great interest was the finding that this chlorine was not affected by annealing of the films. Resistivity increases caused by annealing were shown to arise from film oxidation and interdiffusion of film with glass substrate. Resistivity increases